FATIGUE PERFORMANCE OF NANOCLAY FILLED GLASS FIBER REINFORCED HYBRID COMPOSITE LAMINATE

Submitted in fulfilment of the requirements for the degree of

Master of Engineering: Mechanical Engineering

in the Faculty of Engineering and the Built Environment at the

Durban University of Technology,

KwaZulu-Natal, South Africa

John Olumide OLUSANYA

Approved for final submission:

Supervisor: _____ **Date:** _____

Prof. Krishnan Kanny

Co-supervisor: _____ **Date:** _____

Dr. T.P. Mohan

April, 2017

ABSTRACT

In this study, the fatigue life of fiber reinforced composite (FRC) materials system was investigated. A nano-filler was used to increase the service life of the composite structures under cyclical loading since such structures require improved structural integrity and longer service life. Behaviour of glass fiber reinforced composite (GFRC) enhanced with various weight percentages (1 to 5 wt. %) of Cloisite 30B montmorillonite (MMT) clay was studied under static and fatigue loading.

Epoxy clay nanocomposite (ECN) and hybrid nanoclay/GFRC laminates were characterised using differential scanning calorimetry (DSC) and dynamic mechanical analysis (DMA). The mechanical properties of neat GFRC and hybrid nanoclay/GFRC laminates were evaluated. Fatigue study of the composite laminates was conducted and presented using the following parameter; matrix crack initiation and propagation, interfacial debonding, delamination and *S*–*N* relationship. Residual strength of the materials was evaluated using DMA to determine the reliability of the hybrid nanoclay/GFRC laminates.

The results showed that ECN and hybrid nanoclay/GFRC laminates exhibited substantial improvement in most tests when compared to composite without nanoclay. The toughening mechanism of the nanoclay in the GFRC up to 3 wt. % gave 17%, 24% and 56% improvement in tensile, flexural and impact properties respectively. In the fatigue performance, less crack propagations was found in the hybrid nanoclay/GFRC laminates. Fatigue life of hybrid nanoclay/GFRC laminate was increased by 625% at the nanoclay addition up to 3 wt. % when compared to neat GFRC laminate. The residual strength of the composite materials revealed that hybrid nanoclay/GFRC showed less storage modulus reduction after fatigue. Likewise, a positive shift toward the right was found in the tan delta glass transition temperature (T_g) of 3 wt. % nanoclay/GFRC laminate after fatigue. It was concluded that the application of nanoclay in the GFRC improved the performance of the material. The hybrid nanoclay/GFRC material can therefore be recommended mechanically and thermally for longer usage in structural application.

DECLARATION

I hereby declare that this dissertation is my original work and has not been previously submitted in part or totality for another degree in this or any other university. I further declare that this work does not violate the right of others, as information derived from all published and unpublished sources cited are acknowledged by means of a comprehensive list of references. Furthermore, journal and conference papers have been produced on the basis of this work.

John Olumide Olusanya.

DEDICATION

To the Almighty God, the omniscient, the everlasting father, the beginning and the end, the ultimate teacher.

ACKNOWLEDGEMENTS

All glory and honour be to God Almighty for His mercy upon me to bring this study to a completion. I appreciate Him for the strength given to me and the impartation of knowledge and inspiration throughout the course of this study. I testify to His goodness and His wonderful work in my life. He is my helper through the duration of this study.

For constituting towards the successful completion of this research work, I will like to express my sincere appreciation to the following individuals and institution:

I sincerely appreciate my supervisor, Prof. K. Kanny, for supervising this research work. I thank him for his assistance, motivation and intellectual support throughout the various stages of this study.

I appreciate Dr. T. P. Mohan, for co-supervising this work and for providing guidance in application technically.

My immeasurable thanks to the composite research group (CRG), for their support. Our group discussions and presentations have really been of useful help.

Thanks to my siblings for their support and I also thank my friend Prof. J. A. Adeyemo for his motivation and encouragement at all the time.

To Durban University of Technology and the Postgraduate Research Directorate, I really give thanks for providing the scholarship to pursue this degree and thereby making my dream to come true. The workshops and seminars attended have been instrumental to the success of this research. I will forever be grateful to this wonderful institution.

Finally, my deepest appreciation goes to my loving wife, Dr. Nokhuthula Mavela-Olusanya, who has contributed greatly and immensely towards the completion of this research work. Your sacrifice of love towards my success has been truly wonderful. Thank you my dear for your great support, and for your undiluted love, patience and understanding. I am so grateful.

TABLE OF CONTENTS

LIST OF FIGURES

LIST OF TABLES

SYMBOLS AND ABBREVIATIONS

A_{final}	Final integrated peak area
$A_{initial}$	Initial integrated peak area
A_o	Cross sectional area
ASTM	American Society for Testing Materials
b	Specimen width
°C	Temperature
CD	Crack Density
d	Space between layers of clay lattices
DMA	Dynamic Mechanical Analysis
DMA-RM	Dynamic Mechanical Analysis Reheat Method
DSC	Differential Scanning Calorimetry
ε	Elongation
E	Modulus
E'	Storage modulus
E"	Loss modulus
ECN	Epoxy Clay Nanocomposite
FCG	Fatigue Crack Growth
FRC	Fiber Reinforced Composite
GFRC	Glass Fiber Reinforced Composite
GPA	Giga-Pascal
h	Specimen thickness
Hz	Hertz

l	Specimen gauge length
LR	Liquid Resin
LH	Liquid Hardener
m_c	Mass of composite
m_f	Mass of fiber reinforcement
mm	Millimetre
MMT	Montmorillonite
MPa	Mega-Pascal
MWCNT	Multiwall Carbon Nanotube
N	Number of cycles
N_f	Cycle to failure
nm	Nanometer
OSM	Optical Scanning Microscope
P	Applied load
R	Stress ratio
SEM	Scanning Electron Microscope
T-T	Tension-Tension
TA	Thermal Analyser
tan δ	Tan delta
TEM	Transmission Electron Microscopy
T_g	Glass transition temperature
VARIM	Vacuum Assisted Resin Infusion Method
V_f	Fiber volume fraction

wt	Weight
XRD	X–Ray Diffraction
µm	Micrometre
ρ_c	Composite density
ρ_f	Fiber Density
σ	Stress
σ_a	Stress amplitude
σ_c	Composite stress
σ_f	Fiber stress
σ_m	Mean stress
σ_{max}	Maximum stress
σ_{min}	Minimum stress
σ_{UTS}	Ultimate tensile strength
Δ_σ	Stress range
%	Percentage
λ	Wave length
θ	Angle

CHAPTER 1

INTRODUCTION

1.1 BACKGROUND

Composite materials are known to be ideal replacement of traditional engineering materials such as metals, metal alloys and ceramics [1]. The unique properties of the composite materials have made them to find applications in various structures. Recently, composite materials such as glass fiber reinforced composite (GFRC) have had a steady growth. In performance improvement, products made from GFRC materials are very attractive, durable and profitable. These GFRC materials offer numerous advantages because of their lightweight, high strength, resistance to corrosion, excellent elastic properties and non-conductivity properties [2]. The widespread adoption of the composite materials in many industries has revolutionised metallic components used in structural applications, automobile, aerodynamics, as well as aerospace components, [2]. However, they still remain prone to damage in terms of structural integrity. Fatigue of such composite materials therefore depends on the type of the structure and constituents of the GFRC material.

GFRC materials are finding usage in numerous structural applications, such as aircraft fuselage, boat hulls and wind turbine blade materials. The utilization of GFRC materials instead of conventional materials as structural components under fatigue loading are becoming popular. Moreover, their structures are frequently subjected to fatigue or cyclic loading conditions; and when under pressure, the components are subjected to loadings in all directions. Thus, these GFRC materials require ongoing development to improve their durability, flexibility, impact resistance and fatigue life [3, 4]. In order to take advantage of the composite material system, the complexities and the structure-property relationship of the GFRC materials need to be explored.

One of the common types of failure in service loading of composite structure is fatigue failure [5]. The durability of an aerodynamic component, such as wind turbine blades can be established if the wind blades has high stiffness relative to long fatigue life [6]. According to Richardson [7], the fatigue failure rates of wind turbine blades, when investigated, were discovered to be of the order of 20% within three years. It was suggested that, increasing the reliability and lifetime of such wind blades is important for the developers of wind turbines. In a simple composite wind turbine blade, such as the type shown in Figure 1.1, the majority of the GFRC reinforced structures will undergo twisting (Torsion) and bending during the cyclic period. The damage mechanism that may follow can be catastrophic because the GFRC blade makes use of thermoset resin as matrix phase. This allows the blade structure to be highly prone to matrix cracking. The highly crosslinking nature of resin-matrix in the composite might be favourable properties, but thermoset resin-matrix still exhibits undesirable brittle properties with poor resistance to crack initiation and poor damage tolerance [8].

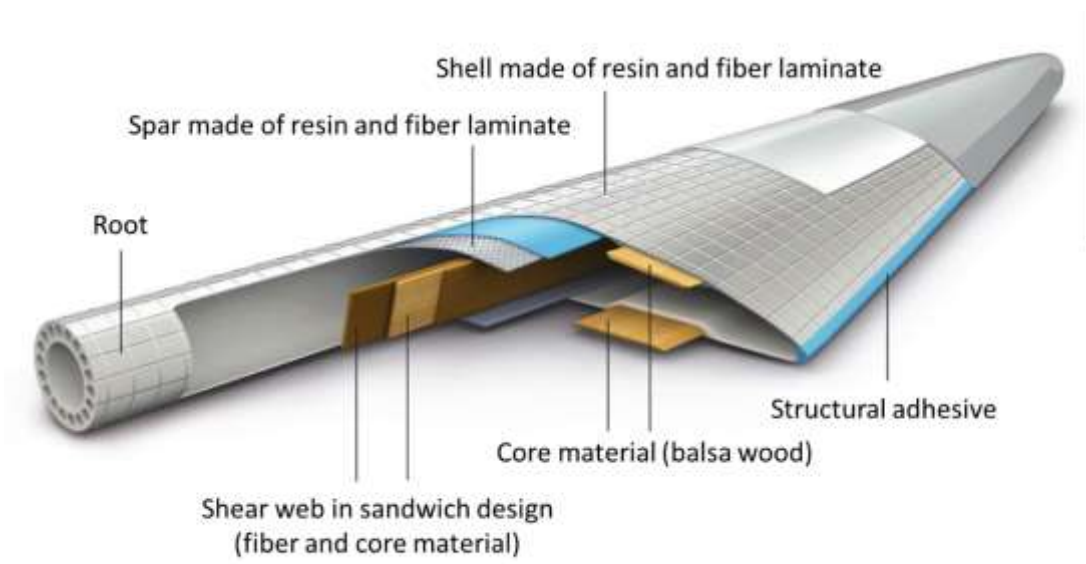

Figure 1.1: Typical wind turbine blade and its cross section [9]

During aerodynamic application of such a wind blade, the initial damage, matrix cracking, can propagate across the composite structure, affect its

structural integrity and the fatigue performance will be seriously affected [10]. Although composite material constituents, fiber lay-ups, fiber orientations and loading modes may differ considerably among such applications, hence, failure in composite material is generally driven by fatigue failure in the polymer matrix [11]. This is because matrix is known to be more susceptible to fatigue than fibers which contain fewer defects; and fiber is more resistant to damage, than matrix to crack initiation [12]. However, fatigue failure of composites can easily occur at the fiber-matrix interface due to poor adhesion strength [13]. That means the fatigue failure through matrix cracking and degradation are the main failure modes that should be avoided in any design. Therefore, the properties of the composite structures should be addressed for maximum fatigue life.

1.2 HISTORY OF COMPOSITE

Composite materials have been in existence and used in one way or the other throughout history of human kind. In 1500s B.C, composite materials were first used when early Egyptians and Mesopotamian settlers used a mixture of mud and straws to create strong and durable buildings [14]. These straws provided reinforcement to ancient composite products including pottery and boats. For example, bricks that are dried out from mud as building material are strong if been squashed because they have good compressive strength. These bricks can break easily if tensile strength is applied on them through bending. Straws on the other hand can be crumpled easily, but seems very strong when they are stretched. By combining the mud and the straws together as composite material, bricks that can be resistant to both squeezing and tearing can possibly be made as excellent building blocks [15]. The mud in the composite material is classified as matrix, while the straws as the reinforcement.

Another common artificial composite material is concrete [16]. Concrete is a mixture of small stones or gravel, bonded together by cement and sand. It has good compressive strength which also resists squashing, but weak tensile strength. In more recent times, it has been found that by adding metal

rods or wires to the concrete, can increase its tensile (during bending) strength. Concrete containing such rods or wires is called reinforced concrete [17].

Also, natural composite exists in plants. Wood is a composite made from long cellulose fibers, held together by a much weaker substance called lignin [17]. Cellulose is also found in cotton, but without the lignin to bind it together, it is much weaker. The two weak substances (lignin and cellulose) together form a much stronger composite. In the present age, advance materials have been developed in the form of synthetic materials and are used as composite materials, even in this study. These synthetic materials are under the basic concept of “matrix” and “reinforcement”, and they are produced in the form of plastic or resin (matrix) and fibers (reinforcement) [18]. The reinforcement is usually much stronger and stiffer than the matrix, and gives the composite its good properties. The reinforcements are held and bound together by the matrix in an orderly pattern. The matrix does not only hold the reinforcement together, it also protects fibers from damage by sharing stress among fibers. Table 1.1 shows examples of some natural and synthetic composite.

Table 1.1: Natural composites and synthetic composites [19].

Natural composites	**Synthetic composites**
Wood : cellulose and lignin	Concrete and reinforced concrete
Bone : collagen and lime	Asphalt paving
Human body	Cements
Sedimentary rocks, e.g. sandstone	Laminates (fiber and matrix)
Leather	Plywood
Metamorphic rocks, e.g. marble	Galvanised Iron
Horn	Vitreous coatings

The role of the reinforcement in this composite structure is to fundamentally increase the mechanical properties of the matrix system. Meanwhile, the reinforcement could be particulate or fiber, and the matrix could be polymer-matrix, metal-matrix or ceramic matrix which surrounds and binds the reinforcement together [18]. Some other composite materials including; particle reinforced composite, fiber reinforced composite (FRC), laminated and sandwich composite has been used in structural applications one way or the other; but the most common composite used is FRC [20]. FRC materials are of two main categories, which are normally referred to as continuous fiber reinforced materials and short fiber reinforced materials. The fiber could be in the form of unidirectional, woven, chopped strand mat or dispersed fabric reinforcement as shown in Figure 1.2. The woven fiber mat showed in Figure 1.2b is interlaced at right angle to create single layer or plain weave.

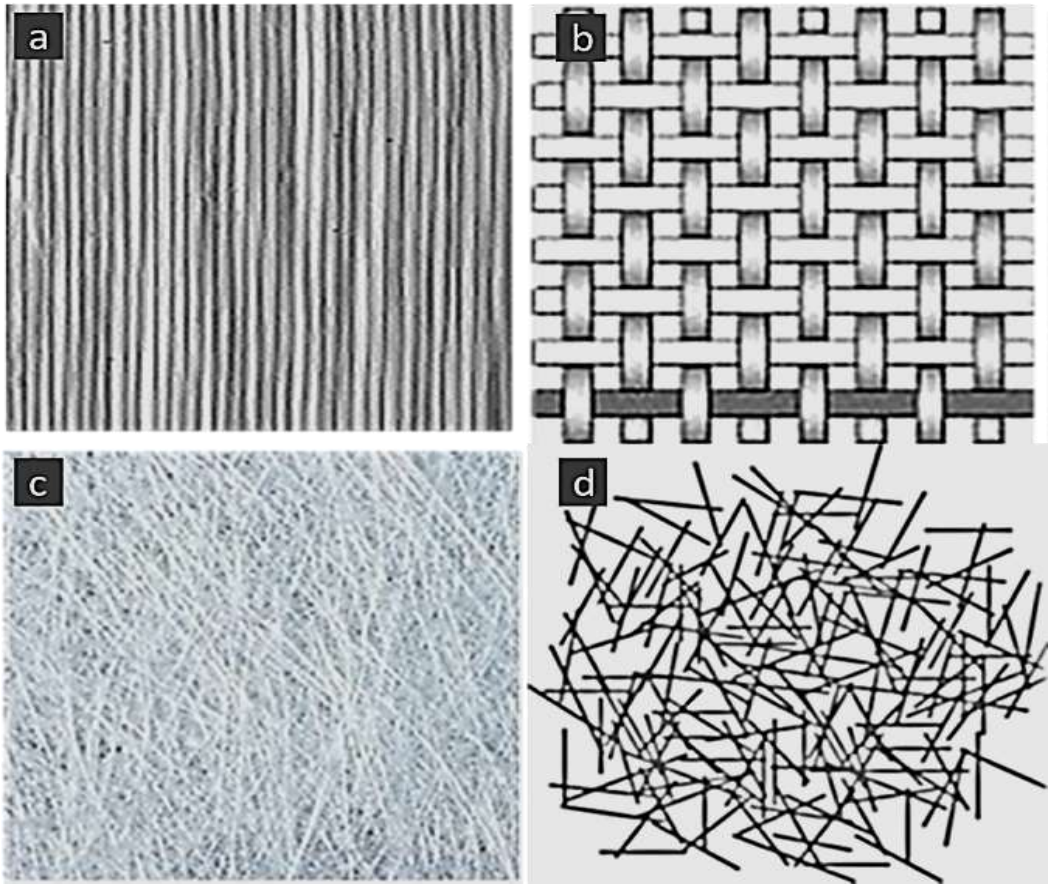

Figure 1.2: Types of fiber reinforcements; (a) unidirectional fiber, (b) woven fiber, (c) chopped strand fiber and (d) short fiber

1.3 CONSTITUENTS PARTS OF COMPOSITES

Composite materials have constituents of the different materials. These constituents are of two or more materials combined to take advantage of the good characteristics of each of the material [21]. The constituents; 'matrix' and 'reinforcement' are mostly assembled to form one single bulk without physical blending to form a homogeneous material. The matrix holds the reinforcement together to form bulk of the material; while the reinforcement impregnated in the matrix lends its advantage (usually strength) to the composite [21].

1.3.1 Matrix

Matrix is a homogeneous material in which reinforced system of a composite is embedded [21]. It is completely continuous. The matrix provides a medium for binding and holding reinforcements together into a solid. It offers protection to the reinforcements from environmental damage, serves to transfer loads, and provides finish, texture, colour, durability and functionality. The three main types of composite matrix materials are ceramic matrix composite (CMC), metal matrix composites (MMC) and polymer matrix composite (PMC). The most common used is polymer matrix composite. However, two types of polymers commonly used as matrix materials for the fabrication of composites are thermosets (epoxies) and thermoplastics (polypropylene, nylon or acrylics); out of which thermoset polymers are the most widely used matrix. These thermoset polymers comprise of different types of matrices which include; Bis-Maleimides (BMI), Epoxy Resin, Phenolics, Unsaturated Polyester Resin, Polyurethane (PUR) and Silicone [22].

1.3.2 Reinforcement

Reinforcement in a composite can be presented in different formats, such as; particle reinforcement, fiber reinforcement and laminates. These are classified by their shapes, aspect ratio, geometric arrangement and concentration. [23]. Figure 1.3 shows examples of reinforcement in composite structure.

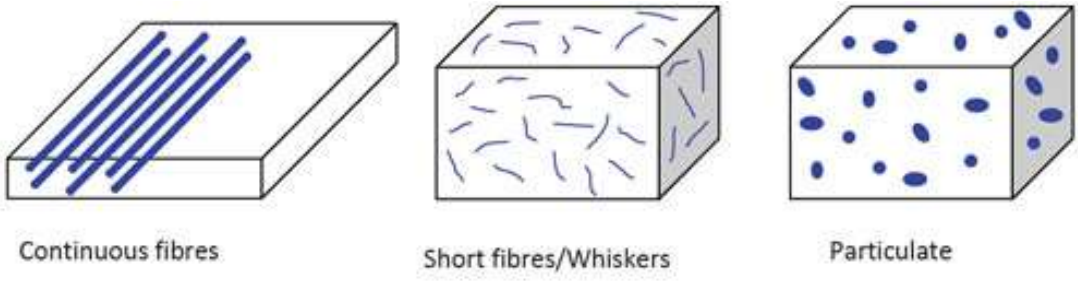

Figure 1.3: Schematic diagram showing specific reinforcing phase: (a) continuous fiber, (b) short fiber/whiskers and (c) particulate [23]

The continuous fiber reinforcement shown above could be uni-directional, bi-directional and multi-directional; by which laminate may be random planar or three dimensional. The particulate reinforced systems are therefore predominantly isotropic in their physical and mechanical behaviour; despite that they are locally heterogeneous in nature. These reinforcements in composite structures formations are classified as:

1. Particulate reinforcement: Particulate reinforced materials are material in which the fillers are roughly round in shape. They are dispersed phase with a physical dimensions approximately 10–100 nm particles. The effectiveness of these particles as reinforcement is when randomly dispersed or evenly distributed throughout within the matrix of composite materials, and the strengthening mechanism of composite material depends on the particle size.
2. Fiber reinforcement: Fiber materials are mostly used to reinforce polymer matrix composites. The most common use are fiber glass and carbon fiber [24]. The presence of fibers in composite materials gives increase to the modulus of the matrix. Fiber reinforced arrangement includes; fiber orientation, fiber concentration and fiber distribution and these have shown significant influence on the strength and other properties of fiber-reinforced composites.
3. Laminar/Sandwich: Laminar is the type of composite that consists of panels or sheets of different materials that are bonded together; while sandwich are the types that uses the filler material known as foam core

or honeycomb materials in the form of face sheet laminated instead of fibers. The matrix (adhesive) material used in the sandwich panel is usually a phenolic type of thermoset polymer. The filler could be any material from craft paper (Formica) to canvas (canvas phenolic) to glass (glass filled phenolic).

Of the various reinforcement types, those based on fiber reinforcement provide the best mechanical properties when loaded parallel to the fiber direction. They exhibit considerable properties along the fiber direction if continuously aligned and their anisotropy behaviour can be beneficial in certain applications. However, if a more isotropic behaviour is desired, then laminates may be assembled, in consideration of fiber layer oriented at a number of different angles. On the other hand, woven fiber cloths and non-crimp fabrics which comprise layers of fibers at various orientations held together with through-thickness stitches provide reinforcement in two or more orthogonal direction [23].

1.4 ADVANTAGES OF COMPOSITE MATERIALS

The widespread adoption of composite structures through many industries was as a result of their unique features and benefits. One of the important features of composite materials is that they are incredibly lightweight; especially in comparison to materials metals and wood. A composite structure will weigh 1/4 that of a steel structure with the same strength. Cars made from composites can weigh 1/4 of cars that is made from steel [25]. This shows that such a car equates to low cost of fuel consumption. In terms of strength to weight ratio, different material has different strength per unit weight. That is, each material can take different amount of load for the same volume (cross sectional area) of the material. For a given design, the material used must be strong enough to withstand the load that is to be applied. An example of this is the high tenacity structural fiber used in composites such as aramid and S-Glass, which are widely used in body armour. Due to the high strength of these composites, soldiers are well protected from blast and

ballistic threats [25]. The strength-to-weight ratio of the body armour is the need of a very high strength material at the lowest possible weight.

Reducing the number of parts in a machine or structure such as an airplane fuselages is another advantages of composite materials [26]. Unlike metallic structures, where parts are joined with screws, composite parts are moulded in order to cut down on the maintenance needed over the life of the structure. A single piece made of composite materials can replace an entire assembly of metal parts. In situations demanding tight fits that do not vary, they are used in aircraft wings to retain their shapes and sizes as the plane gains or loses altitude. Composites are also good insulators and non-conductive materials, especially some composites that are made with fiberglass. Considering a ladder that is required to cross a power line, aluminium ladder can be an electrocution hazard, while ladder made with fiberglass is not a risk for such project. Composites do not easily conduct heat or cold. They are used in buildings constructions parts such as; doors, panels, and windows where extra protection is needed from severe weather. They are also used in electrical components, bath hubs, and households. Structures made of composites stay very long and require little maintenance; and these materials have exhibited apparent infinite life characteristics. Some other important features include; design flexibility, non-magnetic and radar transparency.

1.4.1 Properties of composite materials

Mechanical properties of composite materials are important phenomena to be considered during processing. Their properties can be determined as a function of the fiber and the matrix volume content in the laminate, where strength is required in some specific applications. According to David Cripps [27], the stiffness and strength of a laminate will increase in proportion to the amount of fiber present. When fiber volume (V_f) is above about 60-70%, despite increase in the laminate's strength, the strength will reach a peak and then begin to decrease due to the lack of sufficient resin to hold the fibers together properly [27]. In order to determine the mechanical properties of composite materials, weight fraction or volume fraction of the composite

reinforcement and matrix are required. Based on the volume fraction of the composite constituents, rule of mixture (ROM) for composite materials was derived. The ROM distinguished the relationship between the volumetric fraction and weight fraction of the reinforcement and matrix (for a single composite system) by using Equation 1.1 and 1.2 [28].

$$V_f = \frac{W_f/\rho_f}{W_f/\rho_f + W_m/\rho_m} \tag{1.1}$$

And composite fiber density, ρ_f

$$\rho_f = \frac{W_f \rho_f}{\rho_m/\rho_c(W_m + W_f) - W_m} \tag{1.2}$$

Where; V_f is fiber loading (volume fraction), W_f is the fiber loading (weight fraction), W_m is the matrix loading (weight fraction), ρ_c is composite density and ρ_m is matrix density.

The ROM can be used to estimate the modulus, E_{II} of a continuous fiber laminate when loaded in a direction parallel to its fiber direction from its constituent properties, by using Equation 1.3 [1]

$$E_{II} = E_f V_f + E_m(1 - V_f) \tag{1.3}$$

Where; E_f is the fiber modulus, V_f is the fiber volume fraction, E_m is the matrix modulus and $(1 - V_f)$ = V_m, which is the matrix volume fraction. It is assumed that by using ROM, fibers are uniformly distributed throughout with the matrix and there is perfect bonding between fibers and matrix. Matrix is also free of void, and it leaves no residual stress in the laminate. This makes fiber and matrix to behave as linear elastic materials.

In particle reinforced composite, large particle and dispersion-strengthened composites are the two types involved. The large particle-reinforced is the type that the particle/matrix interactions cannot be treated on an atomic or molecular level. The degree of reinforcement or improvement of its mechanical behaviour depends on strong bonding at the matrix-particle

interface. For effective reinforcement of composite, the particles should be small and evenly distributed throughout the matrix. The volume fraction of the two phases influence the behaviour of the composite, but the mechanical properties are enhanced with increasing particulate content. For the properties of particle–reinforced composite, ROM predicted that the elastic modulus of the composite should fall between an upper and lower bound as stated in the Equation 1.4 and 1.5 [29].

$$E_c(u) = E_m V_m + E_p V_p \tag{1.4}$$

$$E_c(l) = \frac{E_m E_p}{V_m E_p + V_p E_m} \tag{1.5}$$

Where; E_c is elastic modulus of composite, E_p is elastic modulus of particle, E_m is elastic modulus of matrix, V_m is volume fraction of matrix and V_p is the volume fraction of particle.

When proper relationship between the reinforcements and matrices of composite materials are achieved, including their volumetric and weight fraction, the composite materials will equally provide good mechanical properties. Table 1.2 shows mechanical properties of some composite materials. These properties are why composites are used in automobile and to build airplanes.

1.4.2 Strength of composite materials

Strength of fiber reinforced composite (FRC) laminates are generally dependent on the direction of the force or load applied. The stiffness of the FRC panel however, is dependent on the high strength and stiffness of the matrix (epoxy-resin), good adhesion, excellent processability and temperature resistance in the design of the panel [30]. For example, cured epoxy resins are mostly brittle with a low toughness when subject to static and impact loading. That means tougher resin systems are required to be developed without sacrificing the inherent properties of existing resins. Physical strengths of FRC material are generally measured in quasi-static testing.

Table 1.2: Properties of composite materials using polymers as a matrix material and the reinforcement refer to the type of fibers (or fillers) used [31].

Material Properties					
Resin	Reinforcement	Possible Application	Density (g/cm^3)	Tensile Strength (MPa)	Tensile Modulus (GPa)
Polyester	E-Glass CSM		1.44	80-180	7.3-9.3
	E-Glass WR	General Hand Lay-up	1.63	210-300	12-21
	E-Glass uni		1.80	410-1180	12-41
	S-Glass WR	Increased Stiffness	1.64	440	20
	Aramid WR		1.31	430	26
Vinylester	E-Glass WR	General Hand Lay-up	1.89	342	25
	E-Glass WR		1.90	=520	=45
	Aramid WR	Increased & High Stiffness	1.35	=500	=40
	Carbon WR		1.50	=600	=85
Epoxy	E-Glass WR	Higher Strength, durability	1.92	360	17
	E-Glass WR	Fatigue Loading	1.92	1190	39
	Aramid WR	High Stiffness	1.38	1379	76
		High Strength & Stiffness	1.57	2040	134
Phenolic	E-Glass CSM	Non/semi Structural, fire	1.50	85-150	5-7.5
	E-Glass WR	High temperature resistance	1.65	220-330	13-17
Acrylic	E-Glass WR	Structural, Fire/High temperature resistance	170	308	21

These comprise of tensile strength, compressive strength and flexural strength test, interlaminar shear strength test and impact strength test. An

example of a simple composite test can be seen in Figure 1.4, showing tensile loading of unidirectional composite laminate.

In quasi-static testing of FRC materials, the failure behaviour is often complex. The manner in which damage occurs in the material, and the way it accumulates to reach some critical level which precipitates final failure depends on many aspects of the composite construction [32]. This includes the fiber type and distribution, the fiber aspect ratio, and the quality of the interfacial adhesive bond between the fibers and the matrix

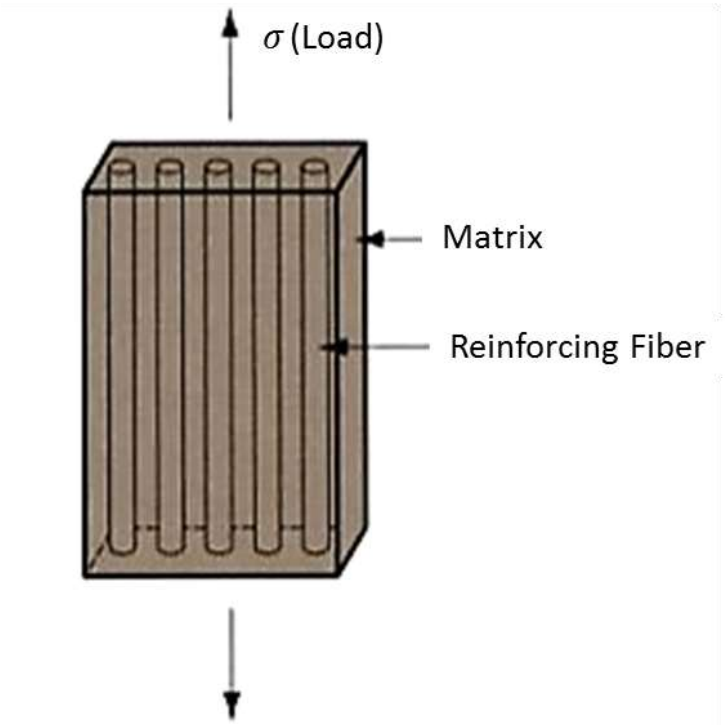

Figure 1.4: Model of a fiber reinforced composite material showing tensile loading of lamina direction [33]

In many types of composites, where consideration for strength and toughness are closely inter-related, fiber failure cannot be the complex nature. When composite laminate reinforced with fibers that are initially well bonded to the matrix is subjected to tensile loading such as shown in the Figure 1.4, the fiber and matrix deform together because the load is shared between them. The stress of such type of composite (σ_c) can be written as:

$$\sigma_c = (\sigma_f) V_f + (\sigma_m)(1 - V_f) \quad (1.6)$$

Where; (σ_f) and (σ_m) are the stress levels in fibers and matrix respectively, and (V_f) is the fiber volume fraction.

When a composite is stressed, both fiber and matrix will stretch by the same amount of load applied in whatever direction the composite is stressed; i.e. they will have equal strain. Since the fiber is stiffer than matrix, the fiber will carry a larger stress. This allows consideration for fiber/matrix stiffness and fiber volume fraction ratio on the composite stiffness during composite fabrication. The continuity of an applied load on composite depends on the nature of the individual components. An illustration of the stress to strain behaviour of two different or common situations in composite is as shown in Figure 1.5. According to Bryan Harris [32], most composites usually regard the high-performance reinforcing fibers as being brittle. That means they deform elastically to failure, showing little deformation. The matrix failure strain is usually much greater than that of the fibers.

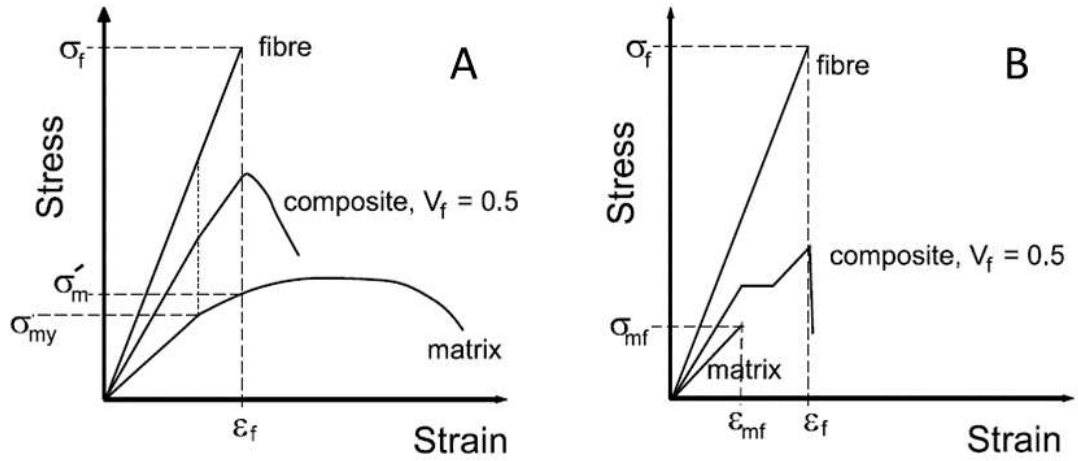

Figure 1.5: Schematic illustrations of the stress/strain curves of two types of composite; (a) with a ductile matrix and (b) with a brittle matrix, which are derived from the stress/strain behaviour of the constituents [32]

From the stress versus strain curve in Figure 1.5a, when the stress in the ductile matrix reaches the matrix yield stress, it can be observed that the

matrix continues to bear load, even though the slope of the stress/strain curve falls almost entirely. But in the brittle-brittle composite system, such as in Figure 1.5b, when there are few fibers present, the stress on the composite may be low enough to break the fibers. This is because the matrix strength was not able to support the load in the composite until its tensile strength is reached.

1.5 PROBLEM STATEMENT

Fiber reinforced composite (FRC) materials are strong lightweight materials. They are internally complex, as they consist of combined order of several architectural parts that makes single structure; hence, not limited to damages. They consist of layers oriented in different directions and those layers in turn are made of individual fibers that vary in composition. Problems with FRC material is that they are brittle materials because they make use of thermoset resin. Their damage behaviour may starts with little cracks which can coalesce to form longer cracks and propagate across the surface of the composite structure. They can undergo temporary damages to permanent deformation depending on stress application, and they can also show little or no damage on the surface until failure occurs [34]. Composite materials are susceptible to a number of failure modes. These occur when composite materials are subjected to an applied load such as static or fatigue test. These modes are related to matrix, fiber and interphase region. The most common failure mode in fiber composite structures is the growth of matrix cracks between different plies within the laminates. These cracks occur when shear loads are applied on the laminate. Since the fibers are significantly stronger than matrix during tension, the matrix starts to crack, leading to interfacial debonding and then delamination may set in [35]. When the delamination propagates through the composite structure upon repeated loading, catastrophic failure occurs if left undetected [36]. Other failure mechanisms in composite materials include intralaminar matrix cracking, longitudinal matrix splitting, fiber-matrix debonding, fiber pull-out and fiber fracture will start to generate; leading the composite material to final failure

[37]. These types of failure mode are as shown in Figure 1.6. They are usually caused by fatigue behaviour in the composite materials.

Matrix cracking is a very important failure mechanism, which is responsible for brittleness of bulk polymer and damages in composite laminate. When the influence of matrix properties on fatigue life of fibre composites was outlined by Jamison et al and Baron et al, reports show that fibre failure, which finalises composite rupture, is strongly dependent on the matrix properties [38, 39]. However, Njuguna et al suggested that, an approach to increase the mechanical properties of such fiber composite is to modify the matrix with nanoparticles [40]. The toughening of the composite material with nanoparticles is to resist fracture, which are mostly initiated by cracks. The durability is to extend the use of the composite material for a long period of time and retaining its physical properties after it has been subjected to stress. Since the fatigue life and the degradation of the mechanical properties are issues of great importance, improvements on the fatigue properties of such fiber composite structures are desirable.

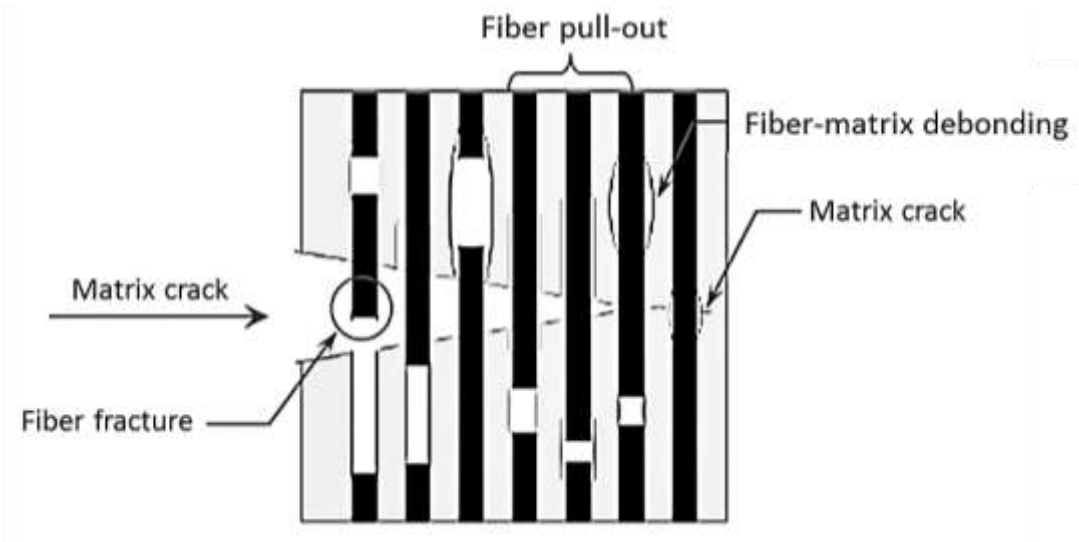

Figure 1.6: Schematic representation of composite material failure mode under fatigue loading [41]

1.6 HYBRID COMPOSITE MATERIALS

Hybrid composite is generally a term used to describe polymer-matrix containing at least two types of reinforcements and the need for this hybrid material is to incorporate the advantage of one material over the other. The categories of hybrid composite materials are based on what is hybridised. The word “hybrid” needed to be explained in terms of difference between hybrid material and composite materials by clarification. The reinforcement materials in hybrid composite structure could either be particle-to-particle, fiber-to-fiber or particle-to-fiber materials; which when combined with composite forms a hybrid composite structure [42]. The combination of these materials has led to new structures that exhibited new properties, not necessarily found in conventional composite structures.

In particle-to-particle reinforced composite, the dispersion of particulates to enhance epoxy matrix of the composite materials have been categorized as hybridisation of inorganic and organic material [43]. This is related to materials hybridised in chemical-bond. An example of inorganic/organic hybrids is organic-modified particulate fabricated by sol-gel processing. The organic-modified silicates shown in Figure 1.7, have excellent mechanical properties due to strong covalent bond between silicate and organic molecules mixed in molecular scale. Hybrid materials fabricated in such a manner are characterized by the particular chemical-bonds between particulate and organic molecules, in contrast with traditional composites.

Hybrid composites materials can also be inter-ply, sandwich hybrids and intimately mixed hybrids, where the constituent fibers are made to mix as randomly as possible, so that over-concentration of any one type is present in the material [44]. According to Daniel and Joel [45], incorporating nanocomposite as a matrix in conventional continuous fiber composites is desirable, in order to produce multi-scale hybrid nano/micro-composites with enhanced properties like fracture toughness. Improvements in damage tolerance are expected from additional energy absorbing mechanisms introduced by the nanoparticles.

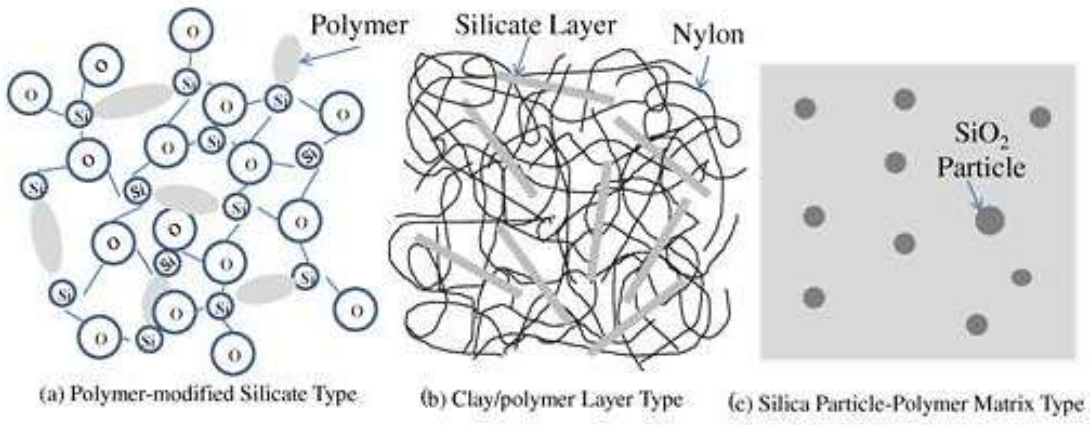

Figure 1.7: Morphology in Inorganic/Organic Hybrid composite materials (a) polymer-modified silicate type, (b) clay/polymer layer type (c) silica particle-polymer matrix type [43]

Hybrid composites are usually used when combination of properties of different types of reinforcements are to be achieved, or when enhancement of the composites are required to achieve better mechanical performance, increase fracture toughness, improve impact damage tolerance and extend fatigue life. To address these properties, there is need to explore the elastic modulus of the hybrid composite.

The elastic modulus of the hybrid composites can be predicted if the individual elastic modulus for particle/polymer composites and fiber/polymer composites are first determined. The values can later be incorporated in the rule of hybrid mixture (RoHM) equations to determine to overall hybrid elastic modulus as suggested by Fu et al [46]. The effect of the assumption will cause the predicted modulus value to deviated from the actual modulus value, and either a positive or negative hybrid effect for certain property of the hybrid composites can be found from the deviation using the RoHM.

By considering a hybrid composites as a system consisting of two single composite systems and assuming that there is no interaction between the two single systems; Mirbagheri et al [47] reported that iso-strain condition can be applied to the two single systems in hybrid composite, such as:

$$\varepsilon_c = \varepsilon_{c1} = \varepsilon_{c2} \tag{1.8}$$

Where; ε_c is the strain of the system in the hybrid composites, ε_{c1} and ε_{c2} are the strains of the first system and the second system respectively in the hybrid composites. Force equilibrium requires that:

$$E_c\varepsilon_c = E_{c1}\varepsilon_{c1}V_{c1} + E_{c2}\varepsilon_{c2}V_{c2} \tag{1.9}$$

Where; E_c is the elastic modulus of the hybrid composites, E_{c1} and E_{c2} are the relative hybrid elastic modulus of the first and the second system respectively, and V_{c1} and V_{c2} are the relative hybrid volume fraction of the first and the second system respectively.

The modulus of the hybrid composites can therefore be evaluated from the RoHM equation by neglecting the interaction between two systems as shown in Equation (1.10).

$$E_c = E_{c1}V_{c1} + E_{c2}V_{c2} \tag{1.10}$$

However, the expressions listed below should also be considered valid for the assumed hybrid composite system [47].

$$V_t = V_{f1} + V_{f2} \tag{1.11}$$

$$V_{c1} = V_{f1}/V_t \tag{1.12}$$

$$V_{c2} = V_{f2}/V_t \tag{1.13}$$

$$V_{c1} + V_{c2} = 1 \tag{1.14}$$

Where;

V_t = the total reinforcement volume fraction.

V_{f1}, V_{f2} = volume fraction of the individual first and second system respectively.

In addition, V_{f1} and V_{f2} are suggested to be used as reinforcement volume fraction for calculation of the elastic modulus (E_{c1} and E_{c2}) of the single

composites. Therefore, a positive or negative hybrid effect is defined as a positive or negative deviation between the elastic modulus of the hybrid composites from the RoHM equation and the actual modulus value.

Different approaches and strategies have been proposed to make hybrid composite materials more damage resistance and less brittle. Hybridising the polymer chemistry with nano-scale reinforcement to toughen the polymer matrix has been the most researched strategies [48]. Progress has been achieved as nanoparticle matrix toughness has been a beneficial effect on the matrix-dominated composite properties. For instance, The effect of carbon nanotubes (CNTs) on the damage initiation and development in a woven carbon/epoxy composite modified with 0.25 wt. % of CNTs was investigated by De Greef et al [49]. The tensile tests in the fiber direction showed a slight improvement of the strength and strain-to-failure by 3.1% and 4.6%, respectively. De Greef et al [50], also reported elsewhere that the presence of CNTs in the matrix of a woven carbon fiber/epoxy composite at 0.25 wt.% improved the composite stiffness and strain-to-failure in the bias direction by about 10% and 15%, respectively.

Several results have been presented on fiber reinforced epoxy nanocomposite, where improvement such as; increase in the flexural, compressive, shear and transverse tensile strength of matrix-dominated properties were reported [51-55]. Hybridising composite systems using glass fibers and carbon fibers have also been proposed [56, 57]. Improvement performances in hybrid composite have been achieved at the incorporation of the different properties of reinforcements. Liao et al [58], has equally reported that both fatigue performance and environmental resistance of such carbon-glass hybrid composite is enhanced when compared to all glass-fiber composites.

Manufacturing process of hybrid structures has provided applicable usage of these materials to various industries such as aeronautics, automotive industries and components for the electronic industry [59]. Considerable efforts are being focused on the applications of Hybrid composites for better

understanding of the phenomena associated to the cutting edge technology. The hybridisation of composite materials to produce hybrid composite and nanocomposite structure will therefore result in the improvement of mechanical properties, when stronger lightweight and stiffer structure are achieved.

1.7 FATIGUE OF HYBRID NANOCOMPOSITE MATERIALS

The fatigue life of hybrid composite structures is of great importance. The cross-linked microstructure of epoxy matrix reinforced by fibers have resulted in many useful properties such as a high modulus, high failure strength, low creep, etc [60]. It has also led to desirable property whereby the materials offer better resistance to environmental factors and fatigue, as well as the advantages of high stiffness-to-weight and strength-to-weight ratios when compared to conventional materials. Improvements in fatigue life of composites are expected from the introduction of nanoparticles in the epoxy, due to dynamic issue arising in engineering components. That is why composite materials have been hybridising with various types of nanoparticles, fibrous and layered nano-fillers for maximum fatigue improvement [61-67]. There have also been reports on fatigue behaviour and improvement of these hybrid nanocomposite [68, 69].

The interphase of composite material is made up of the mechanism of stress-transfer from the matrix to the reinforcement and the process are always influenced by the chemical functionalization of nano-fillers [70]. Fiber-matrix interphase region has a controlling effect on the fatigue of composite. The formation of covalent bonds and interactions between the nano-fillers and the polymeric matrix could lead to a strengthened interface [71]. The benefits of a nanoparticle modification of MWCNTs and fumed silica on the static and dynamic mechanical properties of GFRPs have been investigated by Böger et al [72]. The result reveals that hybridisation of the nanoparticles led to increase in inter-fibre fracture strength up to 16% and the high cycle fatigue life is increased by several orders of magnitude in number of load cycles. A research conducted by Manjunatha et al on fatigue behaviour of a hybrid

GFRP composite containing both micron-rubber and nanosilica particles has equally showed that the fatigue life of GFRP composite was enhanced dramatically by about eight to ten times [73].

Hybrid technique has been revealed as a variable approach to enhanced long-term durable composite materials, out of which the incorporation of nanoclay into an epoxy matrix has been reported to show improvement in the fatigue behaviour of FRC structures. Fatigue life, and related fatigue-fracture crack growth rate, are material properties associated with more long-term or progressive failure processes, and this describe the ability of a material to survive in service over long periods [74]. However, detailed studies on the fatigue behaviour of particle toughened nanocomposites are limited [75]. Hence, the need for further research study on fatigue behaviour hybrid nanocomposite materials is required.

1.8 STUDY OBJECTIVES

The aim of this study is to improve the fatigue strength of GFRC materials enhanced with nanoclay. The specific objective of the study is to determine the percentage weight ratio of nanoclay that will be required to improve the properties of the GFRC material. Attention will be paid to the structure-properties relationship of the high-performance nanoclay in the resin-matrix of the GFRC material, by considering the general state of stress and its physical behaviour during cyclic loading. The effect of the nanoclay on fatigue crack growth rate and fatigue life of the hybrid nanoclay/GFRC in term of stress over the number of cycles to failure will be address.

1.9 SCOPE OF THE STUDY

This research is based on experimental work. For an understanding of the polymer structure, the toughening mechanisms and the failure that is associated with the hybrid nanoclay/GFRC; this experimental work will focus on the follow areas:

(a) Characterisation of epoxy clay nanocomposite (ECN) and its GFRC laminate.

(b) Bulk cure study of the hybrid nanoclay GFRC laminate through dynamic mechanical analysis reheat method (DMA-RM)
(c) Evaluation of the damage behaviour of clay toughened glass fiber reinforced composite (GFRC) laminates subjected to quasi-static loading.
(d) Evaluation of fatigue crack growth behaviour of hybrid nanoclay/GFRC material subjected to cyclic loading.
(e) Study of the residual strength on fatigue induced hybrid nanoclay/GFRC laminates through dynamic mechanical analysis (DMA)
(f) Detailed microscopic analysis of the polymer epoxy nanocomposite and fractured surfaces of the hybrid nanoclay/GFRC optical scanning microscope (OSM) and scanning electron microscopy (SEM)

1.10 SIGNIFICANCE OF THE STUDY

Going by the current use of composites and the adoption of hybrid composite materials, results from this study would help in the development of a more reliable composite with an improved structural efficiency. The fatigue life of composite material was reported to be affected by matrix properties which influenced fibre failure and leading to final composite rupture [63, 64]. The approach proposed by Njuguna [40], which suggested the modification of the matrix was adopted. The toughening of the fiber composite material with nanoparticle is to supress matrix cracking which can lead to quick fracture of the material. The structure-properties relationship of the high-performance hybrid nanocomposite materials will be improved. The general state of stress on the physical and mechanical behaviour during quasi-static and fatigue will be established. The residual strength of the fatigued composite material will be effective for longer duration of use. The nanocomposite structure is expected to continue carrying load irrespective of the structural change, until the material or structure could be replaced. The development of the hybrid nanoclay/GFRC material should therefore be adopted for used in the

manufacturing of lightweight aerodynamic structure in performance that requires high strength, environmental friendly and longer fatigue life.

1.11 THESIS OVERVIEW

Chapter 1: Introduction

This chapter gives a general background of this study, introducing current uses and advantages of composite materials, identification of research problems and an approach to improve the mechanical and fatigue properties. The chapter also outline the hybridisation of the composite material and providing a brief review of hybrid composite materials and the fatigue study of hybrid composite materials. Finally, the chapter outlines the study objectives, the scope of the study, the significant of the study and the structure of the study.

Chapter 2: Literature Review

This chapter provides a comprehensive review of the composite materials and coordinate with respect to the fatigue damage behaviour of FRC structure. Matrix cracking and propagation as well as delamination are discussed in this chapter. Matrix modification approach and toughening effect of nanoparticles for strength enhancement and maximum fatigue life was given detail description.

Chapter 3: Materials, Manufacturing and Testing

This chapter begins with the research design, materials and states the methods used in the development and manufacturing of hybrid nanoclay/GFRC laminates. The chapter describes the modification of epoxy with clay to form epoxy-clay nanocomposite (ECN) and the fabrication of varying clay percentage weight of Hybrid nanoclay/GFRC laminates. The viscosity and flow analysis during vacuum assisted resin infusion method (VARIM), characterisation and thermal analysis of the nanocomposite materials, mechanical and fatigue testing of the neat GFRC and hybrid nanoclay/GFRC laminate were all described in this chapter. Finally, an approach to study the residual strength of the hybrid nanoclay/GFRC laminates was described.

Chapter 4: Morphology, Mechanical and Fatigue Properties of Hybrid Nanoclay/GFRC Laminates

This chapter present internal structure of the ECN material was determined relative to clay dispersion. The performance of the hybrid nanoclay/GFRC material at increasing temperature through thermal analysis was compared with the neat GFRC. Bulk cure properties of the hybrid nanoclay/GFRC laminates was analysed in terms of dynamic mechanical analysis reheat method (DMA-RM) The chapter also present the result of the quasi-static mechanical properties and the fatigue properties of the neat GFRC and hybrid nanoclay/GFRC laminates. Finally, the chapter presents the residual strength of the hybrid nanoclay/GFRC laminates after fatigue. This was investigated by dynamic mechanical analysis (DMA) and result was compared to that of the neat GFRC fatigued laminate.

Chapter 5: Conclusions and Recommendations

This chapter draws out a general conclusion based on the results of the previous chapters. It also provides suggestions in areas that require further investigation and recommendation for future research.

CHAPTER 2

LITERATURE REVIEW

2.1 INTRODUCTION

The need to produce tougher and durable FRC materials to meet their increasing demand for aerodynamic applications has been introduced in the previous chapter. Near to this expectation, research effort in the enhancement of FRC materials' strength and their fatigue life through matrix cracking suppression, propagation and interfacial debonding have become increasingly important. Matrix cracking has been long recognised as the primary defect in composite structures, because of the brittle nature of the thermoset matrix in the fiber-matrix layered configuration. This has led to rapid deterioration of mechanical properties of FRC materials, with which catastrophic failure of composite structure can occur, if matrix cracking is not suppressed.

In this chapter, a concise overview of damage behaviour in composite is given. Various ways by which improvement in composite materials have been achieved over the years are discussed. These attempts involve the improvement of the material property through modification of the matrix and fiber architecture. In the research work, matrix toughening approach through addition of nanoclay has been the focus of the study. The effectiveness of this approach, by which dispersion of the nanoclay/nanoparticles for strength enhancement has led to maximum fatigue life was reviewed.

2.2 INTERPHASE REGION AND DAMAGE BEHAVIOUR OF COMPOSITE

The constituents of FRC are not only dependent on the properties of the composite, but the interfacial bond between the fiber and the matrix also constitute to governing the final performance. The interphase region of composite material is the intermediate boundary governed by the morphology and chemical composition different from either the bulk matrix or the fiber [76]. This interphase region controls fiber-matrix intermediate load transfer

depending on the level of the fiber-matrix interfacial adhesion. The efficiency is determined by the thickness and strength of the interphase region formation, since better bonding is often demanded for composite materials under loading [77]. That means the strength of composite material will increase at the extent of strong interfacial bonding when a functional interlayer is deposited between the fiber and the matrix. Therefore, improvement between the fiber and matrix can be as a result of compatibility between both materials.

Cech et al [78], distinguished fiber and matrix interface surfaces from the interphase region of composite materials. Using the schematic illustration shown in Figure 2.1, by distinguishing two interfaces in the interphase region; one of the interfaces at the fiber surface is relatively sharp, while the other interface at the matrix is a diffused one. However, modifying the fiber surface by a coating (interlayer), a third inner interface occurred between the fiber interlayer and the modified matrix.

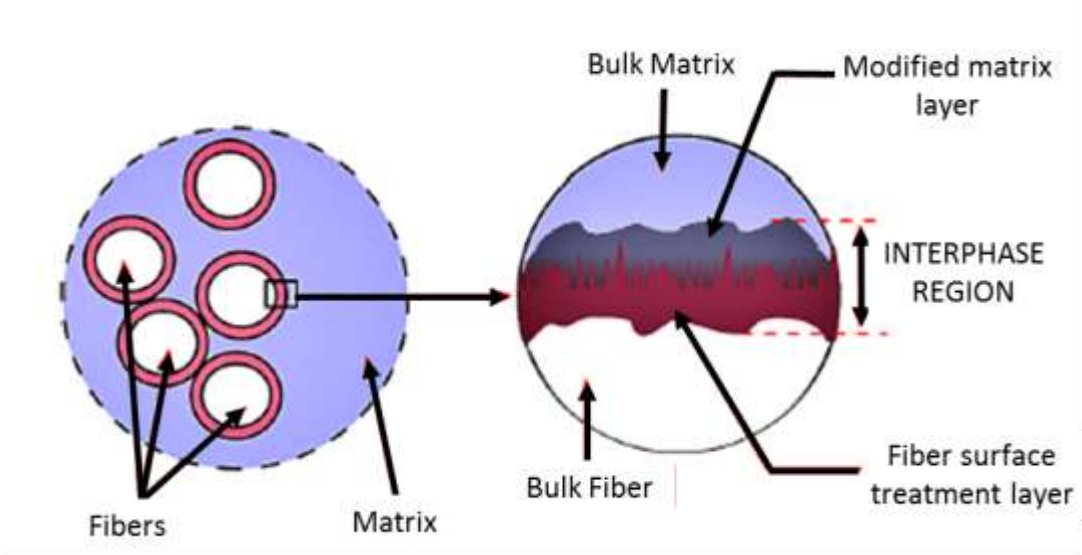

Figure 2.1: Schematic illustration of composite interphase formation between the fiber and the matrix. (Modified) [78]

Interfaces of fiber/matrix in composite materials are formed during the manufacturing process and this determines the performance of the composite materials [79]. The mechanical behaviour of FRC structures leading to their

damages, depend on how much load the matrix can transmit to the fiber, the interfacial bond between the fiber and matrix, and the properties of the fiber itself. The interfacial bond between the fiber and the matrix is an important factor influencing the mechanical properties and performance of FRC [80]. The interface is responsible for transmitting the load from the matrix to the fibers, which contributes greater portion of the composite strength. It is important that the interfacial bond between the fiber and matrix is high because the fiber is stronger material. The complex behaviour of the FRC materials and their properties usually depend on their arrangement and the volume fraction, which can affect the interface between the components [81]. These properties cause a variety of failure mechanisms associated with FRC materials which are more complex under multi-axial loading conditions.

The damage behaviour of composite material is a complex multi-stage process which gets triggered in certain modes; when the damage propagations, final failure modes may be significantly different. When composite is about to fail, the damage processes are observed; it is only when the damages have propagated beyond certain extent that change in composite behaviour and appearance are observed. Under mechanical loadings, depending on the type and direction of the applied load, different damage mechanisms manifest simultaneously. Matrix cracking, fiber-matrix debonding, interlaminar matrix cracking, delamination, fiber separation or fiber fracture and buckling (in compression) may be observed separately or jointly in the damage zone, and may result in component failure [82]. There are cases where very small deformation in composite may constitute failure, whereas in others, only total fracture constitutes failure. According to Okoli and Smith [83], the internal material failure of composite materials generally initiates long before any change in its macroscopic appearance or before any behaviour is observed. Since composite strength is affected by the fiber/matrix condition, the mode of propagation is controlled by the bonding condition. This was confirmed by Baron et al [39], that fiber failure in FRC, which finalises composite failure, is strongly depended on bonding matrix properties. Continual usage of FRC has therefore prompted the need to

ascertain fiber/matrix properties that is necessary to provide essential mechanical properties.

2.3 MATRIX CRACKING IN FRC COMPOSITE LAMINATES

Matrix cracking is usually the initial damage mode in composite structural system. In fiber reinforce composite material, matrix cracking aggravate into multiple of damage modes, such as fiber breaking, interfacial debonding, interlaminar cracking and delamination of the composite laminate. The fracture toughness of a material could be related to the amount of energy required to create a fracture surfaces or break the material. Moreover, in brittle materials such as glass, the energy required for fracture the material is simply the surface energy of the material [84]. In FRC, the matrix absorbs energy in cracking and tearing while the high strength fibers break by brittle cleavage [85]. These contribute to the FRC toughness as a result of debonding between matrix and fibers; and also to the cracks deflection due to tilting or twisting movement around the fiber. The problem of matrix cracking in FRC is that it reduces the stiffness of a structure when occurred, leading to failure during service [86]. Matrix cracking may arise in the form of intralaminar cracks. This is related to the transverse matrix cracking in off-axis plies and interlaminar cracking in between adjacent plies of a laminate. The interlaminar performances of the composite are however characterized by weakness under both tensile and shear stresses. They affect the structural performances of composite laminate, causing debonding and delamination. Such interlaminar stresses become significant and affect the overall performance where geometrical and material discontinuities exist [86].

The complexity of matrix cracking and corresponding degradation of FRC material properties, emphasize the need for enhancement of the material. Numerous works have been carried out to understand the matrix cracking initiation, propagation and its effect on mechanical properties of the laminate [87-90]. Out of which cracking and crack spacing measurements has been one of the primary factors that was considered [89]. While another researcher reported on stiffness reduction in a symmetric cross-ply laminate within the

transverse cracks of the 90° plies [90]. Garrett and Bailey [89] have equally studied transverse cracking in cross-ply laminates. It was observed that matrix cracking occur at a much lower strain than the ultimate resin failure strain. They concluded that spacing between transverse cracks decreased with increasing stress.

In cyclic loading conditions, FRC exhibit gradual degradation of the mechanical and structural performance as a result of damage accumulation. However, the performance in service of composites, involving a combination of fiber and matrix is affected by multi-mechanism of failure under loading throughout the material [91]. For instance, a wide spectrum of failure phenomena under cyclic conditions can be demonstrated by fiber reinforced cross-ply laminates; with the initiation of matrix cracking, interfacial debonding and delamination at relatively early stages of loading. The mutual effect of matrix cracking and delamination can result in significant deterioration of residual stiffness and load-bearing capacity of composite components. This damage evolution is always as a result of the elastic properties in the constituent of the composite, because the regions of stiffness are always attracted by cracks between the bonded solids.

2.4 DELAMINATION IN FRC STRUCTURES

Fiber matrix debonding, as also known as delamination, is a damage that significantly reduces the stiffness and strength of FRC materials. In polymer matrix laminated composites, delamination occurs as a result of debonding between the plies of the glass fibers [92], This is because bonding of the fibers is provided by epoxy resin which is a weaker component. In the manufacturing of composite laminate, depending on the thickness of the laminate, delamination may be introduced due to improper processes and curing; or through machining operations (trimming excess material around the component margin) [93].

Three types of delamination was highlighted by Bolotin [94]. Their modes were analysed depending on their position in the composite structure. The first type depicts internal delamination situated within the fiber layers of the

material as shown in Figure 2.2a. This type of delamination is normally caused by edge delamination in thick structures. The second type is a near-surface delamination, which can be seen in Figure 2.2b. It is a special kind that can be caused by surface buckling. It is typical for component under compression, surface heating and sometimes under tension, to produce this type of delamination due to fiber mismatch effect. The third type of delamination is the one found in composite under fatigue test, with multiple cracks and separation of fiber layers in composite laminates. As shown in Figure 2.2c, this type of delamination significantly affects the load bearing capacity of the composite material because it is often generated under low stress loading.

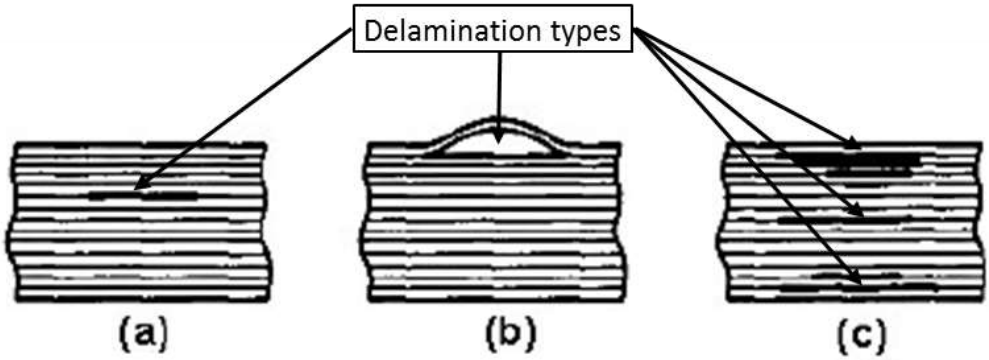

Figure 2.2: Schematic diagram of delamination types in composite structure (a) internal delamination (b) Near surface delamination and (c) Multiple delamination (modified) [94]

Debonding of fiber from matrix in composite materials often cause structural discontinuities. These may occur as a result of interlaminar cracking identified under three basic fracture modes; these include, Mode I (tensile), Mode II (sliding shear), and Mode III (tearing shear). The advantages and limitations of each fracture mode reviewed by Davies et al [95], reveals that each fracture mode gives very similar results for $[0^o]n$ unidirectional laminates. Delamination generally occurs between layers of different orientation, and this is far more complicated for multidirectional laminates that are used in the majority of applications. In the case of woven plies, Hochard [96] mentioned that composite laminates show better resistance to delamination than

unidirectional ply, and they are less sensitive to transverse rupture. However, the rupture of a plies in the fiber direction generally have catastrophic effects on the laminate and the structure itself.

Zhuang and Wightman [97] established that a strong fiber-matrix interface ensures effective stress transfer through the interphase and improves off-axis strength; while a weak interface improves impact strength and fracture toughness of the composite by resisting cracks that would propagate through the matrix. Silberschmidt [98], also mentioned that the place of the matrix crack's arrest at the interface between fiber layers in laminates is characterised by considerable stress concentration and often serves as a nucleus for initiation of delamination along the interface. Although, specimens of the same material loaded identically might demonstrate sufficiently different distributions of matrix cracks and delamination zones; yet, the processes of matrix cracking and delamination depend on both composite structure and loading history.

In a situation where a component is accidentally impacted, such as dropping tools on the laminate, delamination can occur. Due to non-homogeneous and anisotropic characteristics of this material, the failure process often involves very complex mechanisms with a number of failure modes [99], such as shown in Figure 2.3. When the stress within the interphase of the adhesion level between the fiber and matrix exceeds the local strength, fiber matrix debonding occurs and also causing delamination within the plies of the fiber layers. The stress concentration during fiber-matrix debonding affects the overall composite, leading to fibre fracture and/or fiber pull-out. This occurs when the fracture fibers are pulled out of the surrounding matrix, as the crack front continues to advance.

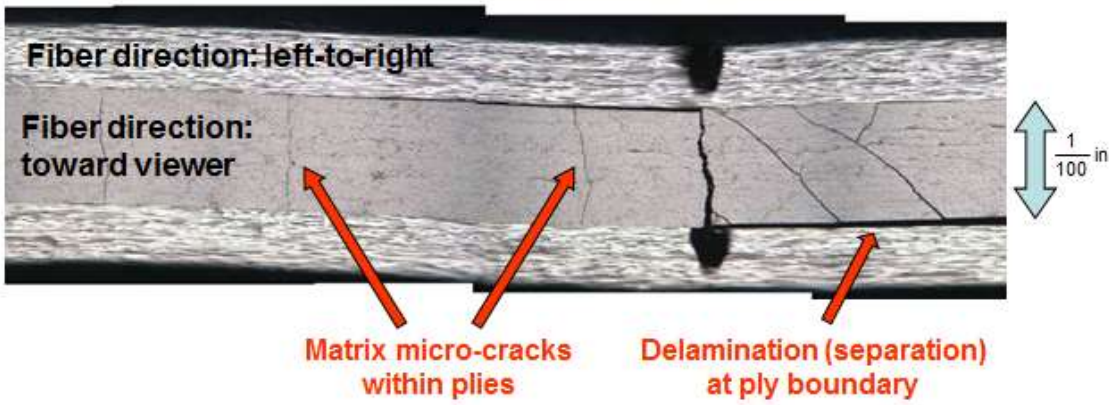

Figure 2.3: Matrix cracking and Delamination in composite laminate structure [99]

The role of delamination in the fracture of composites has been reported in several numbers of papers [100-104]; Interlaminar fracture properties within different fiber reinforced composites are one of the conditions highly observed. The delamination due to interlaminar stresses is strongly dependent on the fiber-matrix interfacial effect due to matrix failure [105]. This interlaminar stress is associated with the specimen geometry and loading parameters. This is because the interlaminar strength is being governed by the brittle matrix and fiber-matrix interface bonding strength, which makes it the weak point in the composite structure. It is therefore important for the matrix to have high tensile strain to failure for good tensile properties and high shear modulus for good compressive properties, because the matrix is responsible for transferring load between the fibers [106].

Delamination also occurs during in-service operation as a result of impact by runway debris, hailstones, bird-strike, or ballistics [107]. This delamination may be barely visible damage, but it can significantly reduce stiffness and strength in the structure, leading to catastrophic failure. For example, the interface layers of an airplane can be subjected to shear stresses causing delamination as a result of erosion by rain impact. Modern composites such as Kevlar can be protected against knives and bullets, but high-speed rain impact can destroy these materials in minutes [108]. At today's flight speeds, the high-velocity water droplet impact can generate pressures of many

damages on the nose of an airplane as shown in Figure 2.4a. This pressure causes stress, which create cracks in brittle materials and deformation of more ductile materials. The outflow of the droplets then picks up on this damage and erodes the material.

Impact damage on aircraft structures depends on the nature of the composite part, its composition, and density. On aircraft composite laminate structures, defects created by impact are mainly delamination between different plies of the fuselage and wing blade skin. Rain impact alone can cause debond between the skin and the stiffeners. Such debond will eventually destroy the integrity of the structures. A wind turbine blade displayed in Figure 2.4b is an example of such impact damage after a thunder's strike. For structural applications in aerodynamics and automobile, the rate of delamination during impact damage of composite laminate are normally measured by the energy absorbed during ballistic impact behaviour of the composite [109-113].

Figure 2.4: Rain droplet; (a) Impact damage to the nose of an airplane [108], (b) Impact damage resulting to debonding between the skins of a wind turbine blade after thunder strike [114].

2.5 DYNAMICS OF FRC STRUCTURES

Dynamic testing of FRC materials is concentrated on cyclic loading of laminates made from different fabrics and matrices. The effect of matrix on the fatigue strength of a composite was described by Broutman and Sahu

[115], to have the best properties for high cycle in low stress fatigue. Material damages from cyclic loading are typically more severe than from static loading. A material that initially survives an applied static stress may catastrophically fail when the same stress is repeatedly applied. Furthermore, a material may fail from cyclic loading in much less time, than from steady loading [116]. From much of the research covered, work done by Mandell et al [117] has shown that the matrix has little effect on the fatigue sensitivity of fiber dominated glass reinforced polymer.

In composite matrix material, crack initiation occurs within the matrix; this is common in the interface between fiber and matrix, and is commonly called interfacial debonding. Fatigue damage and failure of a polymeric material may occur from the initiation and propagation of a single crack [118], or may develop from a complex array of multiple cracks [119, 120]. These initial cracks form and meet axial plies and eventually begin to cause damages in these main load bearing plies. The amount of stress necessary to cause localized cracking is enough to cause cracks spaced far apart in a ply. However, damage comes in the form of broken fibers and delamination. At such a point, the amount of damage in the laminate tends to level off for a period of time. The type of damage which develops depends on the type of material and the test method.

Mandell et al [120] compared slope of maximum stress versus number of cycles (*S-N*) curve and corresponding single cycle strength for different materials strength, fiber orientations, fiber distribution, fiber length and fiber content. The fatigue resistance seems to be insensitive to the listed factors. Basically, all types of glass fiber dominated composites, with the exception of woven fabric composites, tend to lose about ten percentage of their initial strength per decade of cycles. This corresponds to a slope of negative one tenth on a normalized *S-N* curve for most E-glass reinforced composites [120]. By performing a single strand fatigue tests, both with and without matrix material, the *S-N* curve were similar. The crack behaviour of the matrix could not allow the material to achieve a required strength. It was therefore

concluded that the fatigue behaviour is derived primarily from the reinforcement in the material. The stress level to the fatigue life of polymeric materials was correlated by Paris power law relationship [121].

$$S/S_o = 1 - b\ log\ N \tag{2.1}$$

or $$S/S_o = C^* N^{-1/m} \tag{2.2}$$

Where; S is the applied maximum stress, S_o is the UTS, b and C are constants, N is the number of cycles to failure, and m is a power law exponent. If C is equal to 1.0; then the *S-N* curve will pass through the static UTS at one cycle. Typical m values for thermoset materials lie in the range of 11 to 14 [121]. The Paris power law relates the fatigue crack growth prediction generated using fracture mechanics for each cycle (da/dN) to the stress intensity change at the crack tip (ΔK_1):

$$da/dN = A^* (\Delta K_1)^m \tag{2.3}$$

By relating this stress intensity factor to the applied stress (σ) through fracture mechanics, and performing the complex integration from crack initiation to failure, a power law relationship between cycles and stress develops.

$$N\ \alpha\ S^{-m} \tag{2.4}$$

Therefore, the uses of a power law *S-N* trend for fatigue lifetimes dominated by matrix crack growth are both supported by the observations and the theoretical calculations. If specimen lifetime is determined by fatigue crack growth, then the exponent (m) should be the same value in Equations 2.2 and 2.4.

One interesting characteristic of composite materials is the ability to withstand a large amount of damage without a significant loss of strength. In a case where the material temperature increases during service, the increase in temperature can typically lead to quick cyclic fatigue damage [119]. At this point, deformation zone is being formed and energy is set to be released in form of heat. A thermal softening failure may occur if the loading frequency is

too high, by causing heat transfer condition to exceed its glass transition temperature (T_g), which is distinct from the mechanical failure that usually occur under service condition at lower stresses. This condition does not actually represent fatigue resistance. Therefore, to provide accurate fatigue data, test reports should contain maximum stress, strain, and stress ratio (R) values; as well as the loading frequency and waveform, the ambient and internal temperatures, environmental effects, specimen geometry, and crack initiation and propagation times [116].

Fatigue damage within fiber reinforced composites typically initiates at the fiber-matrix interface [121]. The basic load distribution between fiber and matrix results in high interfacial stress, particularly under transverse loading. Once a crack is initiated, interface damage will steadily propagate through further cycling, and typically advances in a direction parallel to the fibers. Therefore, poor fiber-matrix bonding may result in increased crack growth rates, whereas strong interfacial bond strength will increase fatigue crack propagation resistance [121].

2.6 MATRIX TOUGHENING EFFECT

The first form of damage in laminates is usually matrix microcracks [122]; which could be in the form of intralaminar or ply cracks that extend across the laminate thickness and run parallel to the fibers in the ply. Microcracks mostly occur during tensile loading, fatigue loading, changes in temperature, and during thermo-cycling [123]. The effect of microcracks in composite structure initiate excessive matrix cracking, leading to damages; including delamination, fiber breakage and provides pathways for entry of corrosive liquids. Matrix cracking can therefore be considered in a three step process which include; crack initiation, crack growth and localization of different failure modes [87]. This leads to damage growth in the composite, which is associated with stress-strain nonlinearities in the material response, resulting from redistribution of the stress field after matrix microcracking. For composites subjected to quasi-static or cyclic tensile load, matrix

microcracking is often the first defect to occur, which generally triggers the other failure modes.

Matrix materials are known to be widely employed in the manufacturing of aerospace and automotive components. These matrix materials, which are in form of thermosetting epoxy-resin, have been one of the topics most extensively studied because of the brittle nature of the epoxies and their widespread applications for engineering components. Since matrix cracking is an important problem in composites, researchers have proposed toughening of the epoxy by incorporation nanoparticles in composite materials to improve the fracture toughness, stiffness, and strength of epoxy resin [52, 60, 66, 124-126]. Toughening of epoxy has therefore gained a great deal of attention. Hussain et al [127] found that in polymeric nanocomposites; where at least one of the dimensions of the filler material is less than 100 nm, have shown significant improvements in mechanical properties. It was further established by Manias and Evangelos [128], that nanoscale dispersion of filler or controlled nanostructures in the composite can introduce new physical properties and novel behaviour that are absent in the unfilled matrices, by effectively changing the nature of the original matrix. That means the properties can change from brittle to tough, preventing crack propagation and improving the fiber-matrix interfacial adhesion. Also, crack arrest can be generated through particles that delates stress phase transformation [129]; preventing crack bridging by the compliant of particles that are well bonded to a stiff matrix.

2.6.1 Structure of epoxy-clay nanocomposite (ECN)

The nature of polymer nanocomposite depends on the processing condition and strength of the interfacial interaction between the polymer and the layered silicates [130, 131]. Depending on the degree of dispersion of clay into the polymer, different morphological structure including; tactoids (phase separated), intercalated and exfoliated nanocomposite conditions may be formed [132]. An example of nanocomposite in Figure 2.5 displayed different distribution of particulate in the matrix.

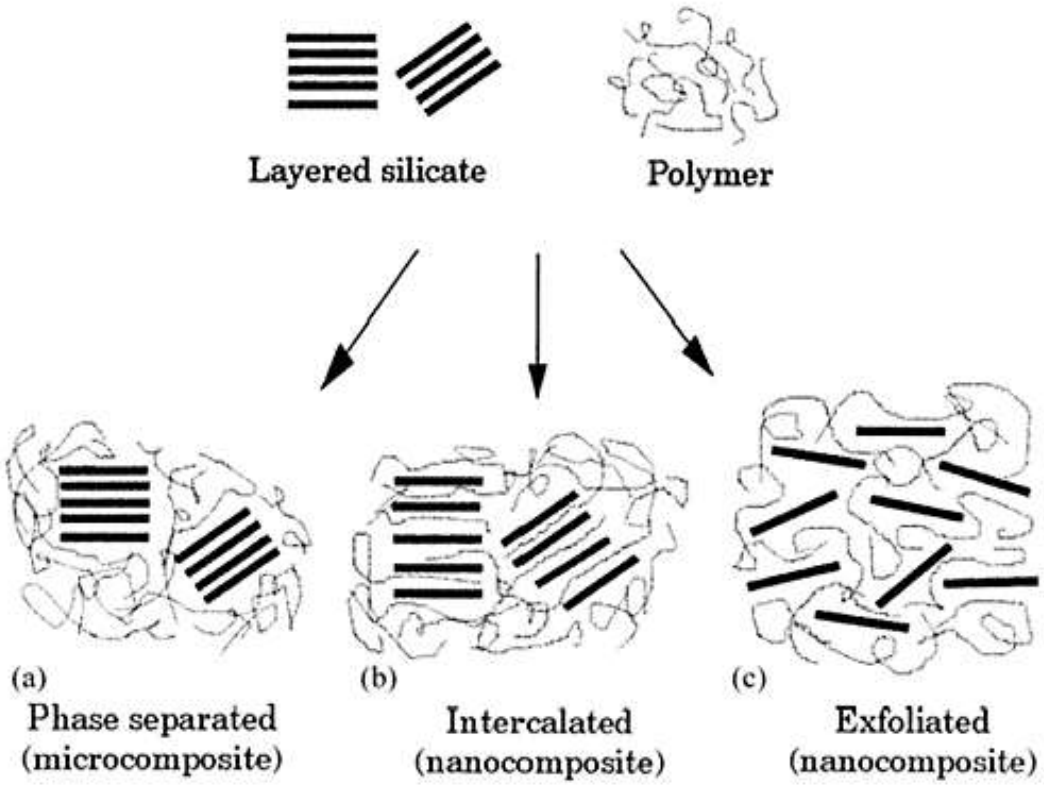

Figure 2.5: Layered silicate and dispersions in composite: (a) phase separated, (b) intercalated and (c) exfoliated [132]

The properties of tactoids (phase separated) polymer/clay composites remain in the range as traditional micro composites**.** The obtained composite structure is considered as “phase separated”, when the polymer is unable to intercalate within the clay layers and the clay is dispersed as aggregates or particles with layers stacked together within the polymer matrix. Meanwhile, when one or more polymer chains are inserted into the inter-layer space and increasing the inter layer spacing, while the periodic array of the clay layer still exist, the intercalated nanocomposite is formed. The presence of polymer chains in the galleries causes to the decreasing of electrostatic forces between the layers but it is not totally dissolved [133]. However, when the insertion of polymer chains into the clay galleries cause the separation of the layers and make the individual layers to disperse within the polymer matrix, exfoliated nanocomposite is obtained. Therefore, due to proper dispersion of individual clay layers, a high aspect ratio is obtained and lower clay content is

needed for exfoliated nanocomposites. Also most significant improvement in polymer properties is obtained due to the large surface interactions between polymer and clay [133]. The separation of the tactoids from the primary particle and the destruction of the order of the clay platelets within the tactoids cause complete exfoliation. In principle, a full exfoliation of the clay platelets will maximise the strength, modulus and toughness improvement in polymer nanocomposite [134, 135]. However a balance between an exfoliated and intercalated structure might be preferable to maximise enhancements in the mentioned properties [136]; hence, intercalated tactoids promoting some toughening mechanisms such as crack deflection or crack pinning [137].

To prepare a polymer/clay nanocomposite, it is important to know the degree of intercalation/exfoliation and its effect on the properties of nanocomposite. For this reason, there is need to analyse the micro structure of the prepared nanocomposite. Two common techniques including; X-ray diffraction (XRD) analysis and transmission electron microscopy (TEM) are widely used to characterize the micro structure of nanocomposite as well as pure nanoclay. Figure 2.6 showed the XRD pattern and TEM images of nanoclay and epoxy-clay nanocomposite. The structure of nanoclay dispersion is easily identified by XRD analysis because all the multilayer structure and interlayer spacing are being determined. Comparing the spacing of the nanoclay and the polymer-clay nanocomposite; unlike the nanoclay, the intercalation of the polymer chain leads to having a shift of the diffraction peak towards lower angle value. The peak is indicative of the platelet separation or *d*-spacing in clay structure as established by Bragg's law [138].

Using the peak width at half maximum height and peak position (2θ) in the XRD spectra the inter layer space can be calculated using equation (2.5).

$$Sin\ \theta\ = \frac{n\lambda}{2d} \tag{2.5}$$

Where λ is the wave length of X-ray radiation used in the diffraction experiments; d is the space between layers in the clay lattice and θ, is measured diffraction angle. Any change in the inter-layer or *d*-spacing of a clay lattice by organic modification or polymer intercalation causes a change in the position, broadness and intensity of the characteristic peak in XRD spectra.

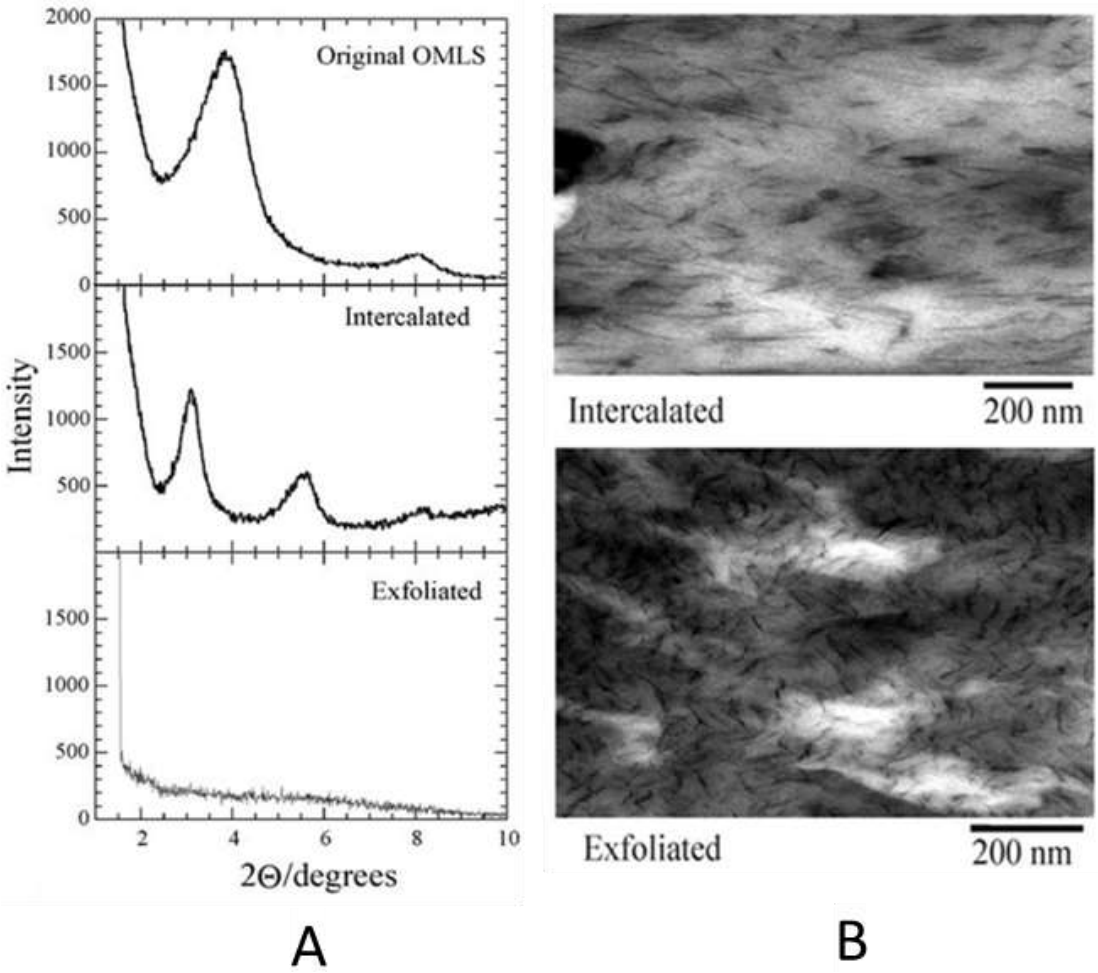

Figure 2.6: Image showing (a) XRD patterns of Organoclay and Organoclay/Polymer Matrix; and (b) TEM images of Intercalation/Exfoliation of nanocomposites dispersion [130]

According to the Bragg law, increasing of d-spacing results in the broadening and shifting of related XRD peak toward lower diffraction angles (2θ); by monitoring the position (2θ), shape and intensity of the characteristic peak for

organoclay in nanocomposite structure it is possible to determine the degree of intercalation/exfoliation.

TEM on the other hand, allows a qualitative understanding of the internal structure. The polymer-clay nanocomposite morphology gives a direct measure of the spatial distribution of the nanoclay layers, and the views of the defect structure through direct visualization [130]. Hence, TEM is mostly used to confirm the result obtained by XRD regarding the face separation of clay in the nanocomposite.

2.6.2 Progress in epoxy-clay nanocomposite

Nanoclay reinforced polymer composites have been widely studied and some researchers already considered nanoclay as supreme reinforcement for improving matrix properties, leading to enhancement of fracture toughness of polymers. Since the first discovery of the reinforcing effect of nanoclay on the mechanical properties of polymeric material by Toyota researchers [139], many other researchers have focused on its applications. Epoxy-clay nanocomposite has become a class of material where the inclusion of clay in epoxy matrices has enhanced the mechanical properties of the matrix. The filler has also caused increase in chemical resistance, barrier properties, and dimensional stability [140].

Wang et al [141]; exfoliated layered silicate magadiite with layer thickness of 1.12 nm in a Shell Epon 828 elastomeric epoxy matrix for the formation of polymer-inorganic nanolayer composite and was immersed in propanol for 50 days. Pinnavaia et al. reported that after 50 days immersion in propanol, that pristine polymer absorbs 2.5 times more than the nanocomposite. They further established that the pristine sample began to crack and break up, whereas the shape and texture of the nanocomposite sample appeared unchanged.

Rana et al. [142] studied moisture diffusion through neat vinyl-ester resin containing nanoclay by performing transient and steady-state diffusion experiments. They illustrated that, montmorillonite (MMT) clay was effective

in reducing the diffusion coefficient of water through the vinyl-ester resin. Rana [143] went on to report that ‘‘the solubility of water in the nanocomposites appeared to increase with the amount of clay, as reflected in the equilibrium moisture content. This was due to water adsorption onto the clay. It was assumed that, the clay act as a moisture scavenger by trapping water and prevented it from reaching any further. The presence of these clay particles still hinders diffusion of water through the sample, thus protecting the structural interfaces.

Sarathi et al. [144] carried out thermo-gravimetric differential thermal analysis (TG-DTA) studies on thermal behaviour of the epoxy nanocomposites; heat deflection temperature of the material was measured to understand the stability of the material for intermittent temperature variation. The dynamic mechanical analysis (DMA) results indicated that storage modulus of the material increases with small amount of clay in epoxy resin.

Quaresimin et al. [145] investigated Mode I fracture toughness and crack propagation resistance for neat and clay-modified epoxy. It was observed from the experimental result that the fracture toughness exhibited a peak value for 1wt% clay-modified epoxy; about a 40% higher than neat resin. Likewise, Mode I fatigue test on clay-modified epoxy Compact tension (CT) Specimen, with a threshold value about 35% higher than that of the neat resin, showed that clay-modified epoxy CT loading equally resulted in an improved crack propagation resistance.

The toughening effect of carbon black and nanoclay on the modified bisphenol-A type epoxy resin was investigated at the room and cryogenic temperatures by Kim et al. [125]. They reported that carbon black (CB) of 3.0 wt. % increased the K_{IC} value by 23% on the average at room temperature, due to the toughening mechanisms of nano-scale crack branching and pinning effects. At the same room temperature, nanoclay of only 0.5 wt. % also increase the K_{IC} value by 20%, while the nanoclay of 3.0 wt. % increased the K_{IC} value by 50% on the average, which was due to the tearing effect by the flake shape of nanoclay. However, at the cryogenic temperature, the

fracture toughness of the epoxy was 2.3 times higher than that at the room temperature. The nano-particles in the epoxy resin decreased the fracture toughness of the composite.

Tensile behaviour of nanocomposites was investigated by Yasmin et al. [146]; the stress–strain behaviour under tensile loading of nanocomposites reinforced with both Nanomer I.28E and Cloisite 30B nanoparticles at room temperature showed that as clay content increases, the strain to failure decreases. However, it is found that the elastic modulus of the nanocomposites increases monotonically with increasing clay content. Both Nanomer I.28E/ and Cloisite 30B/epoxy nanocomposites show similar values up to 2 wt. % clay content. However, at higher clay contents, the Cloisite 30B/ epoxy shows a faster increase in modulus than the Nanomer I.28E/epoxy nanocomposite.

Jumahata et al. [147]; studied the effect of montmorillonite clay on the compressive properties of Epikote 828 epoxy; the evaluation of the performance of the nanocomposites via static uniaxial compression tests indicated that nanocomposites offer higher compressive stiffness when compared to the neat polymer. However, the presence of clusters of intercalated nanomer I.28 and nanovoids reduced the compressive strength of the epoxy system. It was believed that the compressive properties were based on the degree of exfoliation of the clay nano-platelets in the epoxy as revealed by the Transmission Electron Microscopy (TEM) micrographs.

Based on the investigation and application of nanoclay by these researchers, it has been reported that the properties of a composite structures were improved when nanoclay was used as reinforcement in epoxy matrix. However, extensive study on the epoxy-clay nanocomposite is important since it can affect the structural characteristics of a composite structure when used to reinforce matrix of composite laminates.

2.7 MECHANICAL PROPERTIES OF HYBRID NANOCOMPOSITE MATERIALS

The term hybrid has been used to describe the phenomenon of improvement in the properties of a composite containing two or more types of reinforcements [148]. The selection of the components that make up the hybrid composite is determined by the purpose of hybridization and requirements imposed on the material or the designed. The successful use of hybrid composites is determined by the chemical, mechanical and physical stability of the fiber/matrix system. However, different types of materials have been combined to achieve a hybrid composites structures, these comprises of; hybrid resin polymer system, hybrid nanoparticles composite, hybrid fiber/fiber composite, hybrid fiber-reinforced (FR) nanocomposite and so on.

FRC materials are known to re-distribute stresses around local sites of strain concentration through a combination of damage mechanisms, including: fiber failure and pull-out, matrix cracking, interface debonding, and shear band development [149-152]. The structure of the fiber/matrix interface generally affects the overall mechanical properties of all types of composites, by which the durability of the material, such as strength and fracture toughness, are strongly dependent upon the interfacial properties [153, 154]. This is because a strong bond between fiber and matrix facilitates efficient load transfer between the constituents, while a weak interface promotes composite toughness by deflecting cracks into the fiber/matrix interface. Nanocomposites containing organoclay has therefore been employed as the matrix material to produce hybrid nanoparticle/fiber reinforced polymer composites that possess improved mechanical and fracture properties [53, 155]. The incorporation of nanoparticle has led to wide spread of the hybridized composite, and it is believed that the degradation of matrix material and the weakening of fiber–matrix interfacial bonding will be reduced.

Tensile and compressive properties of Glass fiber reinforced plastic with hybrid modified epoxy matrix (GFRC-hybrid) containing 9wt.% of rubber

microparticles and 10wt.% of silica nanoparticles was studied by [4]. When compared to neat GFRP, the compressive properties of the composite were observed to be almost unaffected by the addition of the rubber and silica particles to the epoxy matrix. However, the tensile strength increases by about 6% with the addition of the hybrid nanoparticles [4].

The combination of different fibers such as Glass, Kevlar or Spectra, has led to fibers having high stiffness with fibers having high toughness; by which high load-carrying capacity composite with a high strain-to-failure was achieved [156]. The evidence of this was found in the crack growth in hybrid fibrous composites studied by McColl and Morley [157]. It was found that the stability of transverse crack in a very brittle matrix could be increased substantially by inclusion of a second fiber component, designed specially to increase the work of fracture of the matrix.

Bunsell and Harris [158] showed that the strips of GFRP incorporated into CFRP laminates acts as efficient crack stoppers only if the strip width is greater than a limiting value. This could indicate that hybrids in which the different types of fiber were more intimately mixed and not in well-defined planes would not perform as well in terms of fracture resistance. The same authors concluded that the work of fracture by the impact and the flexural elastic modulus of mixed GFRP/CFRP composites are both simple functions of composition, corresponding to a matrix rule, based on the properties of plain GFRP and CFRP [159].

The structure and properties of hybrid polyurea/vinyl ester resins, produced by dispersing water glass (WG) in a mixture of vinyl ester (VE) and polyisocyanate in the presence of a liquid phosphate as emulsifier was examined by Mingkang et al [160]. The properties of the hybrid resins were compared to those of the neat Es and polisilicate filled polyurea (denoted as 3P resin) as determined by dynamic mechanical thermal analysis DTMA), fracture mechanical tests, thermo-gravimetric analysis and flammability measurement. It was established that stiffness and resistance to thermal degradation of the initial 3P resin was strongly improved by hybridization with

VEs. The fracture toughness (*Kc*) proved to be less sensitive to the formulation of hybrid resin.

Jang et al. [161] showed that hybridizing graphite composites with additional toughing strain-to-failure fibers, give better damage resistance of composite structures under impact loading. The result obtained also implies that the stacking sequence is a major factor governing the overall energy absorbing capability of the hybrid structure, and the penetration resistance of hybrid composites appeared to be dictated by the toughness (strength plus ductility) of their constituent fibers.

The mechanical properties of hand lay-up epoxy/glass/nanoclay hybrid composite was studied by Karippal et al [162]; it was reported that mechanical properties such as ultimate tensile strength, Young's modulus, flexural strength, flexural modulus, interlaminar shear strength, and micro-hardness of the hybrid composites increased with an increase in nanoclay addition up to 5 wt. %. However, glass transition temperature increase marginally at 2 wt. % nanoclay loading and the same decrease at a further addition of the filler.

2.8 FATIGUE PROPERTIES OF HYBRID NANOCOMPOSITE MATERIALS

Fatigue damage of the composite is a common complex process that involves many different damage mechanisms, such as matrix cracking, fiber breakage, fiber/matrix debonding and delamination. Fatigue of composite laminate is one of the primary damage mechanisms parallel and perpendicular to an applied load. Fatigue damage growth in the composite depends on many factors; including the direction of applied load, lay-up, ply stacking sequence, relative stiffness of the fiber and matrix, and loading rate [163]. The fatigue life of composite depends on a large number of variables, stress state, mode of cycling and environmental conditions. Since matrix cracking and delamination always occur together, discerning between the two damages cannot be easily feasible.

Number of published reports regarding fatigue behaviour of nanoparticle modified FRCs have increased in the last few years and various studies involving nanoparticle enhancement have shown specific increases in fatigue life enhancement [70, 73, 164, 165]. With the conception that nanoparticle can have an impressive benefit at low concentrations. In an experimental study conducted by Manjunatha et al [166]; it was observed that the addition of 9 wt% rubber micro particles in the epoxy matrix enhance the fatigue life of a glass fiber reinforced plastic (GFRP) composite by about three times. The incorporation of 10 wt% silica nanoparticles in the epoxy matrix of GFRP composite has also proved to have similar effect, by which the fatigue life is enhanced by about three times [167]. Furthermore, fatigue test was conducted on GFRP epoxy matrix containing hybrid 9wt% of rubber microparticles and 10wt% of silica nanoparticles by Manjunatha et al [4]. The fatigue life of the GFRP-hybrid composite was about 4-5 times higher than that of GFRP-neat composite.

Lars Böger et al [72] modify the fatigue properties of glass fibre reinforced epoxy laminates with small amounts (0.3 wt.%) of nanoparticles (fumed silica SiO2 and multi-wall carbon nanotubes (MWCNT). The fatigue life data were fitted by a linear function, revealing high coefficients of determination (R^2 > 0.8) for the majority of the tested composite systems. They give a strong indication that the addition of MWCNT or fumed silica to the epoxy matrix, led to a delay in the initiation of inter-fibre cracks which finally resulted in an increase in fatigue life up to some orders of magnitude.

Fenner and Isaac [168], hybridised carbon nanotube with carbon fiber reinforced polymer composite for enhanced damage tolerance and fatigue life. It was demonstrated that such hybrid composites, with 0.5 wt% carbon nanotube reinforcement, show a modest increase of approximately 20% in static strength but a much larger enhancement of approximately 180% in interlaminar strain energy release rate. The combination of these effects manifests itself as an order of magnitude increase in interlaminar shear

fatigue life. The interlaminar fatigue crack growth rate was also reduced by nearly a factor of 2 due to the presence of nanotubes in the composite matrix.

Withers et al [169] evaluated fatigue life, strength and stiffness of epoxy glass-fiber composite reinforced with organomodified surfaced nanoclay. Result revealed that both tensile strength and modulus of the nanoclay reinforced composite material at 60^0C in air showed an average 11.7% and 10.6% improvement respectively. However, from tension–tension fatigue tests at a stress-ratio R = +0.9, at 60^0C in air, the nanoclay reinforced composite had a 7.9% greater fatigue strength and a fatigue life over a decade longer or 1000% greater than the pristine composite when extrapolated to 10^9 cycles or a simulated 10-year cyclic life.

2.9 MOTIVATION

These uses of FRC materials are continuously faced with dynamic or cyclic loading conditions. It has been reported by researchers in the literature search that the fatigue failure in composite usually occurs due to poor matrix and fiber-matrix interface adhesion properties [11, 13]. There have been investigations with publications on the use of nanoparticles; such as silica-nanoparticle, carbon-nanotube and nanoclay, as toughening epoxy modifier in FRC, are still relatively new. Also information related to fatigue of hybrid nanoclay/GFRC structure has not been fully explored. Fatigue life and related fatigue-fracture are material properties associated with more long-term or progressive failure processes; which describe the ability of a material to survive in service loading over long periods. It is therefore believed, that the development, processing and testing of the hybrid nanoclay/GFRC material is essential. Evaluation of the nanoclay enhancement in damage tolerance GFRC material for maximum fatigue life will provide additional evidence to the existing research.

CHAPTER 3

MATERIALS, MANUFACTURING AND TESTING

3.1 INTRODUCTION

This chapter discusses the constituent materials that were used in the manufacturing of hybrid nanoclay/GFRC laminates and the method used. The main category of the materials used include; resin and hardener, clay nanoparticle and woven glass fiber. The nanoclay and the glass fiber were used as reinforcement in epoxy-resin to produce the hybrid nanoclay/GFRC. Laminates fabrication method as well as various testing methods of the materials were discussed in this chapter. The experimental design in Figure 3.1 shows the processing, characterization and mechanical testing, both in quasi-static and dynamic loading. This process was used in the fatigue life prediction of the neat GFRC and the hybrid nanoclay/GFRC laminates.

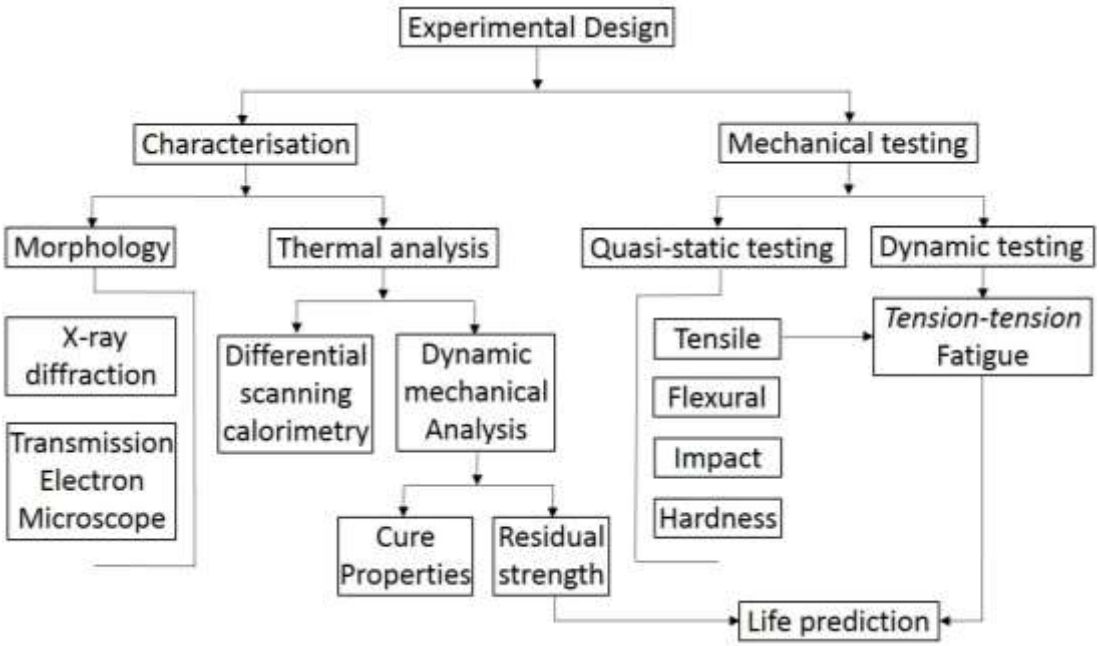

Figure 3.1: Research experimental design

3.2 MATERIALS

A single-component naturally cured formulation was used as the base epoxy. The epoxy-resin used was a commercial bi-functional epoxy resin, diglycidyl ether of bisphenol-A (DGEBA) sold under the name of LR-20. It has a density of 1.13 g/cm^3 and a viscosity in the range 800 – 1100 mPa.s at 25^{0}C. The curing agent used was an unmodified cyclic-aliphatic amine based hardener, LH-281, which also has a density of 1.01 g/cm^3 and a viscosity 650 mPa.s at 25^{0}C. The chemical structure for both epoxy resin and hardener are as shown in the Figure 3.2. Both resin and hardener was supplied by AMT Composite, South Africa.

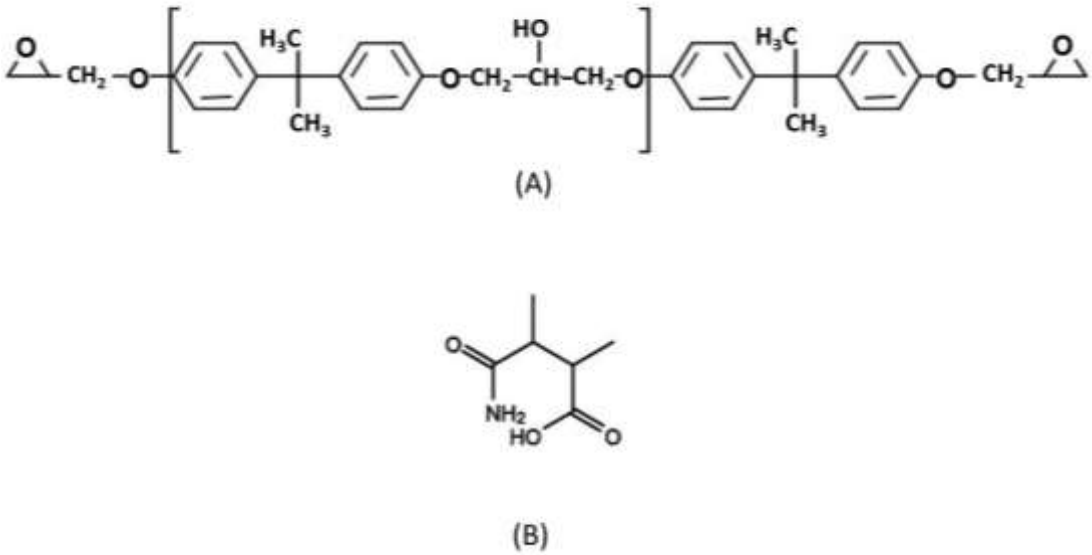

Figure 3.2: Chemical structures for; (a) Epoxy resin: diglycidyl ether of bisphenol-A (DGEBA) and (b) Hardener: cyclic-aliphatic amine based [170]

The reinforcing material used was a silane treated 450 GSM Woven Roving E-Glass fibre with a density of 2.55 g/cm^3. The fibre was a bi-directional (cross-ply) glass fibre, with 0^0/90^0 orientation and a fibre diameter of 20 µm. This was also supplied by AMT Composite, South Africa.

The nanoclay used, Cloisite® 30B, was natural montmorillonite (MMT) clay supplied by Southern Clay Products, Inc., USA. Cloisite 30B is an off white additive particle for plastic and rubber. It is normally used to improve various physical properties, such as reinforcement, synergistic flame retardant and barrier properties. Cloisite® 30B nanoclay was modified with methyl, tallow, bis-2-hydroxythyl, quaternary ammonium chloride (MT2EtOH), a based tallow compound; under an initial Modifier Concentration (MC) of 90 meq/100g clay. Figure 3.3 showed the chemical structure of Cloisite 30B as being modified.

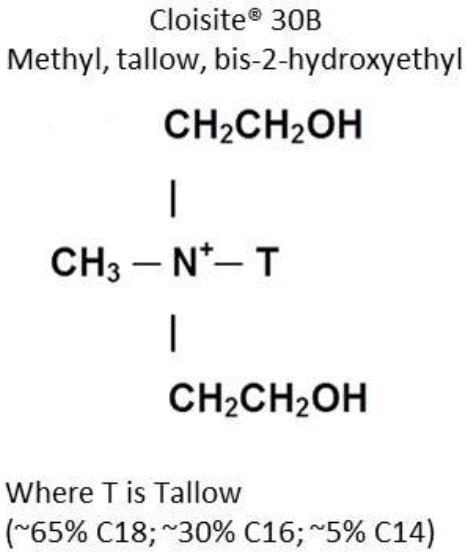

Figure 3.3: Chemical structure for Cloisite® 30B (Southern Clay Products) [171]

3.3 MANUFACTURING

3.3.1 Epoxy-clay nanocomposites (ECN)

Resin of an equivalent weight of six layers of glass fiber (350 grams) was measured in a beaker and heated up to 70^0C on the hot plate, in order to reduce its viscosity. Various weight percentages of Cloisite 30B nanoclay (1 wt. %, 3 wt. % and 5 wt. %) to that of resin and hardener mixtures were measured and mixed with the resin, using magnetic stirrer to form resin-clay solutions. The quantity of clay (in weight percentage) added to the resin was kept low, owing to the fact that benefit of the clay as filler depends on the amount added to the polymer matrix [172]. This is attributed to the fact that,

large amount of the clay tends to agglomerate, increase the viscosity of resin, decrease the reaction enthalpy, and decrease fiber/epoxy interface interaction [173]. Therefore, large clay content can deteriorate the final properties of the nanocomposite.

Considering these factors, various nanoclay/resin solutions were prepared. A magnetic stirrer was used to mix the solution at a constant temperature of 70^0C for one hour and then allowed to cool naturally to room temperature. The hardener was added and manually mixed slowly for about 10mins, thus avoiding formation of bubbles before the infusing process. The resin and hardener was mixed at a ratio of 100:30 by weight parts. It was apparent that mixing or dispersion methods have an influence on the clay (exfoliation) in the polymer matrix [174]. The many different dispersion techniques have led to varying degrees of exfoliation [175-177]. Dispersion methods such as sonication, magnetic stirring, and so on, have achieved reasonable exfoliation of the nanoclay particles in the polymer. For this reasons, magnetic stirring was adopted in order to maintain an exfoliated level of clay dispersion in the polymer-epoxy solution.

3.3.2 Hybrid nanoclay/GFRC

In order to manufacture hybrid nanoclay/GFRC, six plain weave 300 mm by 320 mm glass fiber layers were placed on a glass mould and covered with peel-ply and distribution mesh simultaneously. The setup was further covered with a plastic bag for vacuum infusion process. Unfilled and clay filled GFRC laminates were manufactured through a vacuum assisted resin infusion moulding (VARIM) process. The VARIM system consists of vacuum pump, resin trap and airtight clamping envelopes for laminates as shown in Figure 3.4. The VARIM is a process of transferring resin within fiber lay-up and removing air from the lay-up envelope by using a vacuum pump until the epoxy adhesive cures. The clay/epoxy resin solution was infused on the glass fiber. At the completion of the lay-up process, the excess epoxy was cast in a mould. The epoxy-matrix and the laminate were left to cure naturally at room temperature for 24 hours before demolding. Unfilled and clay filled

polymer nanocomposites as well as their GFRC laminates of ~3mm in thickness were produced and left to cure for 24 hours before demolding. The laminates were then left for 7 days for final curing.

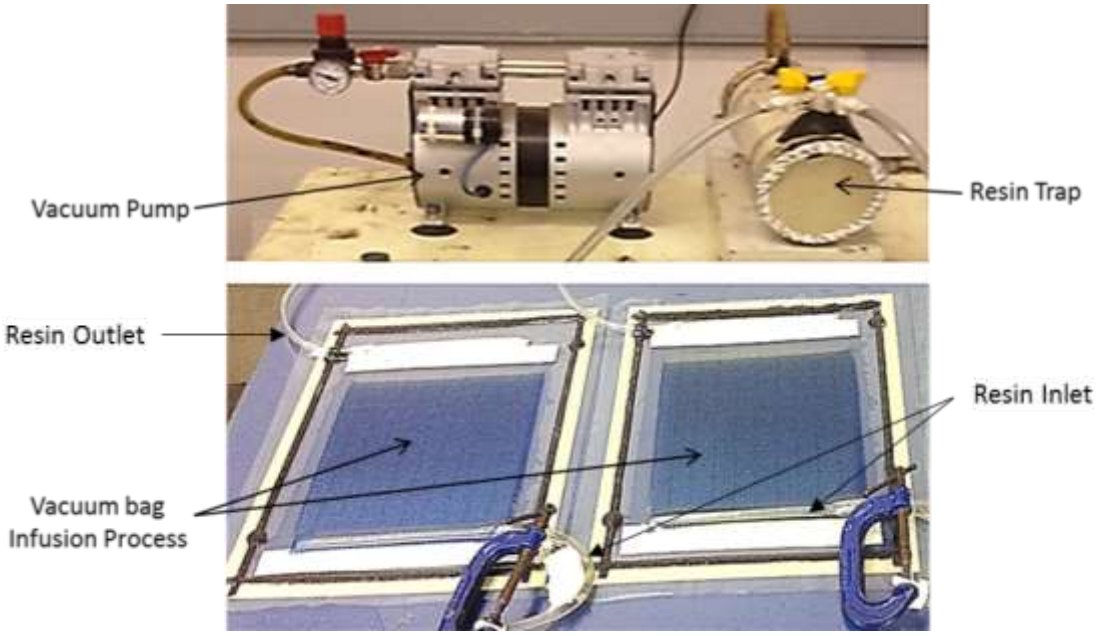

Figure 3.4: Setup of vacuum assisted resin infusion moulding (VARIM) process

3.3.3 Viscosity and flow analysis

Viscosity test of neat and nanoclay/epoxy-resin was carried out on an Elcometer 2300 RV1-L viscometer. This was used to measure the viscous properties of epoxy-resin at 60 rpm. A rotating spindle suspended from the viscometer was inserted into the beaker containing the solution and its resistance to shear or flow was measured. In order to archive homogeneous dispersion of clay in the resin, the resin was heated up to 70 ^{0}C to reduce its viscosity before the clay was added. It was difficult to measure and compare the viscosity of the resin-clay weight percent solution at room temperature because of the clay density (1.98 g/cc). For this reason, the viscosity was taken at 70 ^{0}C during the shear mixing at 60 rpm and recorded.

The flow rate of the neat resin-epoxy and the nanoclay resin-epoxy mixture during VARIM process was equally studied to support the viscosity test. The

flow of the epoxy during VARIM process of the composite laminate is shown in Figure 3.5. This image demonstrates the technique used to measure the time taken by the epoxy to flow across the laminate at different distance intervals. The flow characteristic was studied by placing a rule along the length of the laminate setup. The infusion line was opened at the vacuum inlet and the epoxy start to flow along the laminate length. A stop watch was used to take the time (seconds) at which the resin flows at different intervals. At exactly 30mm away from the infusion line, the first reading was taken. The process was continued with different time intervals throughout the VARIM process.

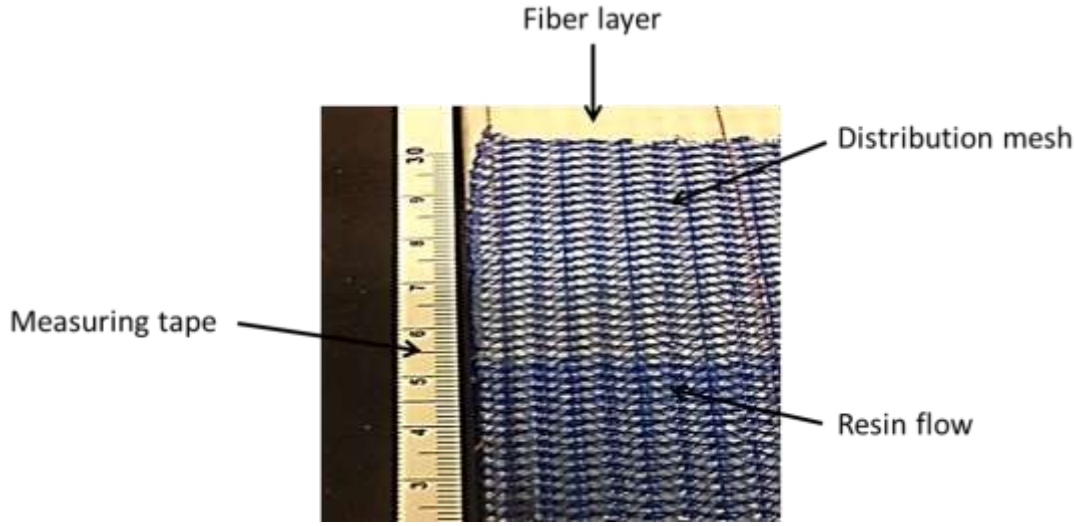

Figure 3.5: Flow measurement of resin-clay epoxy solution during VARIM

The flow of the resin-epoxy and nanoclay/resin-epoxy solution across the laminate was faster at the early stage of the infusion, but later reduced as the flow moved towards the vacuum outlet. The flow characteristics of time dependent gelation per distance interval on the composite laminate was calculated based on different clay percentages and recorded.

3.3.4 Fiber volume fraction (V_f)

The fiber volume fraction of samples was determined through resin burn-off method as per ASTM D 3171 test standard specifications [178]. Two uniform specimens, 25 mm X 25 mm each were cut from different sections of each of

the laminate samples. The specimens were weighed to measure their mass prior to placing them in crucibles and then put inside a preheated furnace set to 560^0C for 5 hours until the resin were burnt off. During the 5 hours burn-off test, the matrix phase was completely removed, leaving behind the reinforcement phase (fiber) inside the crucibles, which were then weighed to measure the reinforcement mass. Having known the mass and densities of different constituents of the laminates, the average fiber volume fraction of the composites was calculated according to Equation 3.1.

$$V_f = \left(\frac{m_f/\rho_f}{m_c/\rho_c}\right) X\ 100 \qquad (3.1)$$

Where;

V_f = Fiber volume

m_c = initial mass of composite specimen

m_f = mass of fiber reinforcement

ρ_c = density of composite and

ρ_f = density of fiber reinforcement.

It is well accepted that V_f is largely dependent on the manufacturing process of composite laminate. Since resin infusion is a variation of resin transfer moulding, the typical fiber volume fraction of the laminate is expected to be in the range of 30-65% [179].

3.4 STRUCTURE AND MORPHOLOGY

3.4.1 X–ray diffraction (XRD)

The structure of the clay and nanoclay/epoxy were examined using X-ray diffractor (XRD). Monochromated Cu K_α radiation of a Philips PW1050 diffractometer was used to obtain the XRD patterns using Cu K_α lines (λ = 1.5406 Å) at room temperature. The diffractrograms were scanned from 3^0 to 16^0 (2θ) in steps of 0.02^0 at a scanning rate of 0.50/min. X-ray diffractrograms

were taken on Cloisite 30B clay and nanocomposites containing 1wt%, 3wt% and 5wt% Cloisite 30B nanoclay to confirm the formation of nanocomposites on addition of organoclay.

3.4.2 Transmission electron microscopy (TEM)

Microscopic investigation of epoxy-clay nanocomposite (ECN) specimens was conducted using a Philips CM120 BioTWIN transmission electron 40 microscope. The operating voltage was 20 to 120 kV. The cryo and low dose imaging TEM has BioTWIN objective lens that gives high contrast and a resolution of 0.34 nm. The microscope is equipped with an energy filter imaging system (Gatan GIF 100) and digital multi-scan CCD cameras (Gatan 791). The specimens were prepared using a LKB/Wallac Type 8801 Ultra-microtome with Ultratome III 8802A Control Unit. Ultra-thin transverse sections, approximately 80-100 nm in thickness were sliced at room temperature using a diamond knife. The sections were supported by 100 copper mesh grids sputter-coated with 3 nm thick carbon layer.

3.5 THERMAL ANALYSIS

3.5.1 Differential scanning calorimetry (DSC)

Differential scanning calorimetry (DSC) measurement of neat polymer epoxy and clay-polymer epoxy samples were performed on a Thermal Analyser (TA) Instruments; Thermal Universal Analyser V4.5A. A power-compensation DSC was performed on three samples each for the neat and clay-polymer epoxy. A heating rate of 10^0C/min was used under a dry nitrogen gas at a flow rate of 100mL/min from 20^0C to 600^0C. The glass transition temperatures (T_g) were determined from the midpoint of the onset to the offset curve along the baseline shift.

3.5.2 Dynamic mechanical analysis (DMA)

Dynamic mechanical analysis (DMA) of neat GFRC and nanoclay/GFRC was performed using a TA Instruments (Model Q800 V20.6). Three specimens of each type measuring 60mm x 10mm x 3mm were tested. The test was carried out according to ASTM D4065-01 [180]. The tests were run in a 3-point bending mode on a support span length of 50mm at a frequency of 1Hz

and amplitude of 20 µm. The heating temperature was ramped from 20^0C to 180^0C at a rate of 3^0C/min. This heating rate was particularly maintained throughout the test runs so that there will be a minimum temperature lag between the sample and the furnace environment. The viscoelastic parameters such as; storage modulus (*E'*), which gives the dynamic elastic response of the samples; loss modulus (*E''*) which gives the dynamic plastic response of samples and damping ratio = tan delta, denoted as tan δ (*E''/E'*), which is the ratio of loss modulus/storage modulus were plotted against the temperature (°C) as determined.

3.5.3 Cure characterization of hybrid nanoclay/GFRC material

In order to study the bulk cure of hybrid nanoclay/GFRC, DMA test was re-performed on another set of separate specimens, cut from the neat GFRC and hybrid nanoclay GFRC samples. The test was conducted in a dual cantilever mode on the same DMA TA Instrument, which was different from the initial test mode used to characterise the thermal properties of the composite material. The heating temperature was ramped using a frequency of 1Hz, at a heating rate of 3^0C/min from 20^0C and were stopped at 100^0C. The specimens were therefore allowed to cool while they were still in the machine. After having been equilibrated at 28^0C, DMA test was re-performed on them again by maintaining the initial heating rate to obtain a difference in T_g values. The dynamic mechanical analysis reheat method (DMA-RM) used, showed changes in T_g values, which were used to calculate the degree of cure of the neat GFRC and that of the hybrid nanoclay/GFRC laminates.

3.6 MECHANICAL TESTING

Considering the factors surrounding composite application in aerodynamic system, the ways and manner the materials are loaded, the condition and environmental factors; the following quasi-static and dynamic testing method are conducted to determine the mechanical properties and fatigue life of hybrid nanoclay/GFRC materials.

3.6.1 Quasi-static test

3.6.1.1 Tensile

Tensile properties were determined according to ASTM D 3039 test standard specifications [181]. The test was performed using MTS 793 servo-hydraulic 100 kN load-cell computer-controlled screw-drive multipurpose testing machine, with the test speed of 5 mm/min. Specimens of 250 mm x 25 mm x 3 mm, in length, width and thickness by dimensions were cut from the neat GFRC and the hybrid nanoclay/GFRC laminate samples using 3000 series CNC router machine. The specimens overall length each was 250 mm and the gauge lengths was 136 mm with tab length of 57 mm on both sides of the grip section as shown in Figure 3.6. The tabs were manufactured and cut from woven glass fiber composite of 1.5 mm thickness. The tabs were bevelled 7 mm away from the gauge length at an angle of 30^0 to avoid stress concentration at the gauge length during testing.

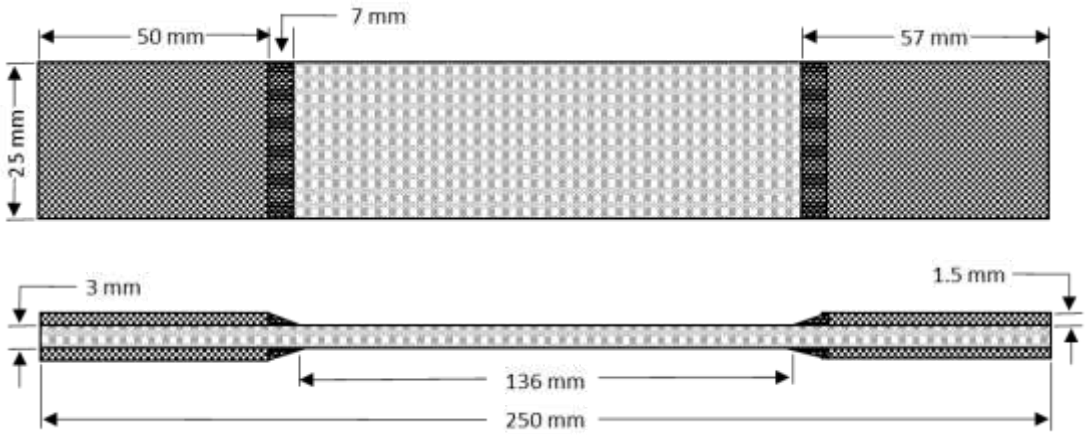

Figure 3.6: Schematic diagram of the tensile and fatigue test specimen

Emery paper was used to sand off the sharp edges left by the CNC machine before the tests were conducted. Specimens were clamped on the MTS servo-hydraulic multipurpose testing machine as shown in Figure 3.7 and the specimen was loaded until it broke within the gauge length. Five specimens were tested for all composite samples and the mean values of the tensile strength, strain at break and modulus of elasticity for all the specimens tested were calculated.

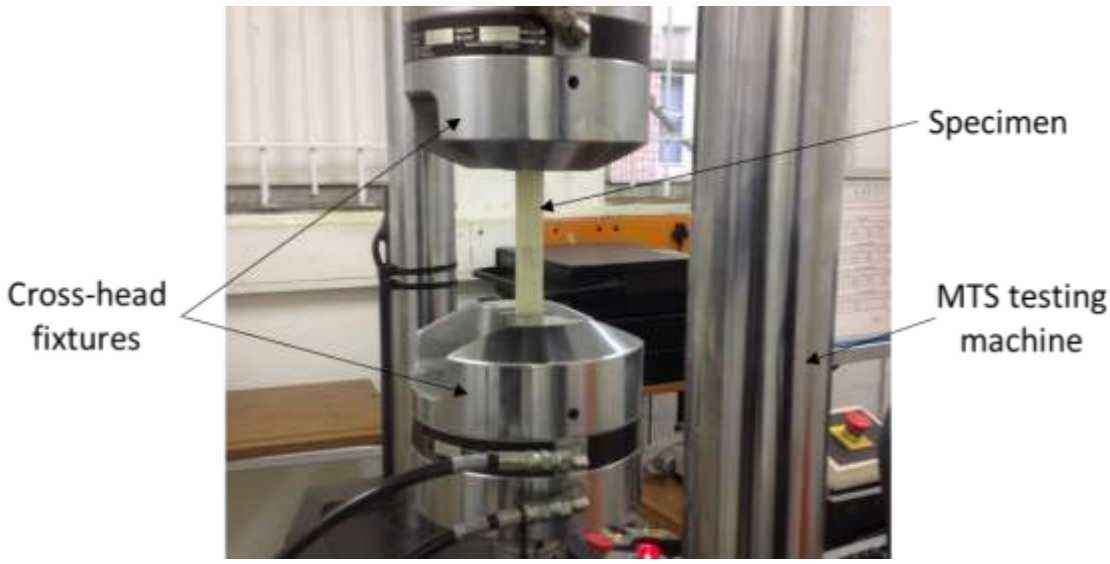

Figure 3.7: Tensile specimen clamped on MTS servo-hydraulic multipurpose testing machine testing

The Young's modulus, E was taken on the linear slope of the curve, between two specific strain, ε_2 = 0.30% and ε_1 = 0.15%. The tensile strength, strain at break and modulus of elasticity were determined from the following equations.

$$\sigma = \frac{P}{A_o} \tag{3.2}$$

$$\varepsilon = \frac{(l - l_o)}{l_o} \tag{3.3}$$

$$E = \frac{\sigma_2 - \sigma_1}{\varepsilon_2 - \varepsilon_1} \tag{3.4}$$

Where;

σ = tensile strength (MPa)

P = applied load (N)

A_o = original cross-sectional area of the sample in the gauge length (mm^2)

ε = Elongation

l_o = original gauge length (mm)

l = instantaneous gauge length (mm) and

σ_1, σ_2 = corresponding stress at the specific strain (MPa).

3.6.1.2 Flexural

A three-point bending flexure test was performed to evaluate the flexural strength and stiffness of the hybrid nanoclay/GFRC material. The test was carried out according to ASTM D790-02 test standard specifications [182]. The test method utilized a simply supported beam of 16:1 span-to-thickness ratio, with center loading support span, developed for design applications as shown in Figure 3.8. Span length of the samples was 48 mm and the nominal thickness was ~3 mm, while the width was maintained at 12.7 mm. Tests were conducted in a displacement control mode with a crosshead speed of 1.3 mm/min. The specimen was deflected until rupture occurred in the outer surface of the specimen or until a maximum strain of 5.0 % was reached; whichever occurs first. Five samples of each type were tested and the average values of flexural strength and modulus were determined.

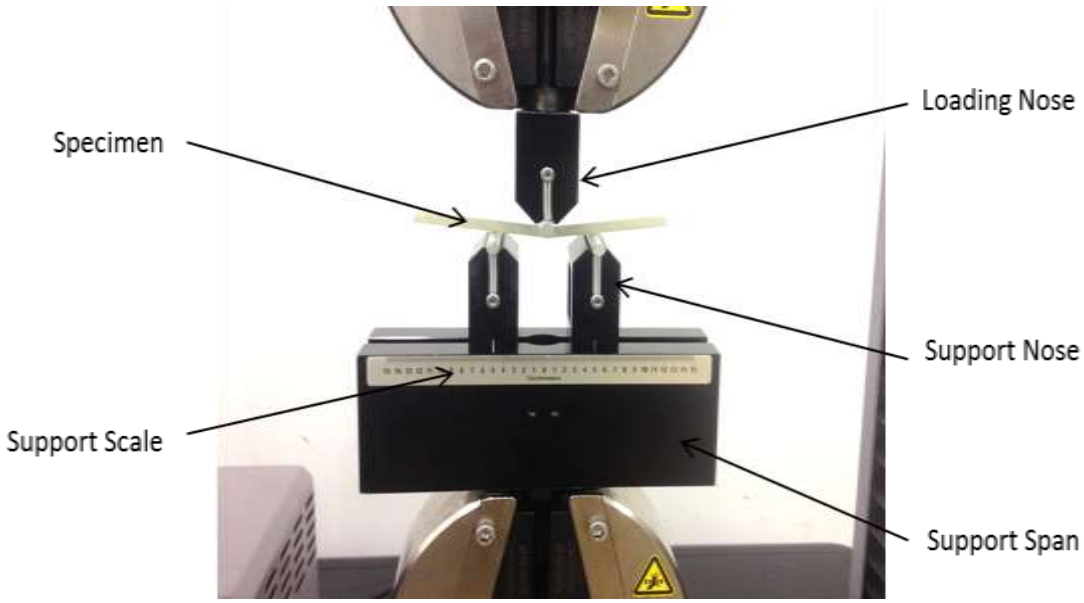

Figure 3.8: Three-point bending test of a composite laminate specimen on a simply supported beam

Load–deflection data for each sample was collected and the maximum flexural stress, strain and modulus were calculated using the following equations:

$$\sigma_f = \frac{3PL}{2bh^2} \tag{3.5}$$

$$\varepsilon_f = \frac{6Dd}{L^2} \tag{3.6}$$

$$E_f = \frac{\sigma_{f2} - \sigma_{f1}}{\varepsilon_{f2} - \varepsilon_{f1}} \tag{3.7}$$

Where;

σ_f= stress at the outer surface at mid-span of the specimen (MPa)

P = load at a given point on the load-deflection point (N)

L = specimen length or support span (mm)

b = specimen width (mm)

h = specimen thickness (mm)

ε_f = flexural strain in the outer surface (mm/mm)

D = maximum deflection of the center of the specimen (mm)

d = depth (mm) and

E_f = flexural modulus (MPa)

3.6.1.3 Impact

To identify the fracture resistance of the neat GFRC and that of hybrid nanoclay/GFRC, charpy impact tests were performed at room temperature using a Hounsfield Balanced Impact Tester (Tensometer Ltd., Croydon, England). The Hounsfield Impact Machine is loaded in a three-point impact manner similar to that created by a charpy apparatus in ASTM D6110 – 10

[183]. Test specimens geometry were modified to a dimension of 50 mm x 12 mm x 5 mm by the length, width and thickness, cut from a separate laminate that was manufactured specifically for the test. This test method permitted a variation in the width of the specimens for many materials, either a brittle or a ductile will occur. All impact specimens were notched 2 mm deep in the middle part opposite the impact area, leaving the impact width to be 10 mm. The impact velocity of the Hounsfield Balanced Impact Tester was approximately 6.7 m/s. Five specimens were tested for the neat and hybrid nanoclay/GFRC.

3.6.1.4 Hardness

Determination of the hybrid nanoclay/GFRC material hardness was conducted using Barber Colman Barcol impresser for the neat GFRC and the hybrid nanoclay/GFRC materials according to ASTM D 2583 test standard specification[184]. The hardness test characterises the indentation hardness of materials by measuring the depth of penetration of the indenter point as shown in Figure 3.9.

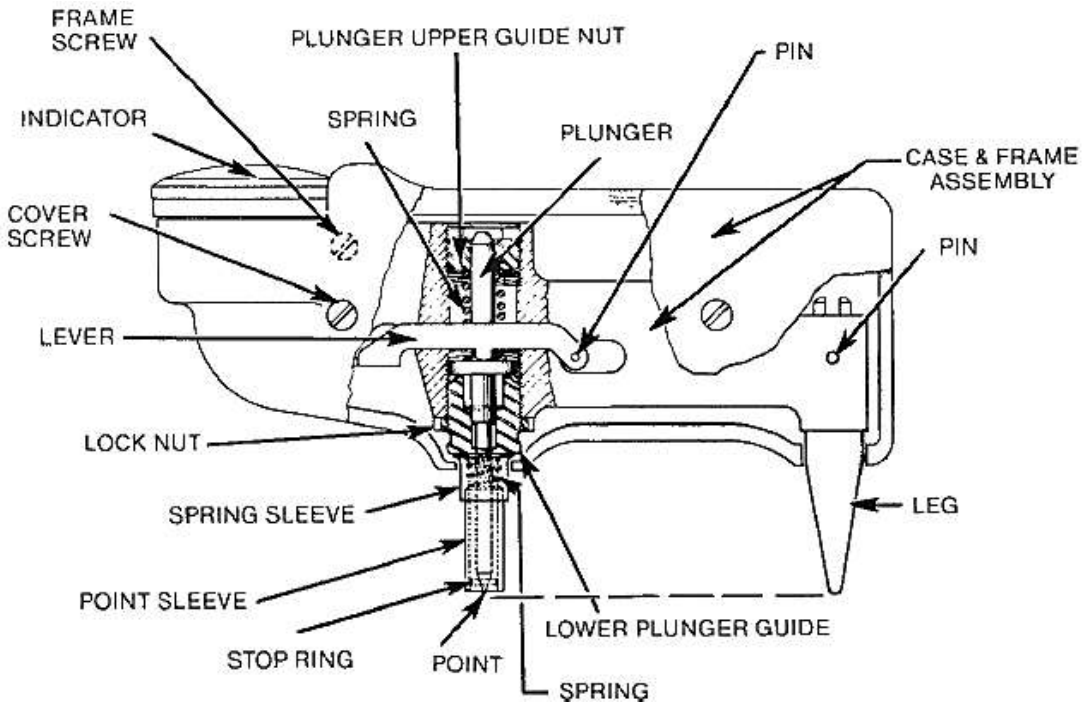

Figure 3.9: Schematic of the Barber Colman Barcol Impressor[184]

The Barcol impresser, model GYZJ-934-1 for harder materials (fiber-glass, Al, Brass and Cu), consist a hardened steel truncated cone, at an angle of 26^0 with a flat tip of 0.157 mm diameter at the spring loading plunger; which was used to make an indentation on the materials. The indenter point and leg of the tester were placed parallel to the sample plate and pressure was applied; increasing the force on the position until the dial indication reaches a maximum. The indenter was sectioned on the reinforced surface as shown in Figure 3.10. Ten consecutive times indentations were conducted randomly on specimens taken from the unfilled and nanoclay filled GFRC laminates. The maximum hardness values were recorded and the mean values for all laminates were taken for graphical representations.

Figure 3.10: Barcol hardness test being conducted on hybrid nanoclay/GFRC laminate surface

3.6.2 Fatigue test

The fatigue life of the neat GFRP and hybrid nanoclay/GFRC composites under the constant amplitude was examined. The fatigue life prediction procedure for the hybrid nanoclay/GFRC laminate involved: (i) matrix cracking and fatigue crack growth (FCG) in the hybrid nanoclay/GFRC laminates, (ii) determination of cycles to failure (N_f), for each of the counted load from the stress versus number of cycles (*S*–*N*), (iii) normalised stress of the neat GFRC and the hybrid nanoclay/GFRC and (iv) residual strength of the hybrid nanoclay/GFRC laminates in comparison to the neat GFRC laminate.

The fatigue test for nanoclay hybrid nanoclay/GFRC laminate was analysed in tension-tension (*t-t*) mode following procedure presented in ASTM D 3479 test standard specifications [185]. The fatigue tests were carried out at constant amplitude loading on MTS 793 servo-hydraulic 100 KN load-cell computer-controlled screw-drives multipurpose testing machine. The loading applications involve a mean stress on which the oscillatory stress is super-imposed as shown in Figure 3.11. The stress ratio R = 0.1 for all tension-tension fatigue testing was used at a frequency of 3 Hz. All tests were carried out at room temperature on four specimens each for neat and hybrid nanoclay/GFRC laminates until final failure. Three displacement levels in the range 80%, 60% and 45% of the ultimate tensile strength (σ_{UTS}) of the composite were applied in the fatigue test.

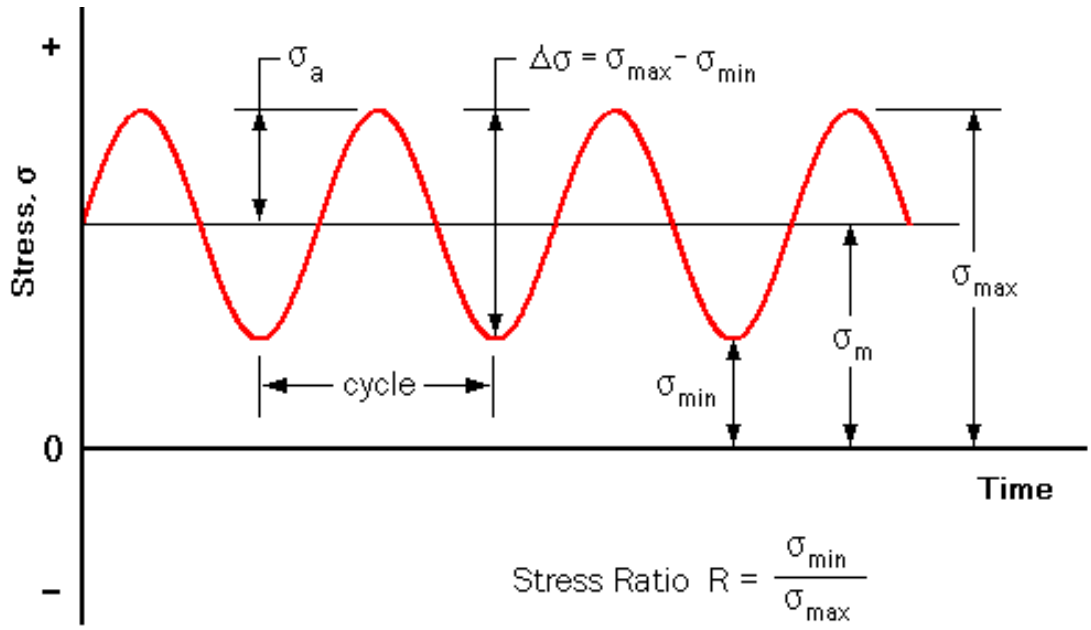

Figure 3.11: Schematic diagram of tension-tension fatigue loading [186]

The following definitions are used to define stress cycle with both alternating and mean stress.

The stress range, which is the algebraic difference between the maximum and minimum stress in a cycle is given by the equation:

$$\Delta_\sigma = \sigma_{max} - \sigma_{min} \tag{3.8}$$

The stress amplitude is one-half the stress range and is given by:

$$\sigma_a = \frac{\Delta_\sigma}{2} = \frac{\sigma_{max} - \sigma_{min}}{2} \tag{3.9}$$

The mean stress, which is the algebraic mean of the maximum and minimum stress in the cycle, is given by:

$$\sigma_m = \frac{\sigma_{max} + \sigma_{min}}{2} \tag{3.10}$$

While the fatigue loading, which is at a stress–ratio is given by:

$$R = \frac{\sigma_{min}}{\sigma_{max}} \tag{3.11}$$

During the tests the number of cycles to failure was registered, as well as the maximum and minimum displacements. The results were analysed in terms of stress (σ) range versus the number of cycles (N_f) to failure, i.e., by representation of data as *S*–*N* Wohler curves. Various observations like crack initiation, crack propagation, crack arrest and delamination were observed during the fatigue test. These were used in the prediction of the fatigue damage behaviour and fatigue life of the hybrid nanoclay/GFRC material.

3.7 RESIDUAL STRENGTH

The residual strength of neat GFRC and hybrid nanoclay/GFRC laminate specimens were evaluated through DMA analysis. Samples conforming to the initial DMA specimen sizes were cut from the already fatigued specimen and tested in 3-point bending mode. The samples were tested using the same TA Instruments (Model Q800 V20.6); both the frequency and heating rate previously used were maintained during the DMA test. Storage modulus (*E′*) values as well and tan δ (*E″*⁄*E′*), derived from the test were compared with the initial results of the un-fatigued samples. The results were used to determine the residual strength of the hybrid nanoclay/GFRC laminates.

3.8 FRACTOGRAPHY ANALYSIS

Conventional and clay filled GFRC of fractured specimens were observed under an optical scanning microscope (OSM) and scanning electron microscopy (SEM). Damage behaviour and analysis were carried out using Olympus BX51M System Metallurgical Microscope, model BX51M, with a maximum magnification 100X; and Carl Zeiss Environmental SEM machine, model EVO HD 15. Fractured samples scanned using OSM were mounted on the platform stage plate below the optical lens to view their fracture surface under low and high magnifications. Fractured samples scanned using SEM was viewed in a high vacuum environmental SEM. The fractured samples viewed under SEM were sputter coated with gold to prevent charging. The microscopic image of the neat and clay filled GFRC fracture samples were compared. The results were used to predict the fatigue life of the hybrid nanoclay/GFRC laminate.

CHAPTER 4

RESULTS AND DISCUSSION: MORPHOLOGY, MECHANICAL AND FATIGUE PROPERTIES OF HYBRID NANOCLAY/GFRC MATERIALS

4.1 INTRODUCTION

In this chapter, the results of the epoxy clay-nanocomposite (ECN) morphology and thermal properties of the hybrid nanoclay/GFRC laminate are provided. Cure properties of the hybrid nanoclay GFRC material studied using dynamic mechanical analysis (DMA) is presented. Mechanical properties of the quasi-static tests and the fatigue test properties of neat GFRC and hybrid nanoclay/GFRC laminates are also reported. Finally, the result of the residual strength of the hybrid nanoclay/GFRC laminate, studied using DMA is presented.

4.2 COMPOSITE LAMINATE CHARACTERISTICS

4.2.1 Viscosity and gel-time behaviour

The viscosity of the neat resin-epoxy and nanoclay/resin-epoxy was taken after stirring on hot plate for an hour. Table 4.1 shows the viscosity values at varying clay loading. The viscosity of neat resin epoxy was measured to be 39 mPa.s, but increased to 46 mPa.s when 1 wt. % nanoclay was added. The reason for the viscosity increase was because the presence of alkyl ammonium ions in the nanoclay acts as catalyst in the resin; by which the cross-linking of the clay with the resin resulted in increased viscosity [187]. As clay percent increases, the viscosity increases. Hence, highest viscosity was observed in 5 wt. % nanoclay/resin-epoxy, having a value of 90 mPa.s.

Table 4.1: Viscosity of neat resin and nanoclay/resin epoxy at 70^0C

Materials (Resin)		Viscosity (mPa.s)
Nanoclay	Neat	39
	1 wt. %	46
	3 wt. %	68
	5 wt. %	90

The time taken per distance interval during the infusion along the laminate was recorded to calculate the velocity at which the neat resin-epoxy and the nanoclay/resin-epoxy solution travelled within the laminate at varying clay loading. Figure 4.1 shows the curve of time versus distance of the neat resin-epoxy and nanoclay/resin-epoxy at varying clay loading.

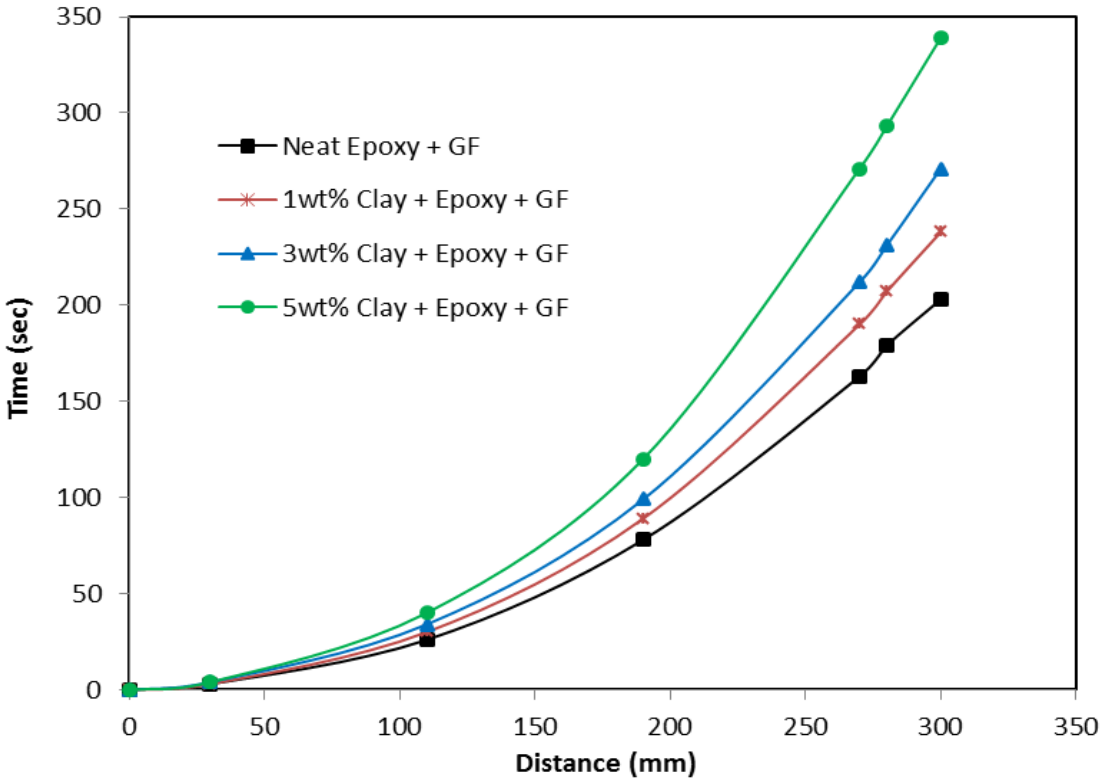

Figure 4.1: Flow behaviour of neat resin-epoxy and nanoclay/resin-epoxy mixture during VARIM processing

The result of the infusion shows that neat resin-epoxy flowed faster than nanoclay/resin-epoxy, and the resin flow speed decreased with increase in the nanoclay content. The flow rate of neat resin-epoxy was 1.48 mm/s and was reduced to 0.9 mm/s at 5 wt. % clay loading, which was 39% difference. The viscosity and gel-time study was stopped at 5 wt. % nanoclay/resin-epoxy because the epoxy has 45 minutes pot life at the addition of hardener into the resin. This affected laminate preparation at higher clay loading, causing incomplete infusion on the fiber during laminate processing, as a result of higher viscous level during infusion. The thickness of the laminate

was not considered in the calculation during the flow analysis, as the flow along the distribution mesh on the surface of the laminate was only required.

4.2.2 Fiber volume fraction (V_f)

Fiber volume fraction (V_f) was calculated from the result of the burn-off test conducted as per the procedure mentioned in section 3.3.4. Table 4.2 shows the results of the fibre volume fraction. Variations were observed in the fiber volume fractions due to the infusion of nanoclay in the laminates. These were insignificant since the values were almost closely related. The average value of the fibre volume fraction derived from all laminates was approximately 0.46 (46%).

Table 4.2: Fiber Volume Fraction

Material (GFRC)	Fiber Volume Fraction			
	Mass of Composite (g)	Mass of fiber (g)	Fiber weight ratio (%)	Fiber volume fraction (V_f)
Neat	2.642	1.675	63.38	0.44
1 wt. % Clay	2.514	1.628	64.76	0.45
3 wt. % Clay	2.549	1.705	66.87	0.47
5 wt. % Clay	2.630	1.732	65.86	0.46

Fibre volume fraction has significant effect on composite properties, including failure mode and ultimate strength. According to Xu Hockin et al. [188], mechanical properties of FRC can be improved with increasing fibre volume fraction. This means that the stiffness and strength of a FRC laminate will increase in proportion to the amount of fibre present [189]. However, when the fibre volume fraction is sufficiently large, the composite ultimate strength will degrade [188]. When fibre volume (V_f) is in the range of 60-70% (depending on the fibres orientation), tensile stiffness may continue to increase. Hence, laminate's strength will reach a peak and then begin to decrease due to the lack of sufficient resin to hold the fibres together [189].

4.3 MORPHOLOGY OF POLYMER NANOCOMPOSITE

The microstructure of epoxy-clay nanocomposite was studied using X-ray diffraction (XRD) and transmission electron microscopy (TEM). The epoxy-clay samples were prepared according to the methods described in sections 3.4.1 and 3.4.2. The diffraction peak at *2θ* and the interlayer *d*-spacing of the Cloisite 30B nanoclay and epoxy-clay nanocomposite material are recorded in Table 4.3. By using the diffraction peak, it was observed that Cloisite 30B has a sharp diffraction peak at *2θ* of 5.63^0 corresponding to interlayer *d*-spacing of 18.2 *Å*. This was consistent with result obtained by Kanny and Mohan [190], where interlayer *d*-spacing of 18.1 *Å* was found in Cloisite 30B. Neat epoxy resin does not have any XRD peaks and this suggests that the material was amorphous. On the other hand, XRD of the epoxy-clay nanocomposite showed a range of peak patterns corresponding to the varying weight ratio of clay. The internal formation in the XRD pattern of the neat polymer composite, epoxy-clay nanocomposite and the Cloisite 30B clay material are shown in Figure 4.2.

Table 4.3: Diffraction peak and interlayer d-spacing of Cloisite 30B nanoclay in resin-epoxy

Material (Epoxy)	X-ray diffraction	
	Diffraction peak at *2θ* (degree)	Interlayer *d*-spacing(*Å*)
Cloisite 30B Clay	5.63^0	18.2
1 wt. % Clay	No peak	Randomly dispersed
3 wt. % Clay	No peak	Randomly dispersed
5 wt. % Clay	5.1^0	20.1

No distinct XRD peak corresponding to the diffraction peak of Cloisite 30B was found in epoxy with nanoclay addition up to 3 wt. %. The absence of diffraction peak may suggest that the nanoclay was randomly dispersed in the matrix. Such type of structure is generally referred as an exfoliated

nanocomposite structure [191]. However, epoxy with 5 wt. % nanoclay shows a sharp diffraction pattern at 2θ of 5.1^0, which corresponded to *d*-spacing of 20.1Å. The increased interlayer spacing suggests that the epoxy was unable to penetrate fully into the gallery spacing of the clays. Such type of structure is referred to as an intercalated structure [191]. In the intercalated structure, the clay nano-layers were arranged in an orderly fashion in the matrix polymer and with increased interlayer distance compared to the clay itself. Hence, the intercalated structure was observed only when the clay content was >3 in percentage. Structural change occurred from exfoliation to intercalation as a function of clay content in epoxy polymer. As the clay content increased, the dispersion of clay changed the structure of the epoxy-nanocomposites. The clay nanolayers separation was restricted and also full dispersion of nanolayers was affected in the epoxy polymer matrix, resulting to an intercalated structure on higher clay content.

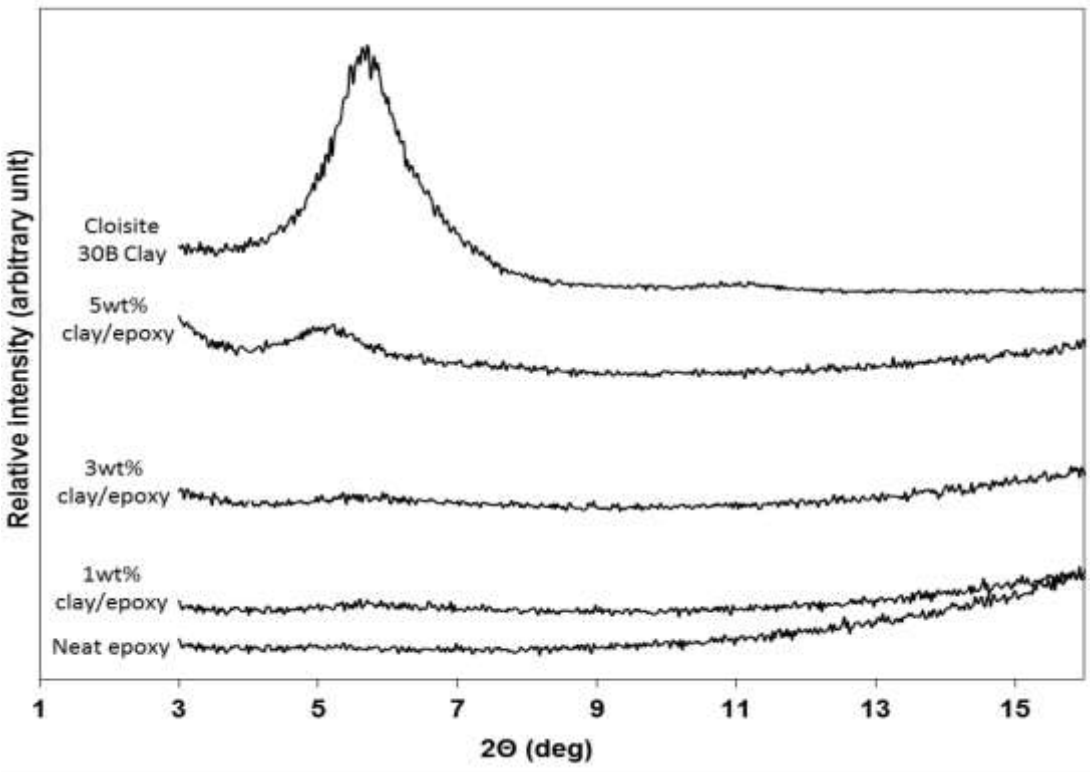

Figure 4.2: XRD pattern of; (a) Neat epoxy; epoxy with (b) 1wt% clay/epoxy, (c) 3wt% clay/epoxy, (d) 5wt% clay/epoxy and (e) Cloisite 30B clay

TEM micrograph of the polymer matrix sample showed homogeneous dispersion of nanoclay in the epoxy-resin. It is apparent that the mixing technique had great influence on the degree of dispersion of the Cloisite 30B nanoclay. That means the magnetic stirring mixing technique produced partially exfoliated and intercalated nanocomposite. The evidence can be observed in the TEM micrograph of the polymer matrix nanocomposite shown in Figure 4.3. Although, homogeneous dispersion nanoclay was found within the polymer matrix; hence, the samples display few clusters of nanoclay within the matrix. Polymer nanocomposite with 1 wt. % and 3 wt. % clay loading can be classified as exfoliated and intercalated nanocomposite as seen in Figure 4.3a and Figure 4.3b respectively. Dispersion of nanoclay into the epoxy-resin up to 3 wt. % clay addition was observed to have resulted into proper homogeneous structures. In polymer nanocomposite sample with 5 wt. % nanoclay addition, agglomeration of nanoclay was observed. Figure 4.3c reveals the dispersion of 5 wt. % nanoclay in the epoxy-resin. The morphology of the polymer nanocomposite can be classified as an intercalated structure. The content of clay clusters in the polymer epoxy at 5 wt. % displayed incomplete dispersion of nanoclay. This may be attributed to high agglomeration of clay particles in the polymer nanocomposite.

The agglomeration of clay in the polymer-matrix was observed to have aggregated high viscosity of the epoxy matrix, leading to incomplete dispersion of the clay platelet. This is because high nanoclay cluster was present in the morphology of the polymer matrix as seen on Figure 4.3c. This observation corresponds to the diffraction peak of the XRD pattern showed in Figure 4.2. The intercalated nanostructure of the polymer nanocomposite at high clay loading was justified by the incomplete dispersion of clay platelet in the polymer matrix during shear mixing at 70 ^{0}C. It can therefore be concluded that the mixing temperature did not influence of the viscosity and shear properties of the polymeric clay nanocomposite at higher clay loading.

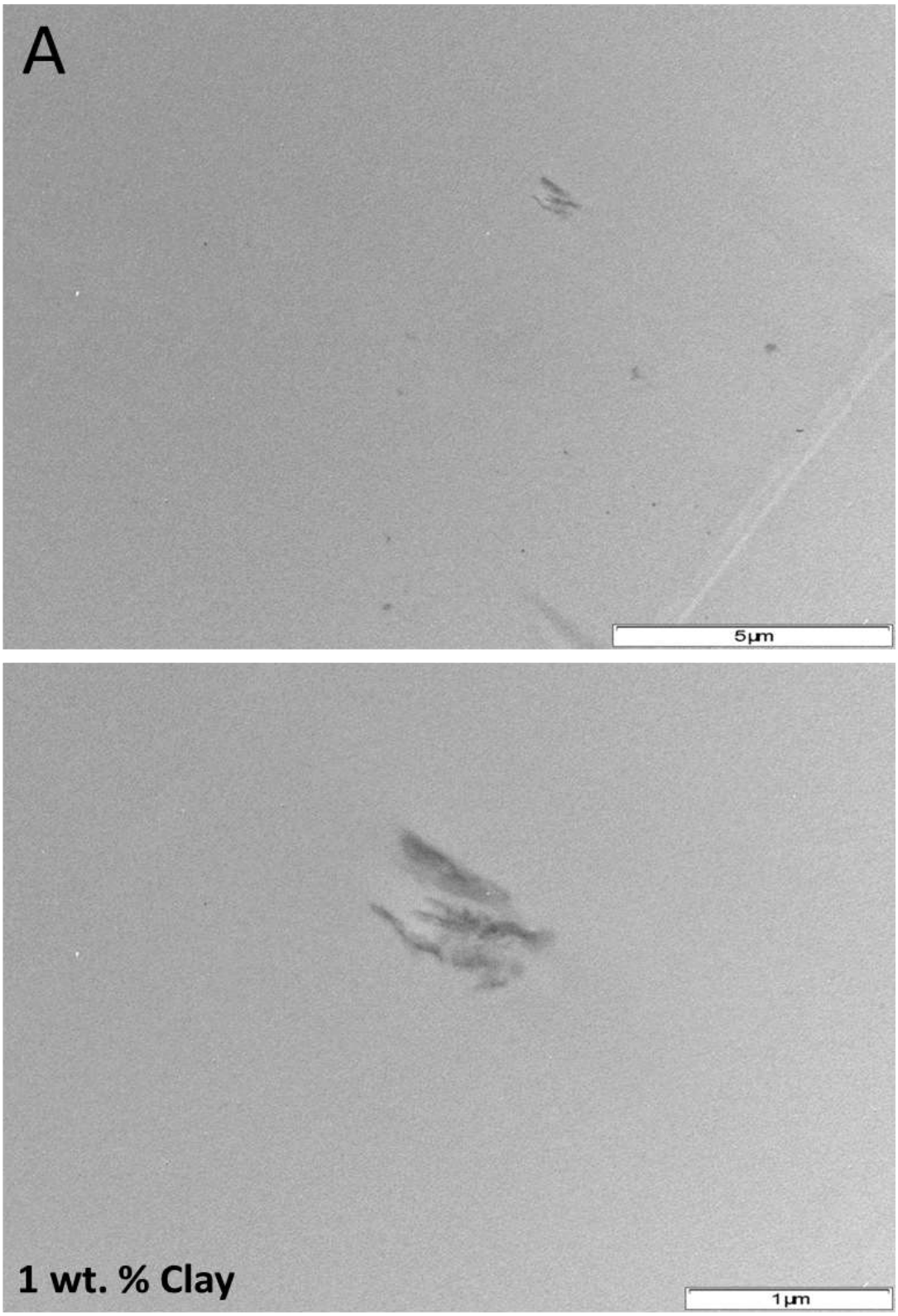
A
5µm
1 wt. % Clay
1µm

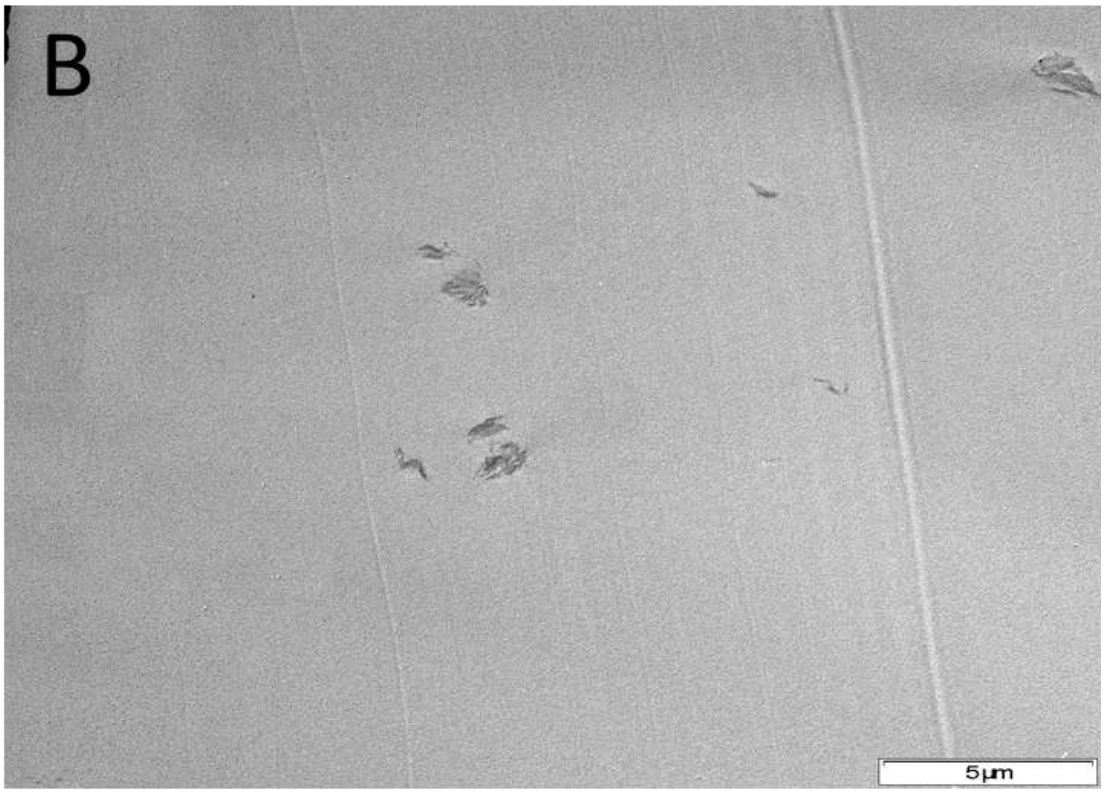
B
5µm

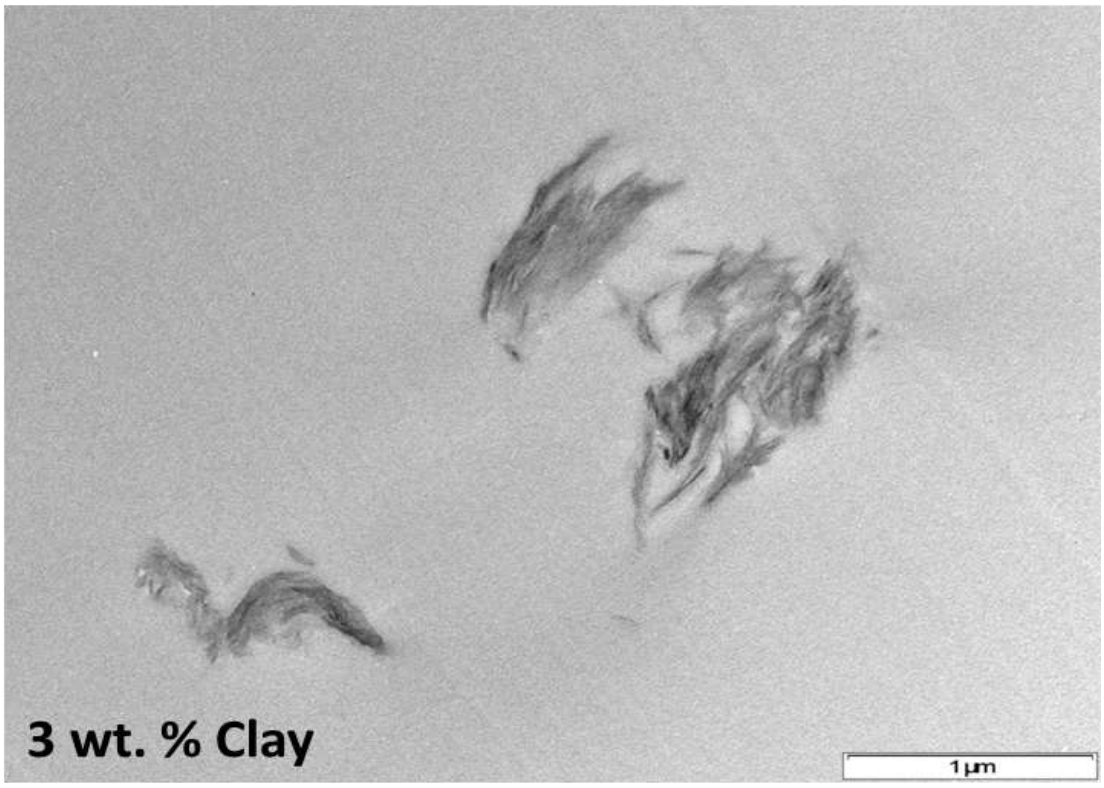
3 wt. % Clay
1µm

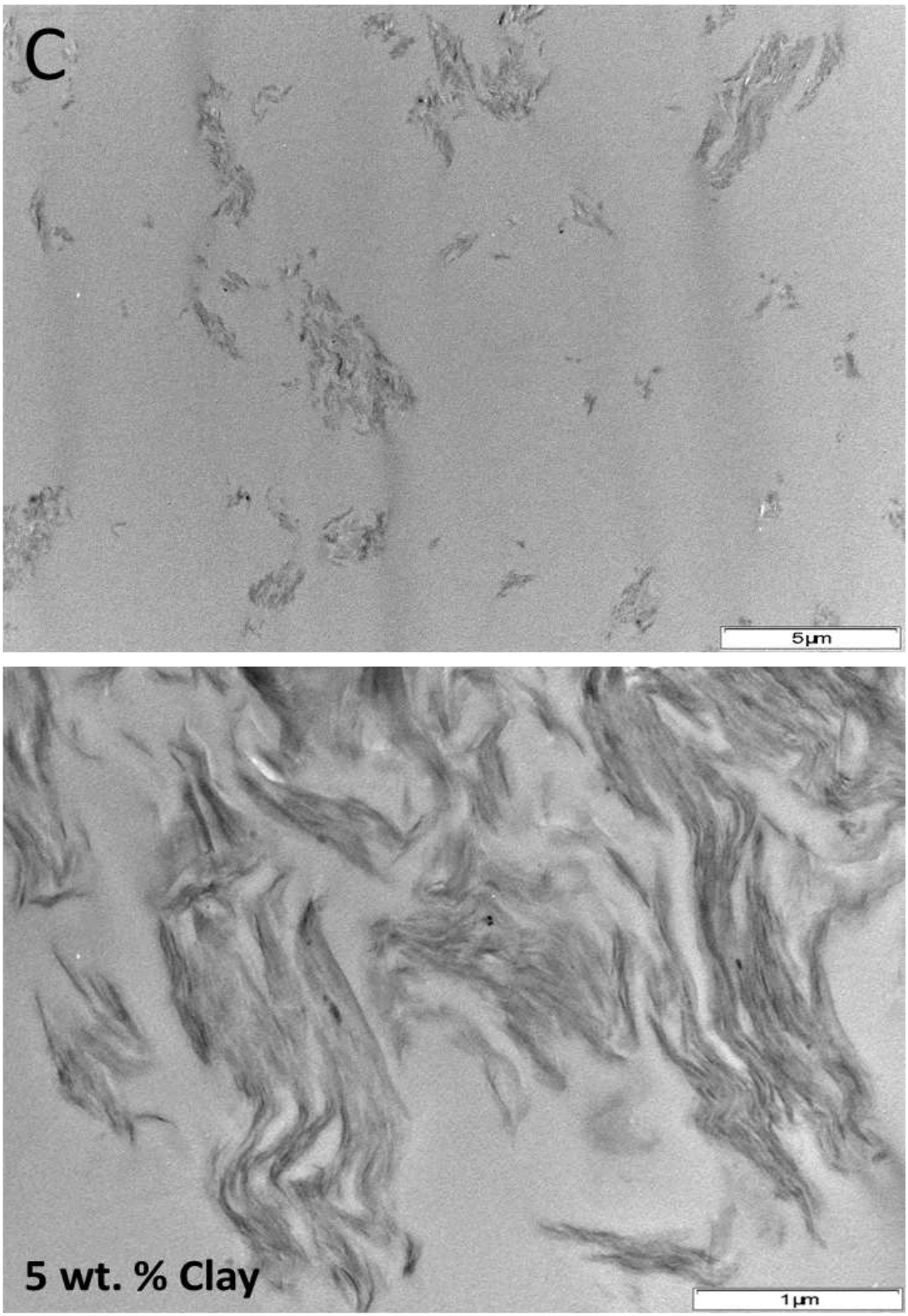

Figure 4.3: TEM image showing low and high magnification of clay dispersion in; (a) 1 wt. % nanocomposite, (b) 3 wt. % nanocomposite and (c) 5 wt. % nanocomposite

4.4 THERMAL PROPERTIES

4.4.1 Differential scanning calorimetry (DSC)

Power-compensation DSC [192], was used to perform the thermal analysis of ECN. Heat flow versus temperature curve with respect to the varying weight ratio of nanoclay in the epoxy is as shown in Figure 4.4. The slope of the thermogram curves of the sample is as determined with respect to the heating rate. The baseline slopes of the DSC which illustrates the differences between the heat capacity of the samples and the reference showed that the samples cured with less absorption of energy during the heating process.

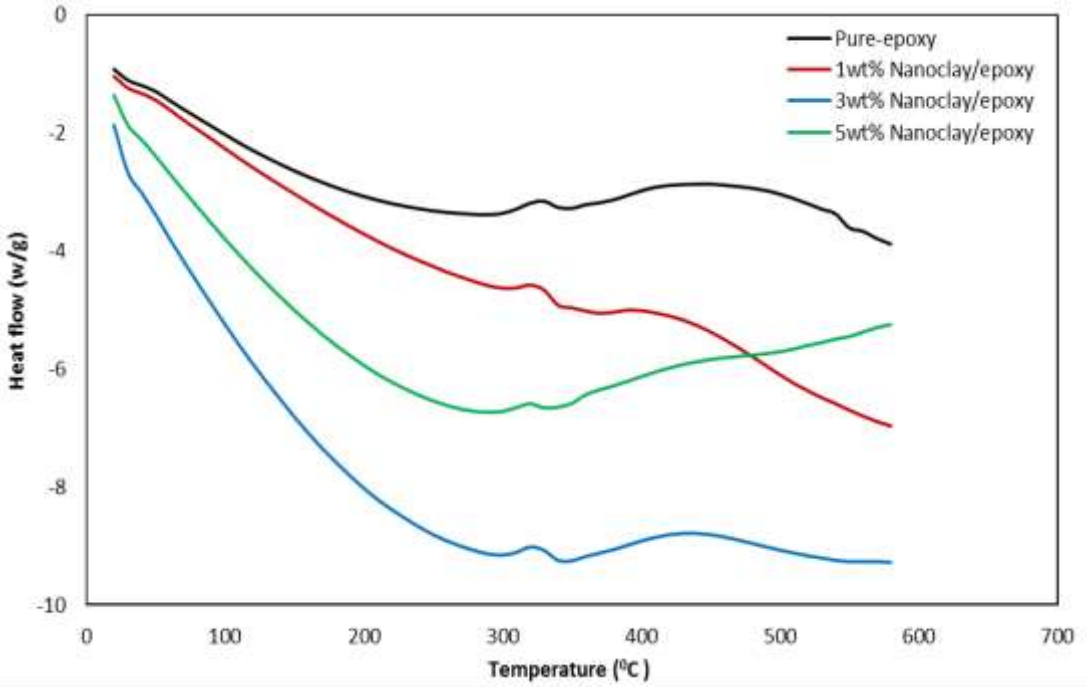

Figure 4.4: DSC thermogram curve showing heat flow versus temperature for neat epoxy and ECN

The nanoclay in the polymer nanocomposite samples slow down the relaxation of polymer chain during the heating process of the samples. This can be attributed to proper crosslink density of nanoclay with the epoxy. Sample with 3 wt. % nanoclay was observed to have shown lowest heat absorption to reach the enthalpy of the rubbery state when compared to other varying clay/epoxy nanocomposites. However, sample with 5 wt. % nanoclay

absorbed more energy than 3 wt. % ECN because of the intercalation of clay particles in the laminate.

The T_g values were derived and recorded in Table 4.4. The glass transition temperatures T_g values of the neat and ECN were determined from the midway of the on-set to the off-set along the baseline slope of the thermogram curve. The initial T_g value of 62^0C increased to 65^0C at the addition of nanoclay up to 3 wt. %. An increase of 3^0C was found in the T_g at the addition of nanoclay up 3 wt. %. Reduction in T_g occurred as clay content was increased to 5 wt. %.

Table 4.4: DSC properties showing the T_g values of neat epoxy and polymer nanocomposites

Materials (Epoxy)	T_g (^{0}C)
Neat	62 ± 0.57
1 wt. % clay	63 ± 0.49
3 wt. % clay	65 ± 0.51
5 wt. % clay	59 ± 0.63

4.4.2 Dynamic mechanical analysis (DMA)

The dynamic mechanical analysis (DMA) gave an indication of the phase structure of neat and hybrid nanoclay/GFRC over a temperature range of 20^0C to 180^0C. The phase structure was dependent on various factors such as fibre loading, fibre orientation and the nature of fibre–matrix interface region, which are sensitive to all kinds of transitions and relaxation processes of resin-matrix and the blends of the nanoclay morphology. DMA's sensitivity was based on the significant change in modulus and damping which occurred in the T_g value. Generally, T_g in DMA is taken as the peak in tangent delta [193], but ASTM [194] recommends the peak in the loss modulus. The viscoelastic properties of the GFRC such as the peak of the loss modulus or

tan delta (Tan δ) characteristics were considered as the T_g; these are relatively frequency independent at the increasing temperature.

The storage modulus measures the stored energy in the elastic portion of the composite. In Figure 4.5, an increase of 18% in the storage modulus (*E'*) peak of the nanoclay/GFRC was observed in 3 wt. % when compared to the neat GFRC. However, the Loss modulus (*E''*), which measures the energy dissipated at heat per cycle under deformation of the material showed varieties of trends in the neat GFRC and hybrid nanoclay/GFRC laminates systems.

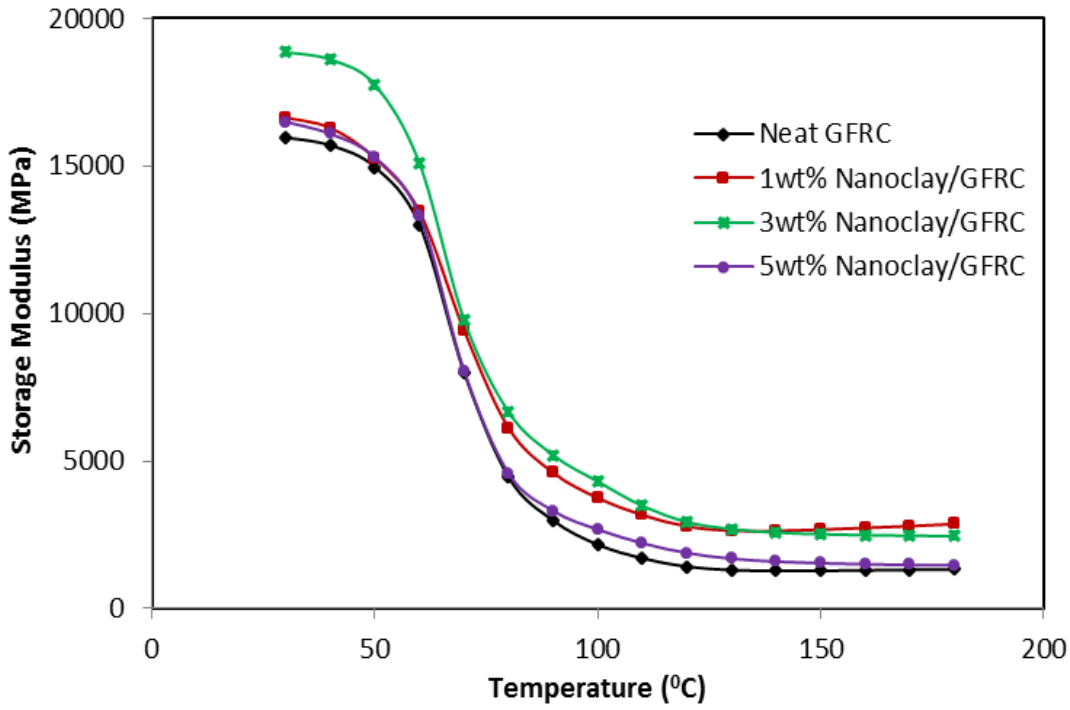

Figure 4.5: Temperature dependency of storage modulus for neat GFRC and hybrid nanoclay/GFRC laminates

It was observed in Figure 4.6 that incorporation of nanoclay in the glass fibre laminates caused broadening of the loss modulus peak. This was more visible at hybrid nanoclay/GFRC with 3 wt. % clay loading. Highest peak value of 41% was observed in the loss modulus peak, which was more than the neat GFRC peak value. Hence, a shift of 2^0C increase in the loss modulus T_g towards the right was found at 3 wt. % clay loading. This is due to the

increase in the number of chain segments upon clay addition. This shift in the temperature was quite significant; and this depicted an improvement in the T_g with addition of nanoclay. Furthermore, amorphous polymeric materials have different T_g values above which materials' stiffness reduces with increased viscosity at the rubbery state.

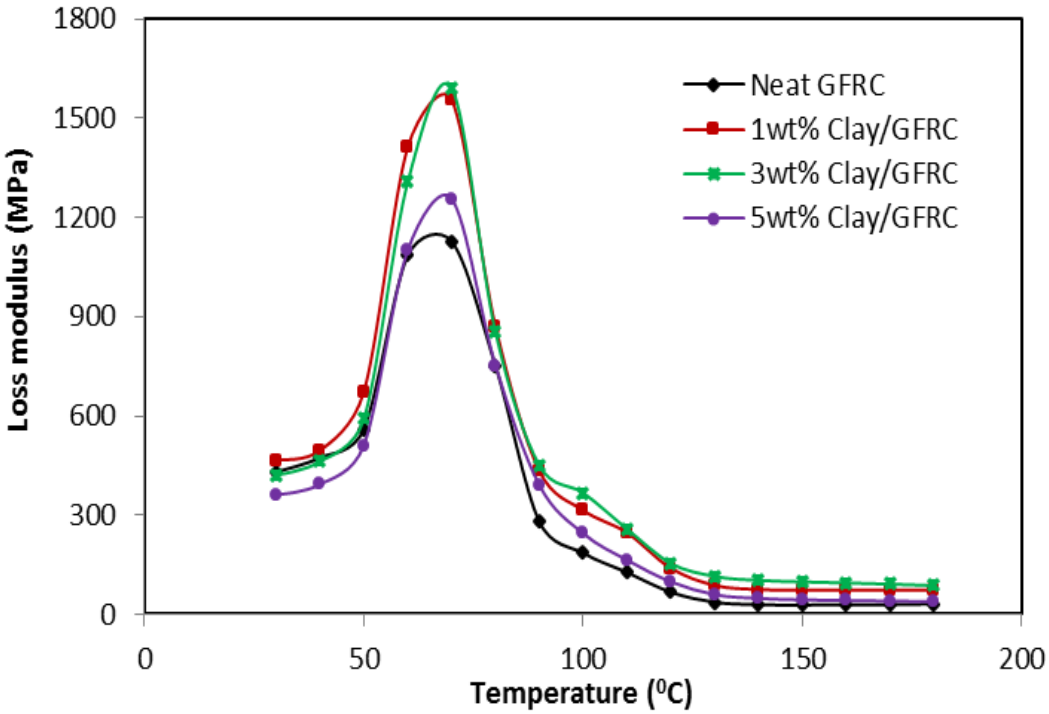

Figure 4.6: Temperature dependency of loss modulus for neat GFRC and hybrid nanoclay/GFRC laminates

The variations in tan delta of neat GFRC and hybrid nanoclay/GFRC are shown in Figure 4.7. This measures the ratio of the loss modulus to the storage modulus; which is also known as the mechanical loss factor. Tan delta curve with the highest peak value was observed in 5 wt. % clay loading to be 9.3% higher than neat GFRC. The peaks increased in intensity with increase in the amount of nanoclay content. The broadening of the glass to rubbery state is likely to restrict the movement of molecules in the epoxy by incorporation of nanoclay. The lowering of the peak height also indicated good interfacial adhesion.

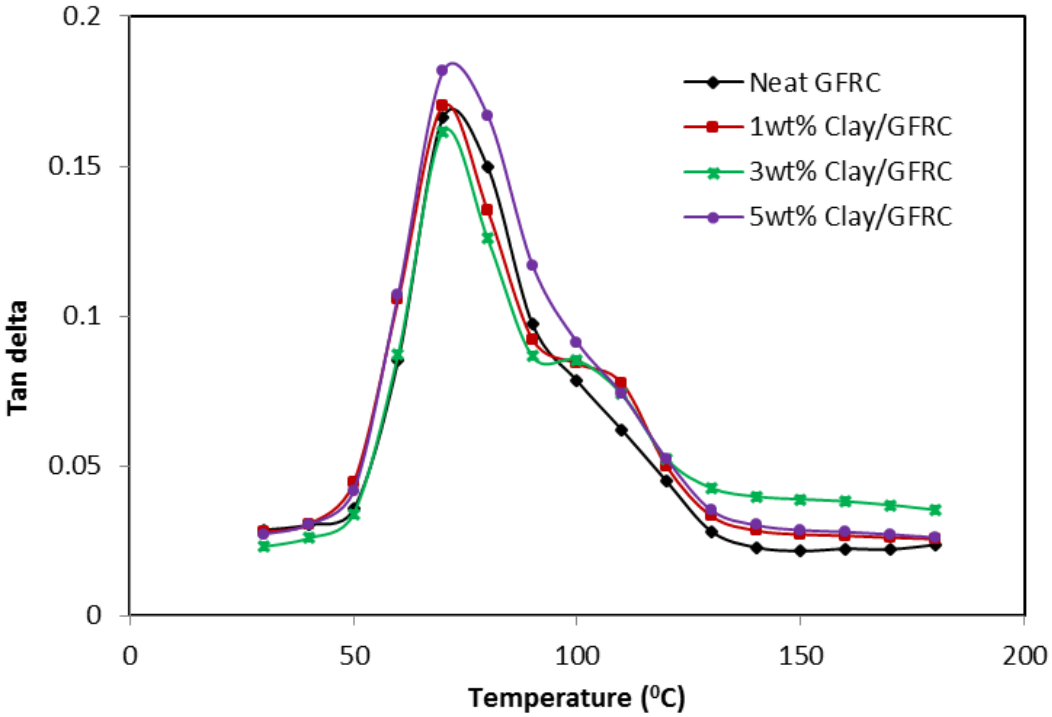

Figure 4.7: Temperature dependency of tan δ for neat GFRC and hybrid nanoclay/GFRC laminates

At a point between 90^0 and 110^0, there occurred another peak within the variation of tan δ at 1 wt. % and 3 wt. % nanoclay/GFRC. This shift was as a result of the barrier properties, which is indicative of improved clay-epoxy interaction in the glass fibre reinforced laminate. The polymer surrounding the clay undergoes a high T_g because the clay acts as a thermal barrier in the medium of the soft segment. This shows the effectiveness of clay as a reinforcing agent. Apparently, tan δ T_g values reduced with nanoclay increase in the hybrid nanoclay/GFRC materials except for 5 wt. % nanoclay/GFRC. It is not a surprise that no change or a significant increase occurred in tan δ T_g values of the hybrid nanoclay/GFRC materials; this has also been previously reported [195, 196]. With the little increase in T_g value of the loss modulus, it showed that clay acts as catalyst in the medium by which the polymer was made to undergo high-viscous response as energy was being dissipated. The effectiveness of the clay as a reinforcing agent was therefore justified. Table

4.5 shows the values of DMA properties of neat and hybrid nanoclay/GFRC samples.

Table 4.5: DMA properties of neat GFRC and hybrid nanoclay/GFRC materials

Materials (GFRC)	DMA properties					
	Storage modulus		Loss modulus		Tan δ	
	Peak (MPa)	T_g (^{0}C)	Peak (MPa)	T_g (^{0}C)	Peak	T_g (^{0}C)
Neat	15964 ± 416	66.10	1128 ± 96	68.24	0.1662	74.84
1 wt. % Clay	16635 ± 303	68.17	1556 ± 88	69.84	0.1701	72.91
3 wt. % Clay	18856 ± 284	68.32	1592 ± 82	70.28	0.1615	67.28
5 wt. % Clay	16496 ± 422	66.26	1257 ± 102	68.91	0.1816	75.08

4.4.3 Bulk cure properties of hybrid nanoclay/GFRC materials

Dynamic mechanical analysis reheat method (DMA-RM) was employed to determine bulk cure of the neat GFRC and the hybrid nanoclay/GFRC. The composite laminates were heated according to the DMA test reported in section 3.5.3. The loss modulus T_g value in the neat GFRC was found to be the same value as that of 1 wt. % hybrid nanoclay/GFRC at the first heating process. These T_g values are shown in Figure 4.8a and 4.8b. The T_g values later increased by 0.21% (although minimal) as clay was increased to 3 wt. % in the GFRC. The T_g eventually dropped by 1.35% as clay was increased to 5 wt. % in the GFRC. The low increase in 3 wt. % was unlikely to be accepted because the change was too small and negligible. Some investigators have reported increase in T_g values with the addition of clay [197, 198]; while others found a slight decrease or no change in T_g values [199-201]. This is in agreement with the increase observed in this study. With the minimal increase in T_g, it can be deduced that clay serves as a physical cross-linker

with the epoxy in the fibre glass materials by which the T_g value was extended.

In order to determine the degree of cure; the materials were reheated. The initial heating process did not actually finalize the curing process because the samples were ramped at a slow heating rate of 3^0C/min from 20^0C to 100^0C. However, interesting changes in the loss modulus values were found after reheating of the composite materials. The change in the loss modulus T_g values of the first and second heating of the laminates were used to determine the cure rate of the composite materials. From the tests results, Figure 4.8a shows the loss modulus T_g value of the neat GFRC, while Figure 4.8b shows the loss modulus T_g value of the 1wt% hybrid nanoclay/GFRC laminates at the first heating of the laminates. After the DMA Instruments have been equilibrated to 28^0C, the same materials were further reheated. By reheating the specimens, increased the T_g value in the neat GFRC and hybrid nanoclay/GFRC laminates was observed. The increasing T_g values after reheating of the samples are shown in Figure 4.8c and 4.8d. The value was observed to be lower in the hybrid nanoclay/GFRC when compared to the neat GFRC. The difference in loss modulus T_g value between the first and the second heating process depicted the level of cure, and this observation with cure level was better in hybrid nanoclay/GFRC samples.

From the DMA-RM, it can be reported that uncured properties of the materials cured with respect to the increase in the loss modulus T_g. However, the T_g value of neat GFRC was higher than that of the hybrid nanoclay/GFRC after reheating of the same samples. The evidence of the increase is recorded in Table 4.6. The increase of T_g in the neat GFRC laminate after reheating of the material was about 11^0C higher than the initial T_g. However, the initial uncured properties as a result of clay addition in the GFRC laminate increased the T_g by 7^0C in both 1 wt. % and 3 wt. % nanoclay/GFRC after reheating. Meanwhile, samples with 5 wt. % clay loading also show T_g increase of 9^0C, which was equally lower to that of the neat GFRC.

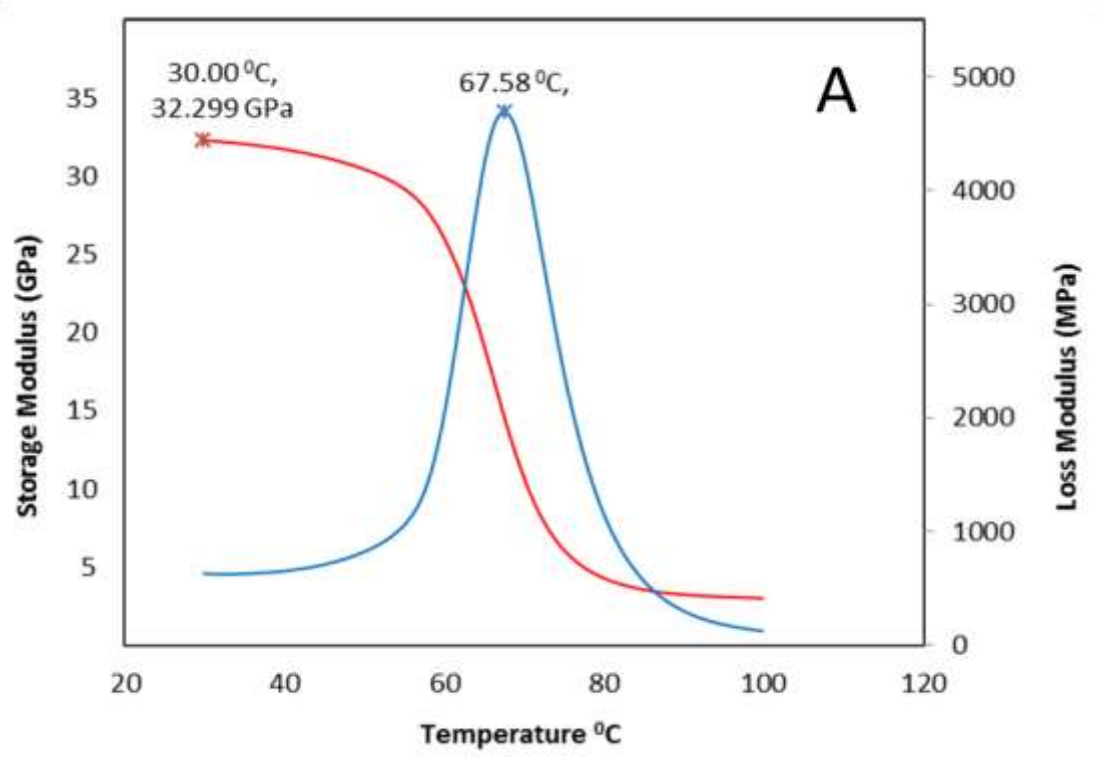
30.00 °C,
32.299 GPa
67.58 °C,
A
Storage Modulus (GPa)
Loss Modulus (MPa)
Temperature °C
35
30
25
20
15
10
5
5000
4000
3000
2000
1000
0
20
40
60
80
100
120

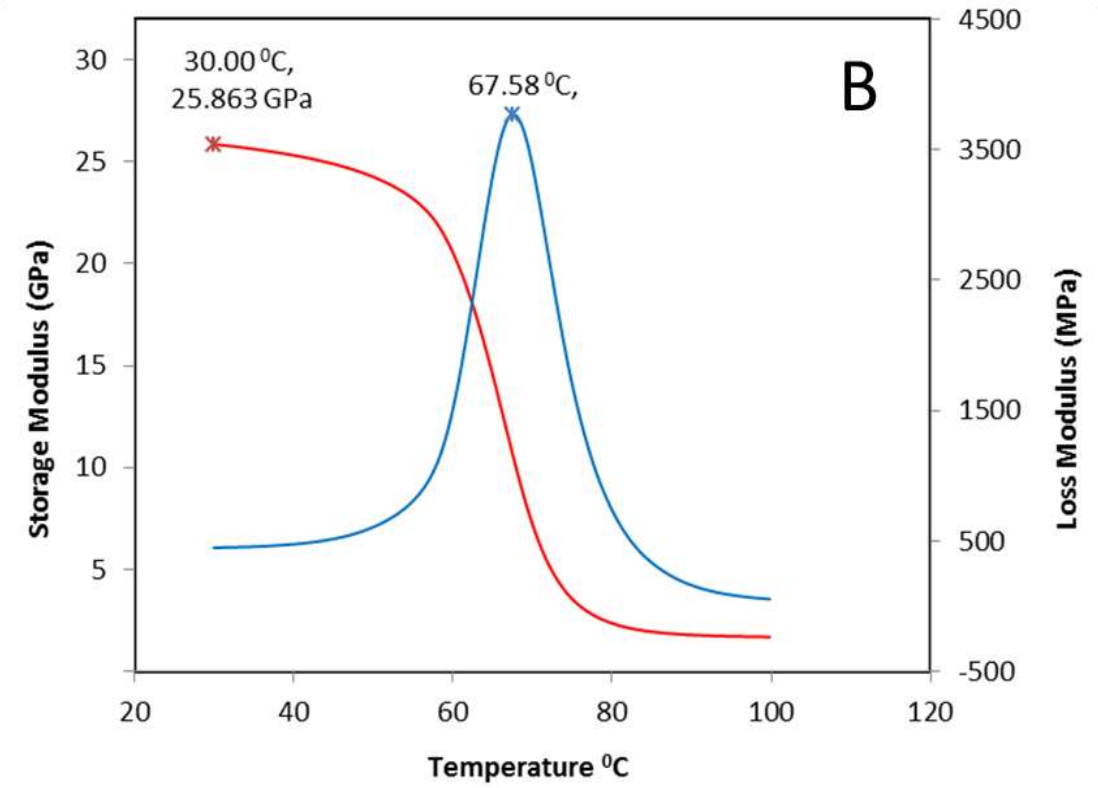
30.00 °C,
25.863 GPa
67.58 °C,
B
Storage Modulus (GPa)
Loss Modulus (MPa)
Temperature °C
30
25
20
15
10
5
4500
3500
2500
1500
500
-500
20
40
60
80
100
120

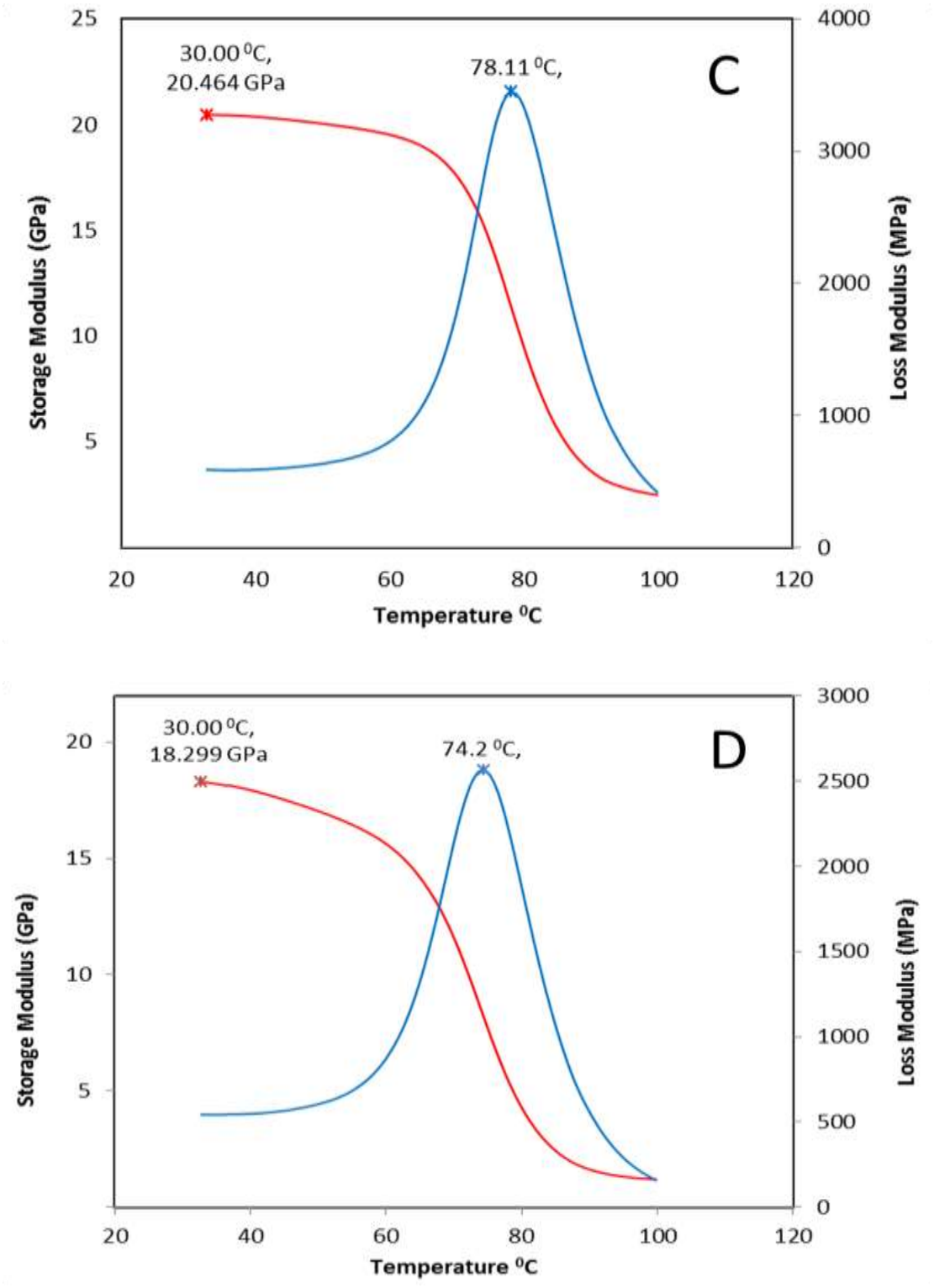

Figure 4.8: Variation in loss modulus T_g value and storage modulus peak value for the determination of composite cure in (a) initial GFRC, (b) initial 1 wt. % nanoclay/GFRC (c) reheated GFRC, and (d) reheated 1 wt. % nanoclay/GFRC laminates

The lower increase in the loss modulus T_g for all the hybrid nanoclay/GFRC laminates was justified by proper crosslink density of nanoclay with the epoxy during the curing process. This prevents the relaxation of molecules in the matrix of the composite laminates. Hence, clay filled GFRC laminates was more fully cured than the GFRC laminate.

Table 4.6: T_g values and degree of cure of neat GFRC and hybrid nanoclay/GFRC materials

Materials (GFRC)	Cure properties					
	Initial heating		Final heating		Change in T_g (^{0}C)	Degree of cure (%)
	Peak Area (MPa*min)	T_g (^{0}C)	Peak Area (MPa*min)	T_g (^{0}C)		
Neat	20001 ± 603	67.58	15847 ± 558	78.11	10.53	74
1 wt. % Clay	16182 ± 419	67.58	13254 ± 299	74.2	6.62	78
3 wt. % Clay	16433 ± 424	67.79	13442 ± 302	74.55	6.76	78
5 wt. % Clay	19120 ± 562	66.23	15001 ± 480	75.48	9.25	73

Reduction in the storage modulus also occurred after reheating both neat and hybrid nanoclay/GFRC laminates. As mentioned in chapter 3, section 3.5.3, the materials have lost some strength at the first heating process. However, by ramping up the samples again, the specimens' stiffness at this time was lower in comparison to their initial stiffness. The specimens were therefore left with residual stiffness, which were obtained after the second heating. The residual stiffness in the samples produced lower storage moduli; these were recorded in Table 4.7 for all storage moduli at reheating of the samples. The highest reduction in storage modulus observed in 5 wt. % hybrid nanoclay/GFRC laminate by about 16 GPa, while the neat GFRC laminates reduced by about 12 GPa. From this occurrence, it can be said that uncured properties in all specimens cured with respect to the second heating of the composite material. This gave some of the material a hedge over the others in terms of the residual strength of the composite laminates. The observation

with lowest storage modulus reduction was found in 1 wt. % clay loading by about 8 GPa.

Table 4.7: Storage modulus cure properties of neat GFRC and hybrid nanoclay/GFRC materials

Materials (GFRC)	Storage modulus properties		
	Initial heating (GPa)	Final heating (GPa)	Reduction (GPa)
Neat	32.3	20.46	11.48
1 wt. % clay	25.86	18.3	7.56
3 wt. % clay	25.39	15.49	9.9
5 wt. % clay	27.25	11.76	15.49

The degree of cure was however calculated from the percentage difference of the cured to uncured values derived from the initial and final area of the integrated peak values of the DMA loss modulus. The loss modulus integrated peak values of the materials at the first and second stage of their heating process for the determination of composite cure in the neat GFRC and hybrid nanoclay/GFRC were recorded in Table 4.5. However, the degree of cure (α) was calculated using the formula in equation (4.1).

$$\alpha = \left[1 - \frac{(A_{initial} - A_{final})}{A_{final}}\right] \times 100 \qquad (4.1)$$

Where; $A_{initial}$ and A_{final}, are the area of the integrated peak value of the Initial and final Loss Modulus peak. Changes in area of the Loss Modulus peak over its final area was subtracted from the fully cured value to calculate the percentage value of composite cure in unfilled and clay filled GFRC laminates.

The composite cure percentage value was observed to have increase with increase in clay ratio in the GFRC up to 3 wt. % but further reduced at 5wt%

clay addition. This was as a result of the plasticization effects at the clay-epoxy interphase in the presence of the clay surfactant, with reductions being more pronounced in systems of high clay loading [202, 203]. The degree of cure derived from the loss modulus value, showed that the composite was observed to be more fully cured with the addition of nanoclay up to 3 wt. % in the GFRC laminate. The highest degree of cure is 78%, which is 4% higher than neat GFRC laminate.

4.5 MECHANICAL PROPERTIES OF HYBRID NANOCLAY/GFRC

4.5.1 Tensile properties

Tensile properties of neat GFRC and hybrid nanoclay/GFRC are shown in Table 4.8. Tensile strength of the neat GFRC laminate was 332 MPa, while that of the hybrid nanoclay/GFRC laminates were 370 MPa, 360 MPa and 357 MPa, for composite with 1 wt. %, 3 wt. % and 5 wt. % respectively. The higher stress values found in all nanoclay/GFRC samples indicate significant improvement. It was observed that 1 wt. %, 3 wt. % and 5 wt. % nanoclay/GFRC all improved by 12%, 8% and 7% respectively. The reason for the improvement found in the tensile strength is attributed to the significant effect of clay filler as a result of its homogeneity when dispersed in the resin-epoxy of the composite laminate.

Table 4.8: Tensile Properties of neat and hybrid nanoclay/GFRC materials

Materials (GFRC)	Tensile properties					
	UTS		Modulus		Stain at max. break	
	Mean (MPa)	Increase (%)	Mean (GPa)	Increase (%)	Mean (mm/mm)	Increase (%)
Neat	332 ± 9	-	17.6 ± 0.5	-	0.0276	-
1 wt. % Clay	370 ± 6	12	19.8 ± 0.3	13	0.0299	8.3
3 wt. % Clay	360 ± 5	8	20.6 ± 0.2	17	0.0296	7.3
5 wt. % Clay	357 ± 8	7	18.4 ± 0.5	6	0.0295	6.9

Figure 4.9 shows linear trends in the stress-strain curves in the neat GFRC and hybrid nanoclay/GFRC laminates until their ultimate strength is reached. According to the varying weight percentage of clay content in the hybrid nanoclay/GFRC as shown in Figure 4.10, higher tensile stress levels were observed in the stress versus strain curve of the hybrid nanoclay/GFRC when compared to neat GFRC. Owing to the observed result, it has been previously observed by Withler [169], that tensile properties of Cloisite 30B nanoclay epoxy GFRC laminate was increased slightly at 2 wt. % but decrease by more addition of nanoclay filler. The strength reduction found Cloisite 30B nanoclay epoxy GFRC laminate was also consistent with some other research studies [204, 205]. From the studies, it was explained that the addition of more filler may have led to incomplete dispersion and thus more agglomerations of the clay, causing reduction in the mechanical properties [206, 207]. However, the case was quite different in the tensile properties observed in this research work.

The tensile strength and modulus shown in Figure 4.10 and Figure 4.11 at all nanoclay/GFRC loading were higher than the neat GFRC properties. In the tensile modulus, GFRC laminate at 1 wt. %, 3 wt. % and 5 wt. % clay addition gave modulus of 19.8 GPa, 20.6 GPa and 18.4 GPa respectively; while neat GFRC modulus was 17.6 GPa. The tensile modulus percentage increase was in the order of 13%, 17% and 6% accordingly. In the tensile properties of composite materials, there is a diverse improvement as a result of the nanoclay dispersion in the matrix of the laminates. The evidence of these improvement can be found on the stress versus strain curve in Figure 4.9. Form the sub-image of the stress versus strain curve that 3 wt. % nanoclay/GFRC laminate sample exhibit better slope at the elastic region. However, 1 wt. % nanoclay/GFRC laminate sample progresses as the slope move to the plastic region. It was apparent that nanoclay was homogeneously dispersed in the epoxy through magnetic stirrer, with which agglomeration of the clay was avoided. This caused an improvement in the properties of hybrid nanoclay/GFRC laminates at all clay loading. The higher value of tensile strength found in 1wt% was a result of the full homogeneous dispersion of

clay in the polymer matrix. However, the lower percentage of nanoclay at 1 wt. % could not influence the stiffness as much as 3 wt. % clay loading. The improved modulus can be attributed to the stiffening enhancement effect of clay fillers in the nanoclay/GFRC, since clay has higher modulus properties than epoxy. The reduction in the storage modulus above 3 wt. % could be attributed to an intercalated nanocomposite structure at 5 wt. % clay loading. Although, agglomeration of clay platelets was avoided during preparation/mixing of clay/resin-epoxy to prevent formation of microstructures during the VARIM process of the nanoclay/GFRC laminates. Hence, full dispersion could not be totally achieved at higher clay loading.

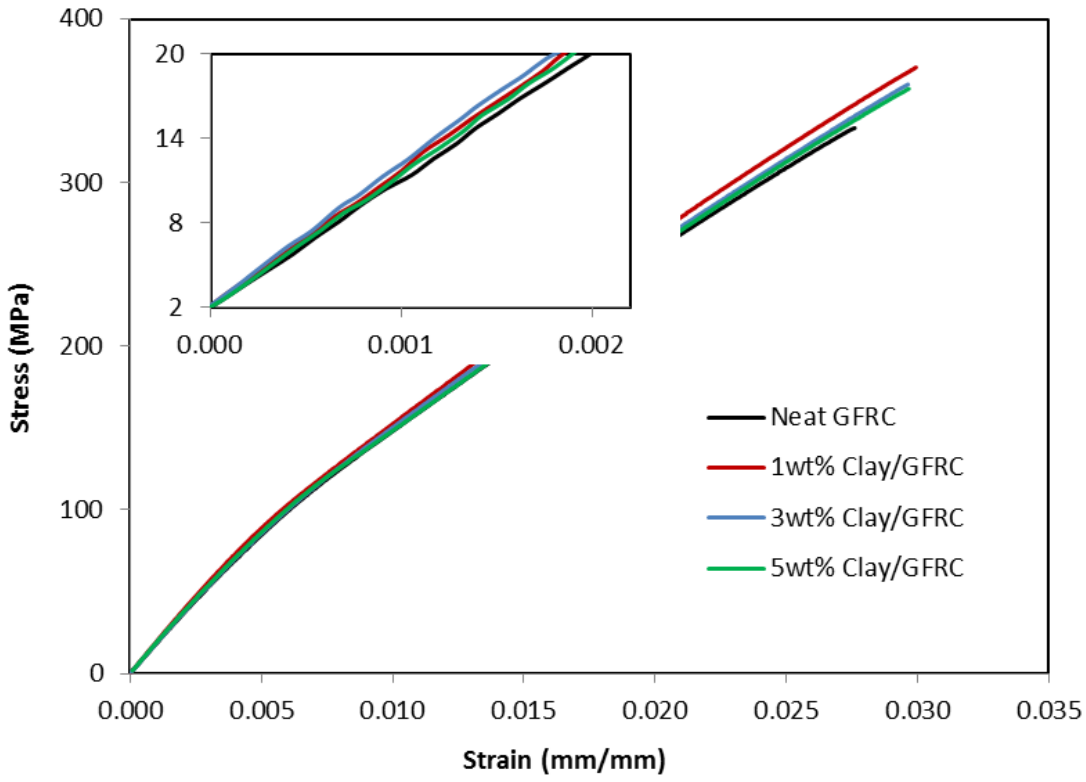

Figure 4.9: Tensile stress versus strain curve of neat and hybrid nanoclay/GFRC materials

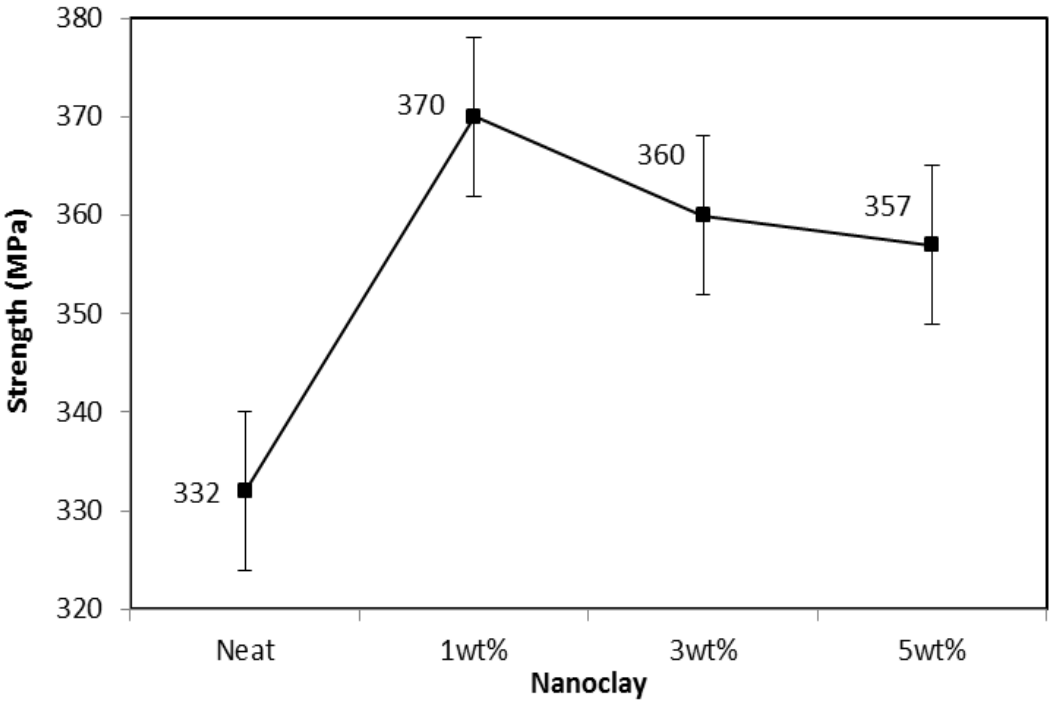

Figure 4.10: Ultimate tensile strength of neat and hybrid nanoclay/GFRC materials

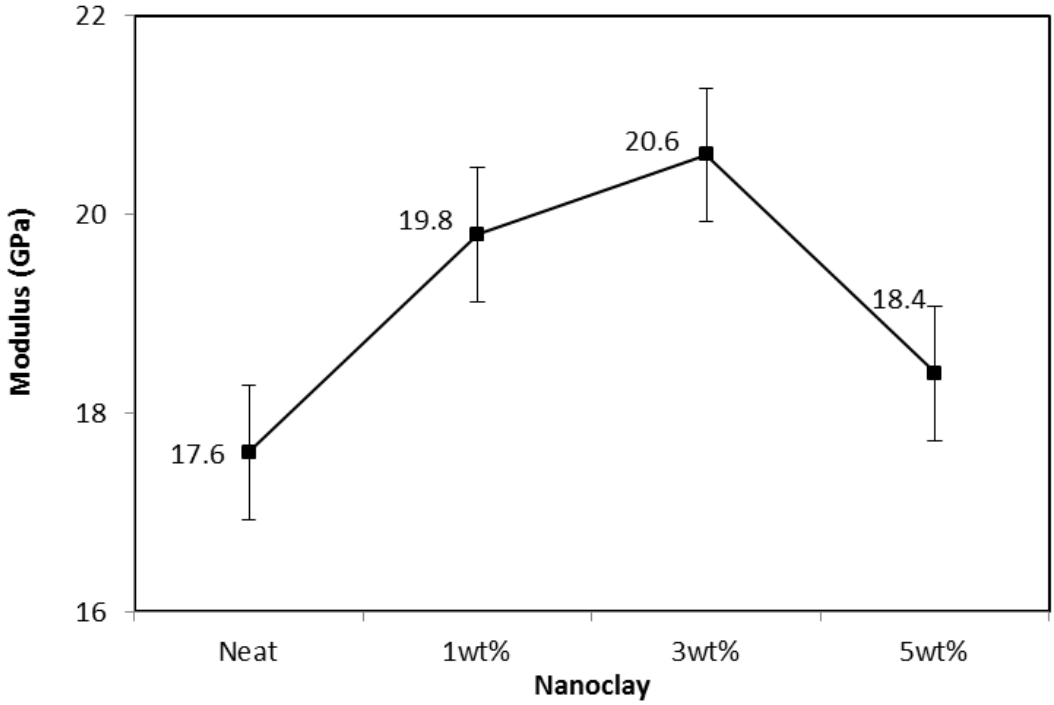

Figure 4.11: Tensile modulus of neat and hybrid nanoclay/GFRC materials

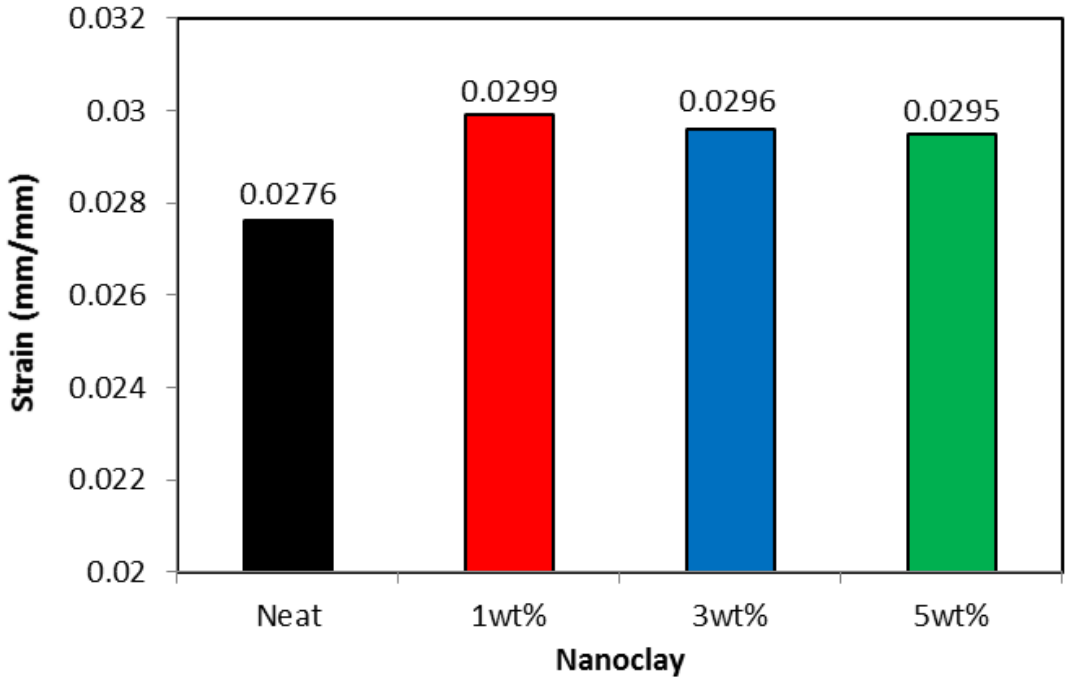

Figure 4.12: Strain at maximum stress of neat and hybrid nanoclay/GFRC materials

Higher failure strains were also observed in hybrid nanoclay/GFRC laminates when compared to neat GFRC laminates. The evidence of this failure strain is shown in Figure 4.13. The increase can be described to the crosslink effect of clay and the epoxy within the laminate, which aggravated ductile behaviour in the hybrid nanocomposite, leading to significant plasticity of the material. It can also be attributed to the homogeneous dispersion of clay in the resin-epoxy, with an evidence of highest strain found in nanoclay/GFRC material at 1 wt. % clay loading. The materials undergo longer strain in 1 wt. % nanoclay/GFRC with favourable increases in the extension before they breaks.

To further understand the enhancing mechanism, the failure surfaces of the samples were examined using optical scanning microscope (OSM). The fracture behaviour in the tensile specimen was observed to determine the effect of nanoclay in the hybrid nanoclay/GFRC laminates and compared with the neat GFRC. It was found in Figure 4.13a, that the neat woven GFRC failure surface was smooth as it shattered; an indication of matrix cracking

leading to fiber fracture was the failure mechanism, which led to the brooming of the fiber at final fracture. However, there was a different observation in the sample with nanoclay shown in Figure 4.13b. The hybrid nanoclay/GFRC tensile fracture sample has an interface deformation as the nanoclay/resin-matrix bonded to the surface of the fibers. From the observation, the resin-matrix glued the fiber ‘warp’ to the ‘weft’ as the specimen fractured, rather than shattering like neat GFRC. From this result, it can be depicted that the fiber was surrounded by the matrix and consequently, fiber/matrix fracture can only be considered as the failure mechanism. The application of nanoclay enhanced the binding effect of the matrix by improving the fracture properties of the hybrid nanoclay/GFRC laminates. This showed that both fiber and nanoclay act as hybrid reinforcement in the nanoclay/GFRC laminates.

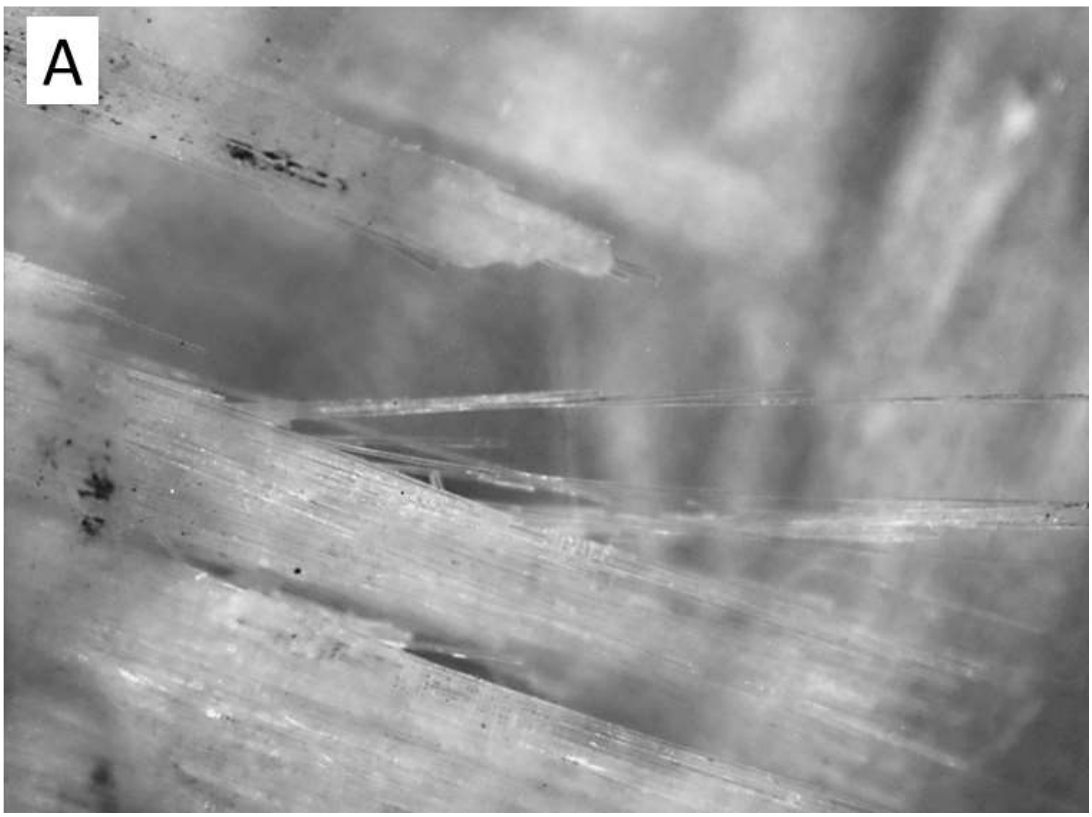

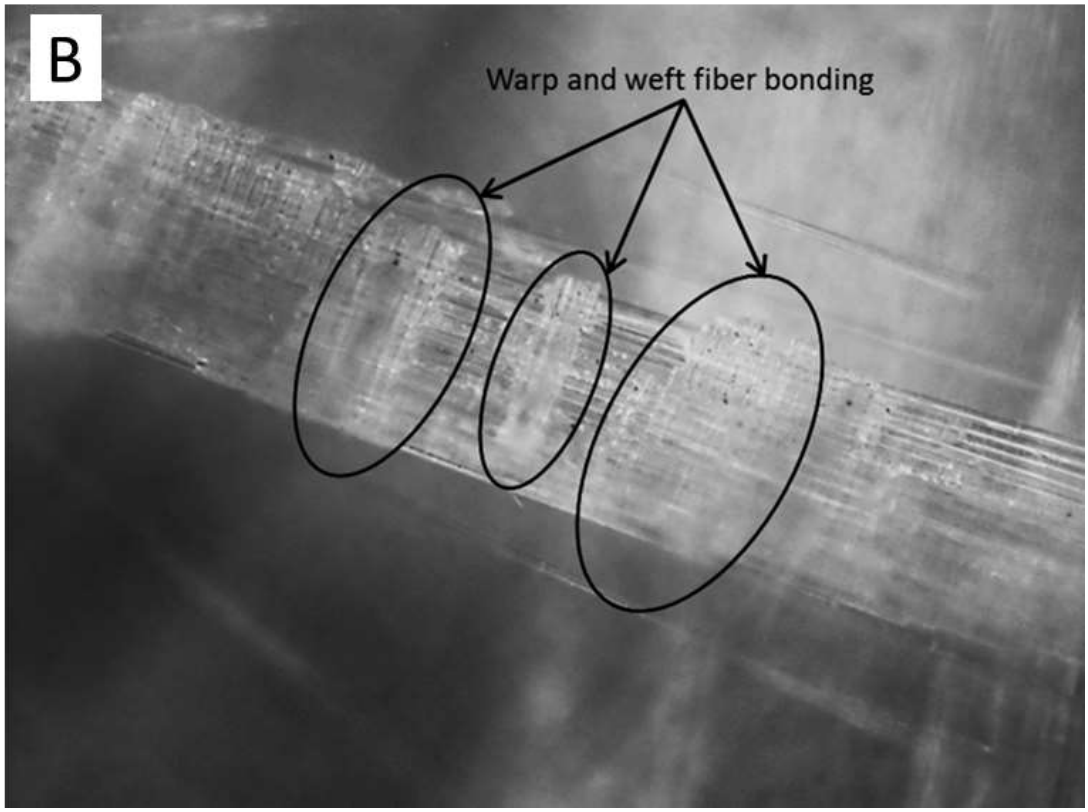

Figure 4.13: Optical micrograph showing tensile fracture surface of: (a) Neat GFRC and (b) hybrid nanoclay/GFRC laminate specimens

4.5.2 Flexural properties

Flexural tests were performed to evaluate the strength and stiffness of neat GFRC and hybrid nanoclay/GFRC laminates. The average flexural properties of the neat GFRC and hybrid nanoclay/GFRC obtained from these tests are recorded in Table 4.9. During the test, some samples failed rapidly before the strain of 5.0% after experiencing their maximum load, showing brittle nature of failure; while in some other cases, when a maximum strain of 5.0% was reached, the test was stopped and maximum strength were considered for such cases. Typical stress versus strain behaviours from the 3-point bending flexural test are shown in Figure 4.14. The curve showed a nonlinear deformation before reaching the maximum stress and the evidence of the irregularities in the curve can be related to random fiber breakage during the flexural loading.

Table 4.9: Flexural properties of neat and clay hybrid GFRC materials

Materials (GFRC)	Flexural properties					
	Flexural strength		Modulus		Strain at max. stress	
	Mean (MPa)	Increase (%)	Mean (GPa)	Increase (%)	Mean (mm/mm)	Increase (%)
Neat	335 ± 7	-	16.1 ± 0.1	-	0.0278	-
1 wt. % Clay	388 ± 12	16	19.3 ± 0.4	20	0.031	12
3 wt. % Clay	396 ± 5	18	20 ± 0.2	24	0.0315	13
5 wt. % Clay	356 ± 10	6	18 ± 0.5	12	0.0248	-11

Flexural Strength as well as the flexural modulus shown in Figure 4.15 and 4.16 for all hybrid nanoclay/GFRC samples are larger than the neat GFRC sample. From the test result, it was found that 3 wt. % nanoclay/GFRC depicted the highest strength and modulus values of 396 MPa and 24 GPa respectively; which are 18% and 24% higher than the neat GFRC values. The improvement in flexural properties could be attributed to the improved matrix and interfacial properties due to nanoclay addition as previously reported by Wetzel [208]. Flexural strain at maximum strength as shown in Figure 4.17 was increased up to 3 wt. % clay loading and decreased at 5 wt. % clay loading when compared to the neat GFRC strain value. It can be depicted from the strain values that the addition of clay into the epoxy appears to be more effective at low content. The detrimental effect of clay content higher than 3 wt. % in the composite may arise from the formation of clay agglomerates in the epoxy. Therefore, clay agglomerations are particularly harmful to the fiber-matrix interfacial adhesion, which has more significant influence on the flexural strain of the hybrid nanoclay/GFRC materials.

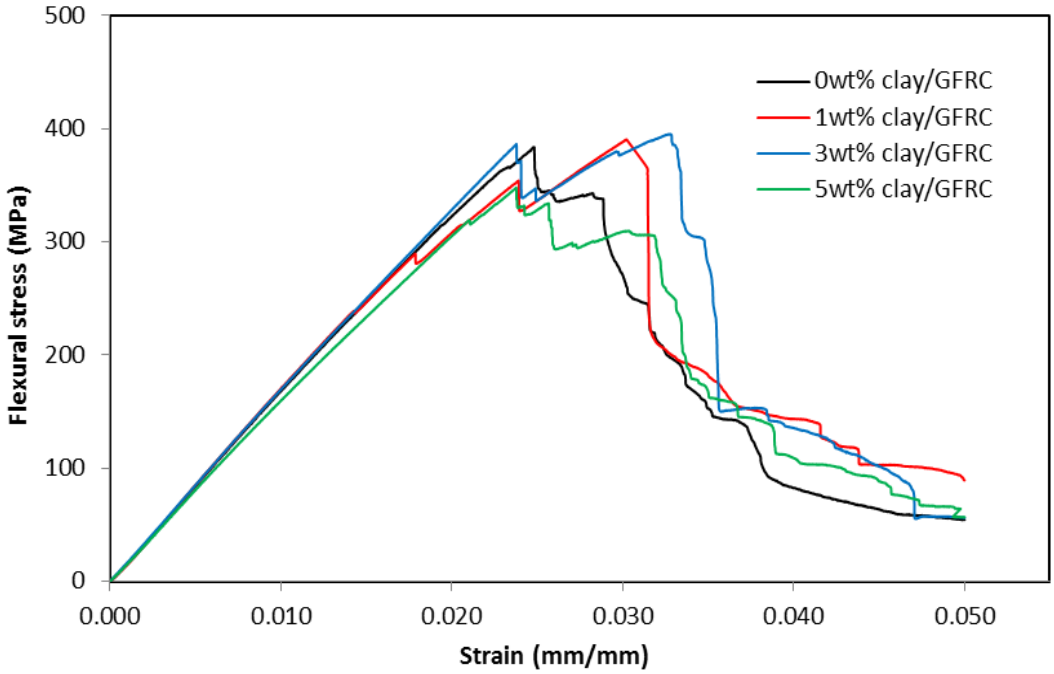

Figure 4.14: Flexural stress versus strain curve of neat and hybrid nanoclay/GFRC materials

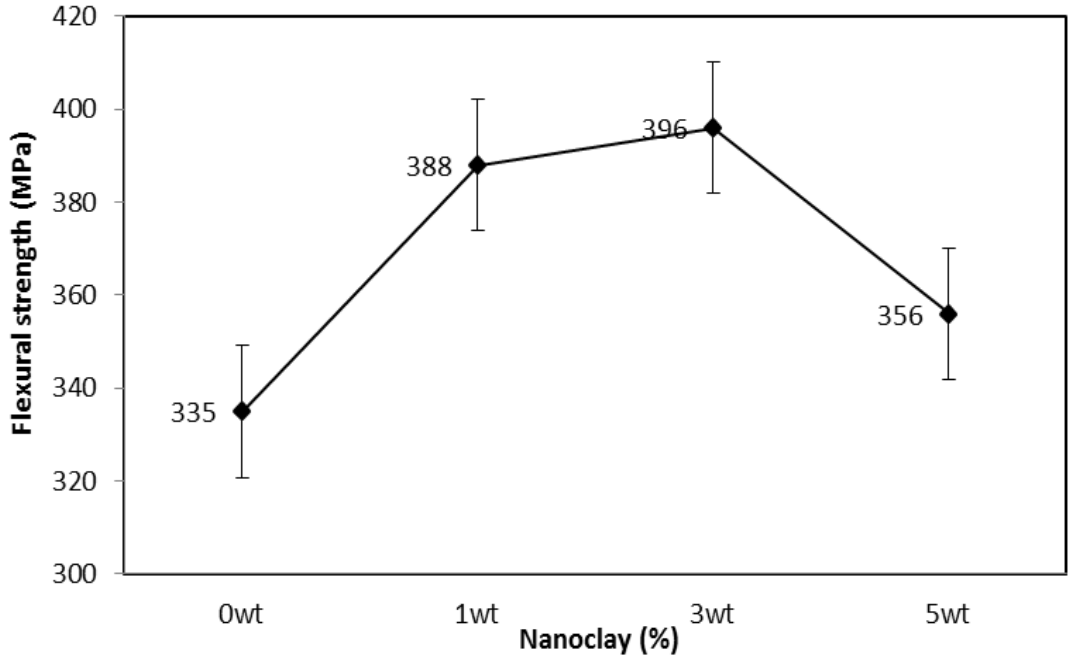

Figure 4.15: Flexural strength of neat and hybrid nanoclay/GFRC materials

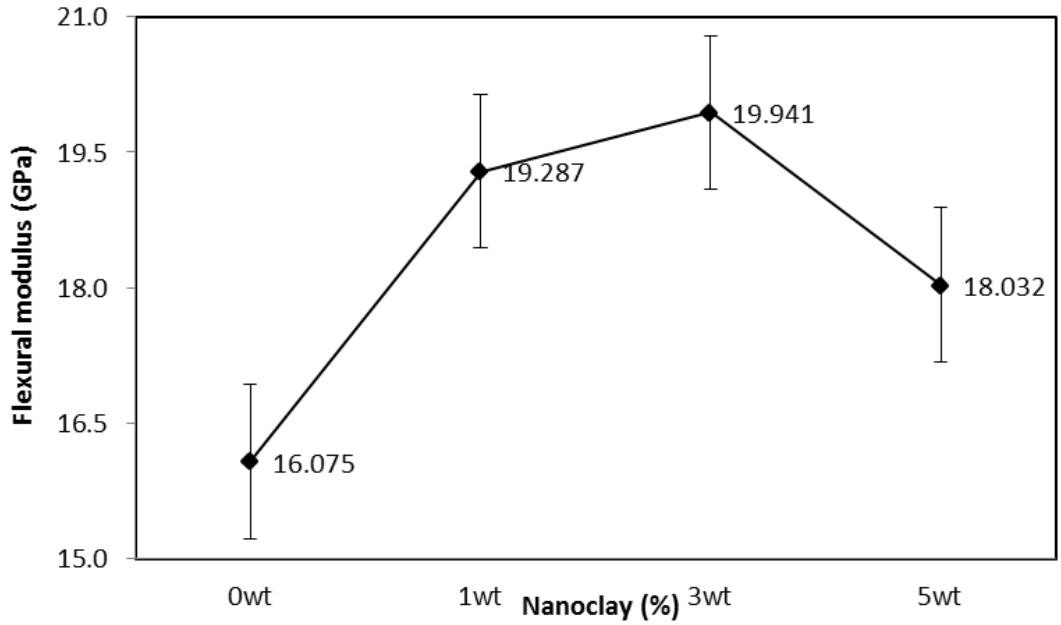

Figure 4.16: Flexural modulus of neat and hybrid nanoclay/GFRC materials

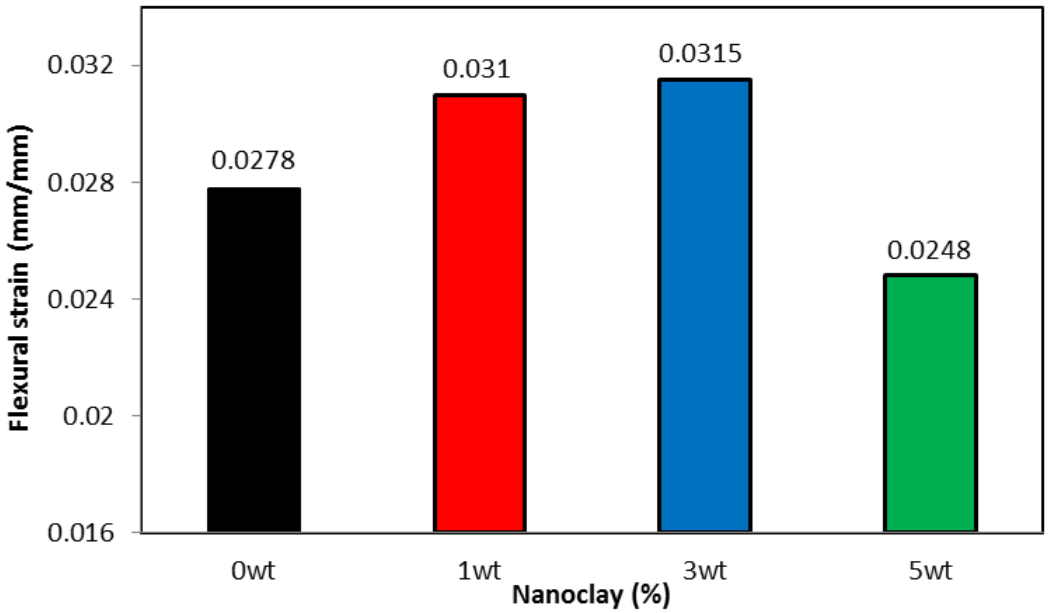

Figure 4.17: Flexural strain of neat and hybrid nanoclay/GFRC materials

Results from SEM study provide evidence to support quantitative results obtained through the flexural test of the neat GFRC and the hybrid nanoclay/GFRC composites. Their fracture surfaces are shown in Figure 4.18a to 4.18d. The fracture mode in the neat GFRC is quite different from the hybrid nanoclay/GFRC. In Figure 4.18a, the neat GFRC sample suffered

severe fiber breakage in form of tensile mode up to the mid-section of the laminate; while fiber shrinkage is the form of damage mode that occur at the compressive section. On the other hand, as shown in Figure 4.18b and 4.18c, inter-layer delamination was the damage mode that occurred in the hybrid nanoclay/GFRC. These occurred at 1 wt. % and 3 wt. % clay loading. It is evident that excellent bridging effect in the interfacial region of the nanoclay, matrix and fiber was observed. This shows that the nanoclay in the laminate, promotes good interfacial bonding between the matrix and the fiber.

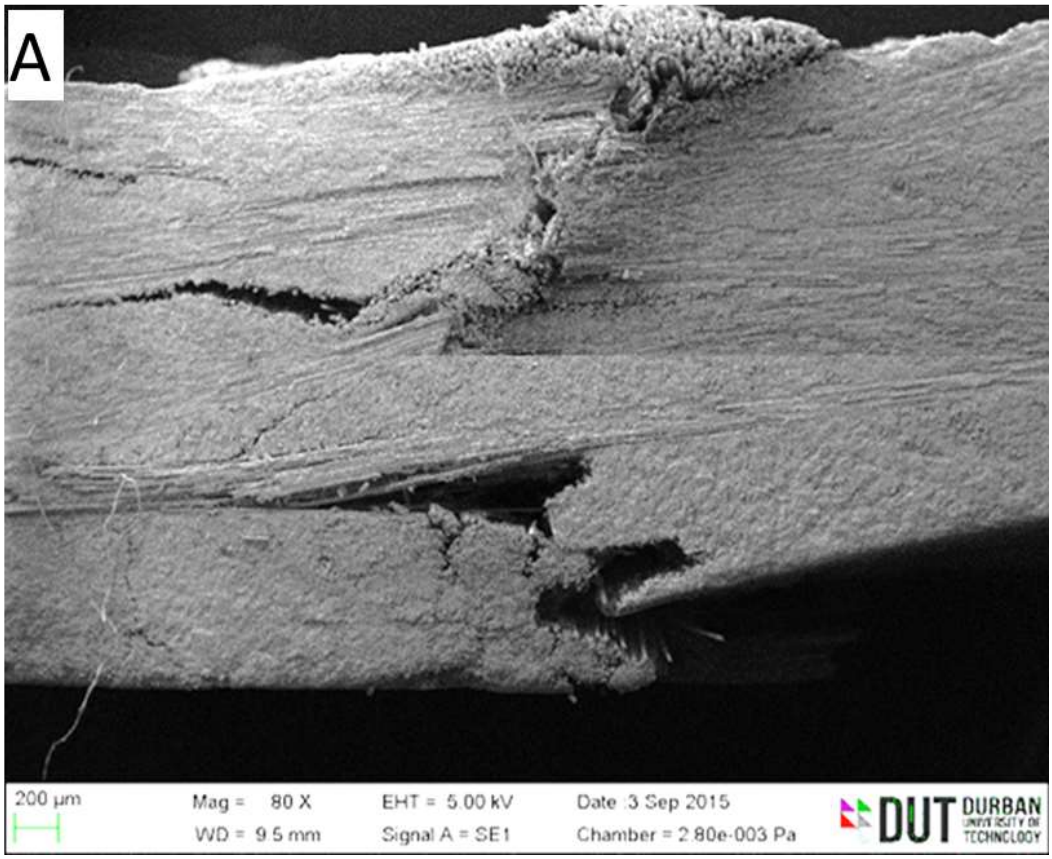

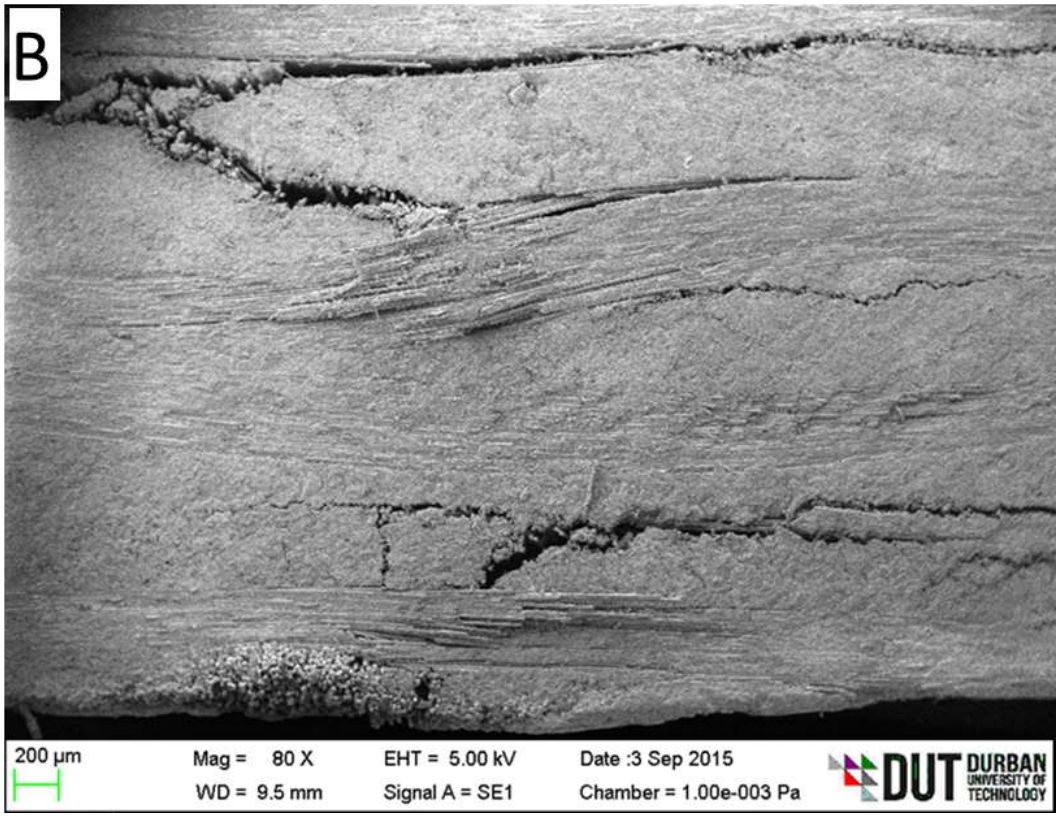
B
200 µm
Mag = 80 X
EHT = 5.00 kV
Date :3 Sep 2015
WD = 9.5 mm
Signal A = SE1
Chamber = 1.00e-003 Pa
DUT DURBAN UNIVERSITY OF TECHNOLOGY

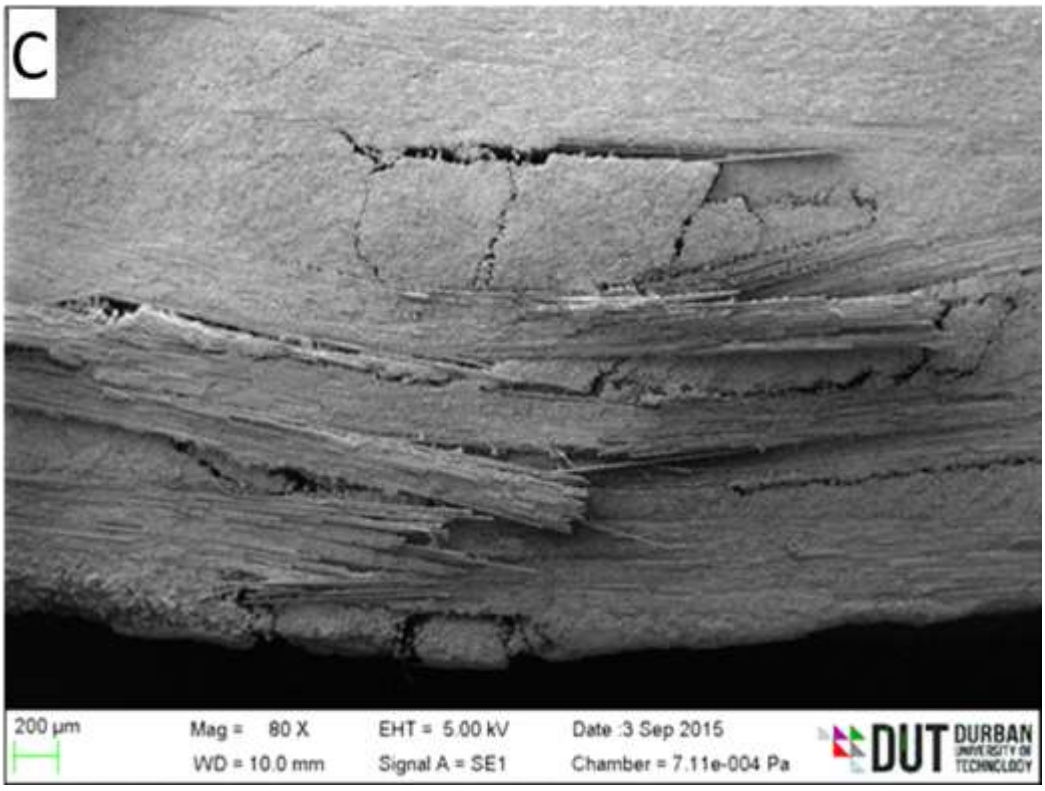
C
200 µm
Mag = 80 X
EHT = 5.00 kV
Date :3 Sep 2015
WD = 10.0 mm
Signal A = SE1
Chamber = 7.11e-004 Pa
DUT DURBAN UNIVERSITY OF TECHNOLOGY

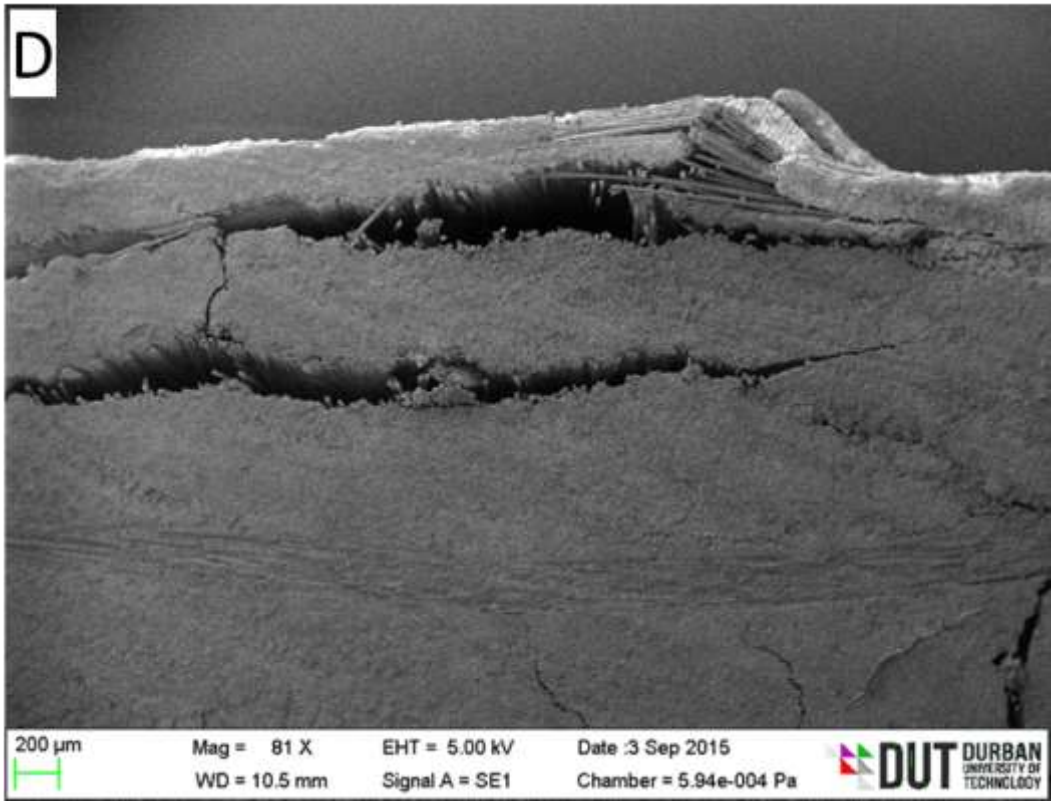

Figure 4.18: SEM micrograph showing flexural fracture surface of: (a) neat GFRC, (b) 1 wt. % nanoclay/GFRC, (c) 3 wt. % nanoclay/GFRC and (d) 5 wt. % nanoclay/GFRC laminate specimens

From the hybrid nanoclay/GFRC at 5 wt. % clay loading shown in Figure 4.18d, the higher percentage nanoclay in the composite laminate caused stress concentration. This act as crack initiation sites that led to delamination and fiber fracture of the composite laminate. The present of nanoclay on the composite up to 3 wt. % clay loading, have shown good interfacial adhesion of the clay/matrix interaction. The better fiber/matrix interfacial bonding and delamination propagation resistance found at 3 wt. % clay loading resulted in higher strength and improvement of modulus of elasticity of the hybrid nanoclay/GFRC laminates.

4.5.3 Impact properties

Impact strength properties of the hybrid nanoclay/GFRC measured by charpy impact test were recorded in Table 4.10. The impact strength of the neat GFRC, as well as the corresponding hybrid nanoclay/GFRC is as shown in

the Figure 4.19. It was apparent that the impact resistance of the neat GFRC laminate was 201 KJ/m^2. At the addition of nanoclay, impact resistance was increased at all varying clay loadings, with the highest impact resistance of 314 KJ/m^2, observed at 3wt% clay loading. This gave 50% impact resistance increase. The impact strength, however, decreased to 268 KJ/m^2 at 5wt% clay loading. This was therefore classified as a diminished improvement.

Table 4.10: Impact fracture resistance properties of neat and clay hybrid GFRC materials

Materials (GFRC)	Impact properties	
	Mean (kJ/m^2)	Increase (%)
Neat	210 ± 24	-
1 wt. % Clay	254 ± 25	21
3 wt. % Clay	314 ± 27	56
5 wt. % Clay	268 ± 21	28

The reduction at 5wt% clay loading as a result of diminished improvement was attributed to the high possibility of agglomeration of the clay in the epoxy, which in turn reduced the energy absorbing efficiency in the hybrid nanoclay/GFRC materials. It is worth mentioning that the high impact resistance values of the hybrid nanoclay/GFRC at 3wt% clay loading over the corresponding neat GFRC material, depict great improvement of the composite material.

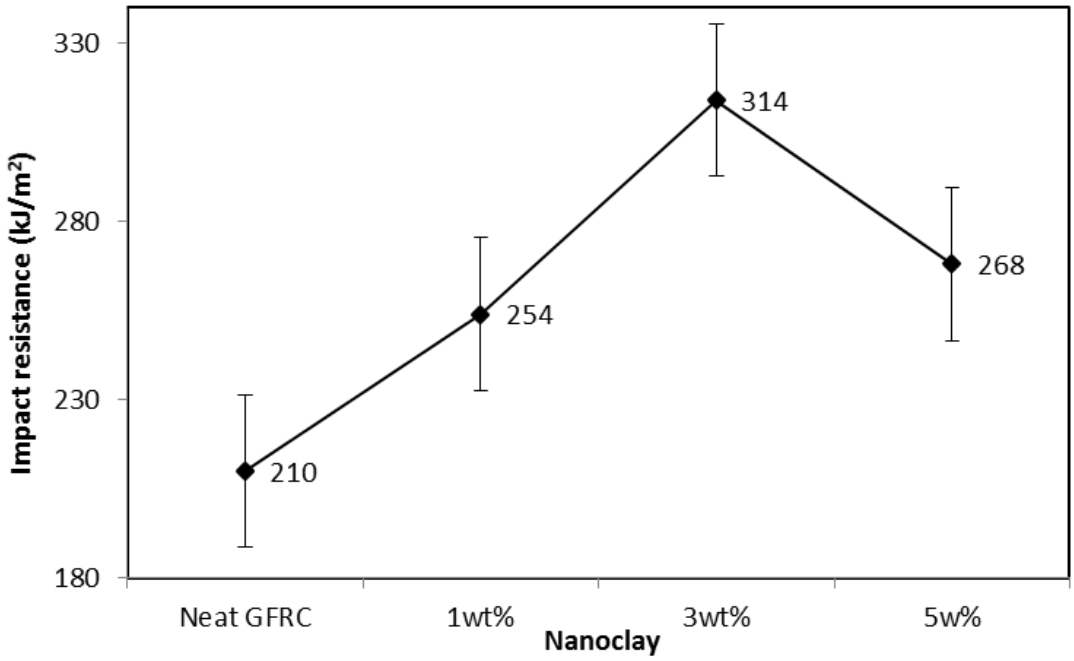

Figure 4.19: Impact fracture toughness of neat and hybrid nanoclay/GFRC materials

SEM images taken for the neat GFRC and the hybrid nanoclay/GFRC materials were presented in Figure 4.20a – 4.20d. From the image shown in the Figure 4.20a, the neat GFRC exhibited a typical fiber separation after the impact test, leaving the impact surface to exhibit a scattered brittle failure. Fracture became difficult as soon as clay is being added to the GFRC. This can be observed in Figure 4.20b, showing fiber and matrix separable resistance as they stuck together at 1wt% clay loading, with a tough fracture surface induced as a result of clay addition. This fracture resistance is more confirmed in Figure 4.20c as the clay was increased to 3wt%, and was equally observed in 5wt% clay loading in Figure 4.20d. Matrix was found to have glued the fibers together, even after fracture. The total absorbed energy required to break the hybrid nanoclay/GFRC was thought to be dependent on both the matrix and the interface properties between the clay-epoxy/glass-fibers. Therefore, the increase energy at which the hybrid nanoclay/GFRC broke, which was recorded in Table 4.9, was confirmed by with the SEM images.

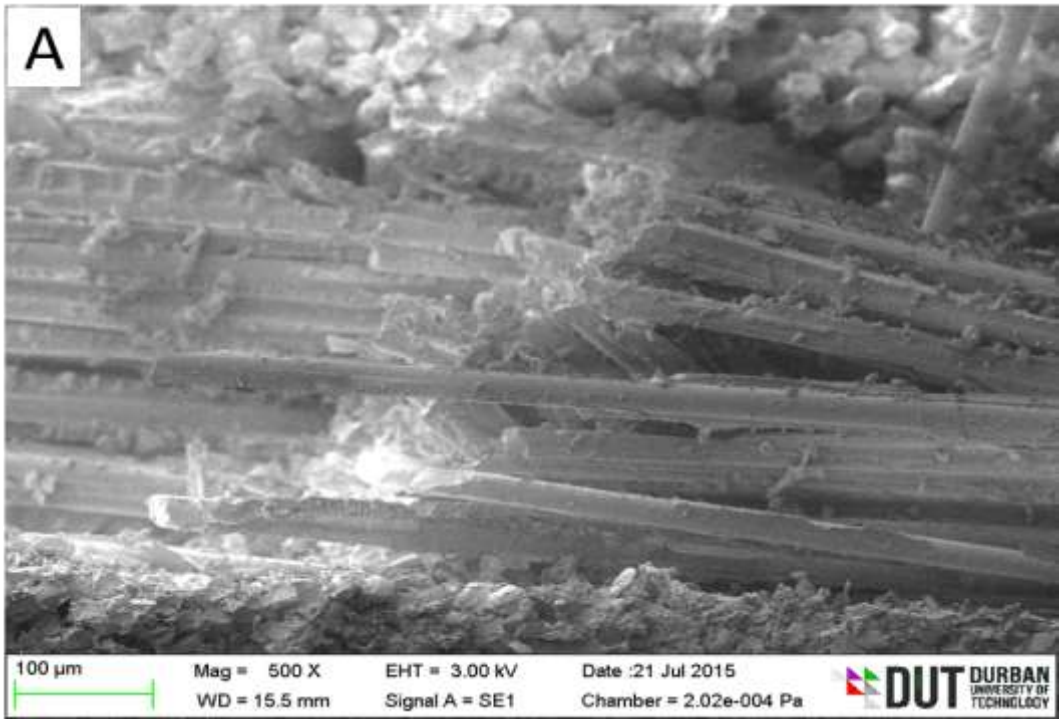
A
100 µm
Mag = 500 X
WD = 15.5 mm
EHT = 3.00 kV
Signal A = SE1
Date :21 Jul 2015
Chamber = 2.02e-004 Pa
DUT DURBAN UNIVERSITY OF TECHNOLOGY

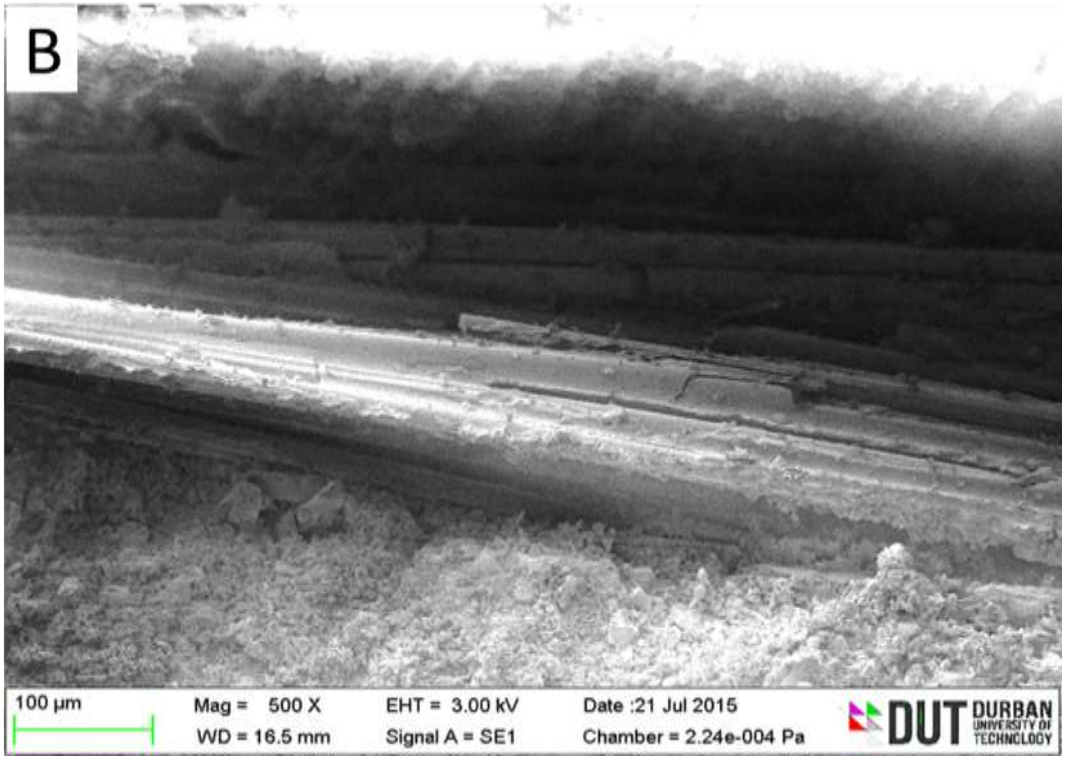
B
100 µm
Mag = 500 X
WD = 16.5 mm
EHT = 3.00 kV
Signal A = SE1
Date :21 Jul 2015
Chamber = 2.24e-004 Pa
DUT DURBAN UNIVERSITY OF TECHNOLOGY

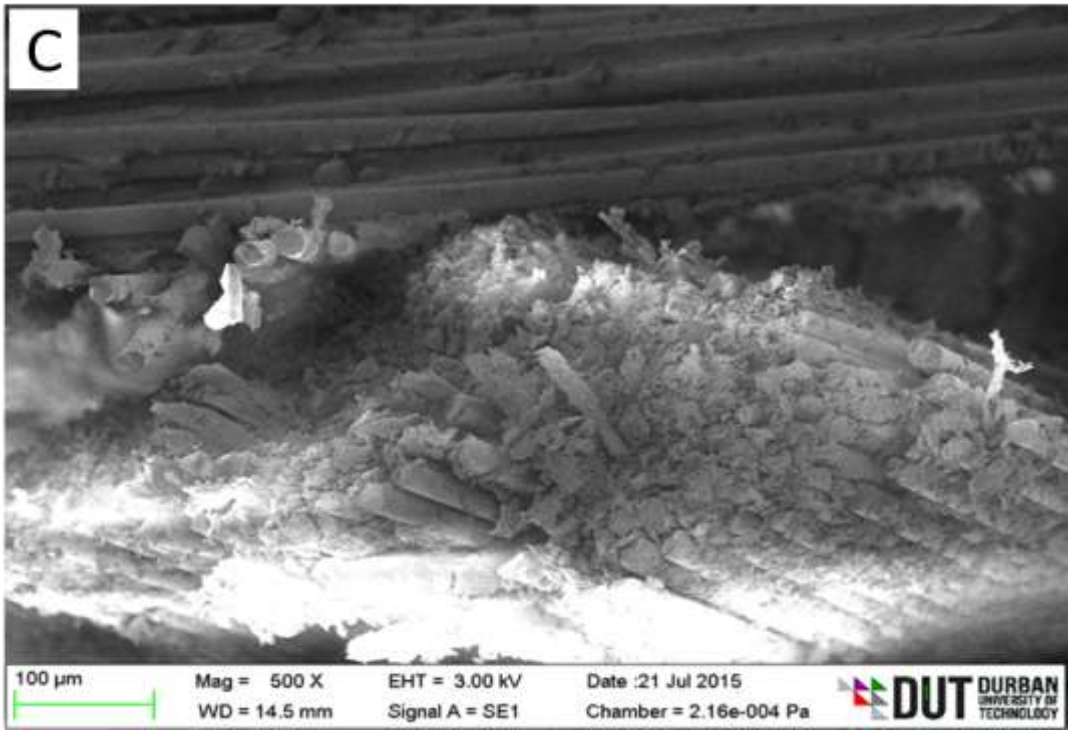

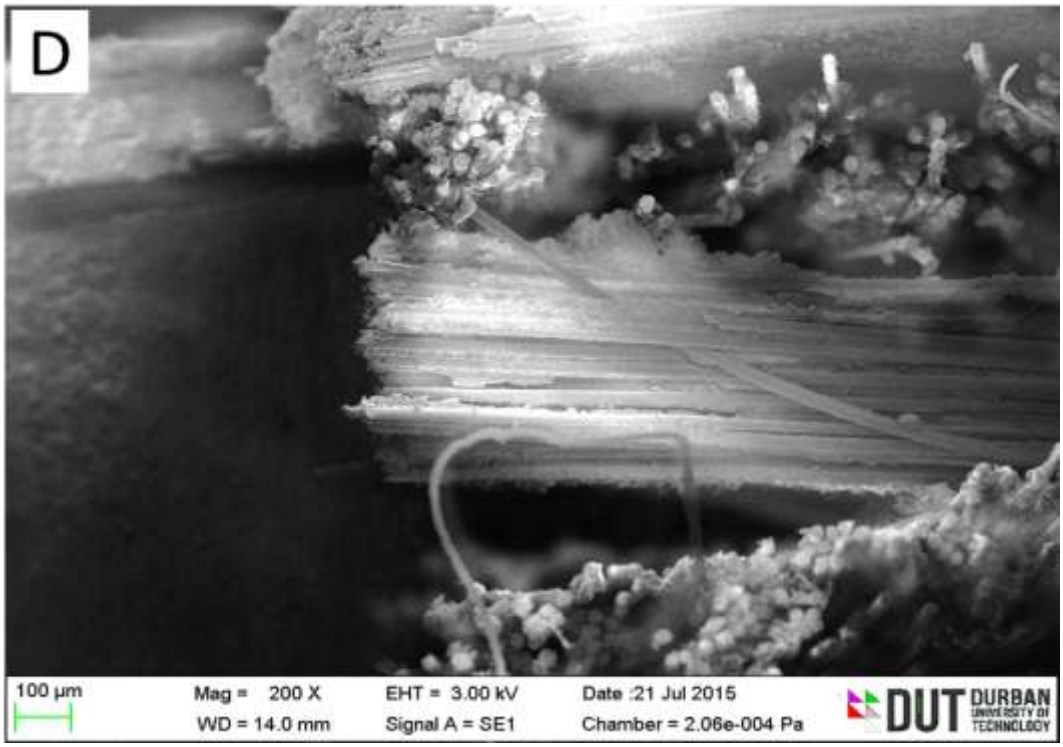

Figure 4.20: SEM micrograph showing impact fracture surface of; (a) neat GFRC, (b) 1 wt. % nanoclay/GFRC, (c) 3 wt. % nanoclay/GFRC and (d) 5 wt. % nanoclay/GFRC laminate specimens

4.5.4 Hardness properties

Hardness test results of the Barcol impresser taken from the surface of the neat and hybrid nanoclay/GFRC were recorded in Table 4.11. Following the ASTM standard prescribed in Section (3.4.1.4), neat and hybrid nanoclay/GFRC samples were all tested ten consecutive times and their averages were taken as the hardness values. All the samples were statistically similar, therefore confirming the accuracy of the VARIM process of the laminate preparation. The addition of 1 wt. % nanoclay gave the best hardness value of 61.8 Hv. The Barcol hardness testing was confirmed to be satisfactory, after ten readings on the materials have produced variance-of-average of 0.8 in 1wt% hybrid nanoclay/GFRC hardness value, having 1.3 as the coefficient of variation value. However, 3wt% hybrid nanoclay/GFRC equally depict a good variation in the hardness reading values closer to that of 1wt% clay loading.

Table 4.11: Barcol hardness properties of neat and hybrid nanoclay/GFRC

Materials GFRC	Barcol hardness properties		
	Hardness value (Hv)	Increase (%)	Coefficient of variation
Neat	56.6 ± 1.5	-	2.7
1 wt. % Clay	61.8 ± 0.8	9.2	1.3
3 wt. % Clay	61.4 ± 1.1	8.4	1.6
5 wt. % Clay	58.2 ± 3.1	3	5.3

The Barcol hardness values with varying weight ratio of nanoclay in GFRC were shown in Figure 4.21. The hardness value increased by 9.2% with the addition of 1wt% nanoclay, but starts to drop as clay weight was increase. 3wt% hybrid nanoclay/GFRC had a hardness value closer to 1wt% hybrid nanoclay/GFRC material. The reduction at 3 wt. % was as a result of higher clusters found in the clay/resin-matrix when compared to 1 wt. %. It can be

established that both 1wt% and 3wt% hybrid nanoclay/GFRC hardness values are commendable as materials with better surface toughness. The agglomeration of clay particles at 5wt% loading in the matrix provided variations in the hardness values, leading to a higher coefficient of variation.

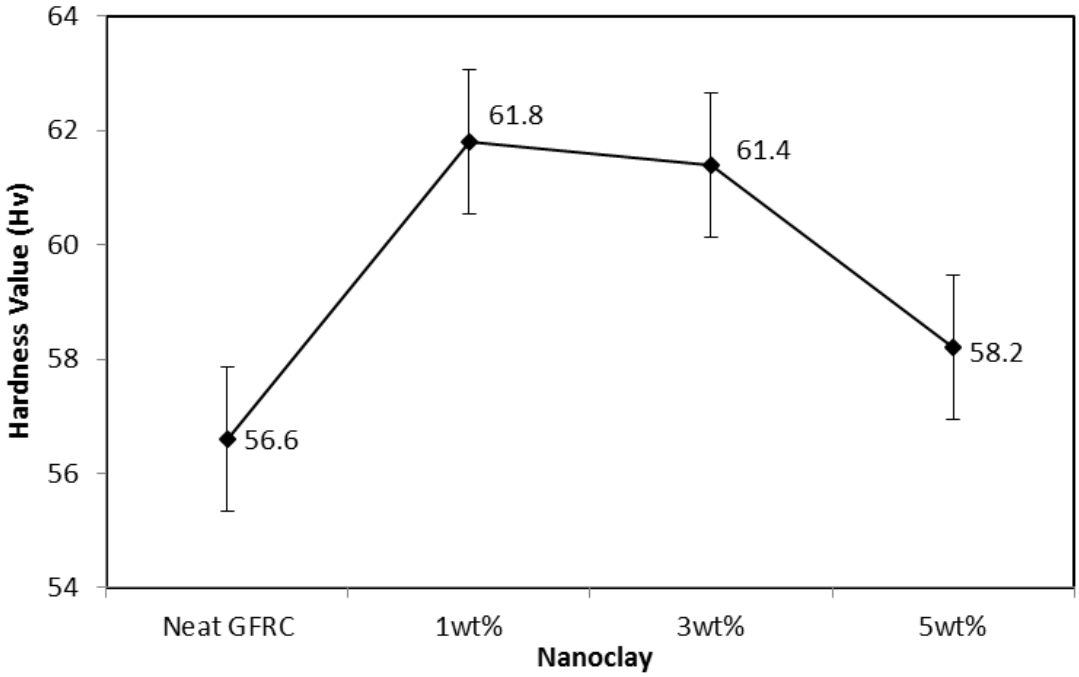

Figure 4.21: Hardness value of neat and hybrid nanoclay/GFRC materials

4.6 FATIGUE PROPERTIES OF HYBRID NANOCLAY/GFRC

4.6.1 Fatigue properties

Tension-tension (*t-t*) fatigue test was carried out on neat and hybrid nanoclay/GFRC on the MTS servo-hydraulic machine operated under applied stress control mode at a frequency of 3 Hz. The specimens for the fatigue test were cut from the same laminates used in the quasi-static tensile test. On the basis of load histories for the prediction of fatigue life of the composite material, strength requirement calculated in terms of stress ratio R = ($\sigma_{min}/\sigma_{max}$) = 0.1 for all the test specimen were employed in the fatigue testing. In order to verify the fatigue strength of the fiberglass material, three different loading conditions at 80%, 60% and 45% stress levels were considered as previously stated in section 3.6.2 of chapter 3. Several fatigue tests coupons of four specimens each were conducted for the neat and hybrid

nanoclay/GFRC laminates at all stress levels. The fatigue test appeared to exhibit crack initiation, crack growth and delamination leading to failure of the materials. To understand the fatigue stress level loading conditions, Talreja [209] had described the fatigue failure mechanisms in three regions: at high loads, leading to fiber failure; at medium loads, leading to combined matrix and interface failure; and at low loads, leading to matrix cracking. He proclaimed that the damage mechanisms were observed to be different in the different regimes of the *S-N* curve; by which, accelerating the fatigue tests into another regime and estimating between the different regimes might lead to wrong results.

4.6.2 Fatigue crack growth (FCG)

Fatigue crack growth (FCG) of the neat GFRC and hybrid nanoclay/GFRC materials was monitored by studying the matrix crack growth rate within the laminate. The crack growth was monitored at the cyclic low stress levels (45%). At the beginning of the fatigue cycle, multiple cracks were initiated at the edge and surface of the specimen. These cracks were considered negligible because they were so small in length (less than 5 mm). Since the initiation of cracks, growth and propagation were the primary concern in the fatigue test, the cracks initiation in the laminate were considered full cracks as soon as the length grew up to about 5 mm. At the growth of full crack length, with increasing loading of the specimen, numbers of cracks observed were counted from specific marked length of 50 mm along the specimen gauge length. The specimens were unloaded to determine the number of cracks throughout the marked areas. These were done visually and periodically as the cycle increased with the propagation of more cracks along the marked areas. The cracks were taken at different intervals to calculate crack densities (CD), which were plotted against the number of cycles. After the numerous cracks have been recorded, the laminate specimens were subjected to continuous fatigue at stress amplitude until fracture occurred. It was observed that the cracks grew rapidly in neat GFRC laminate specimens with more CD than hybrid nanoclay/GFRC laminate specimens. There was no evidence of saturated FCG in neat GFRC before fatigue fracture. However, saturation of

FCG was reached around 400,000 to 500,000 cycles in hybrid nanoclay/GFRC laminates before fracture occurred. Figure 4.22 shows the matrix CD over the number of cycles. This relationship between the CD and the cyclic number was achieved at a lower stress level of 45% fatigue loading.

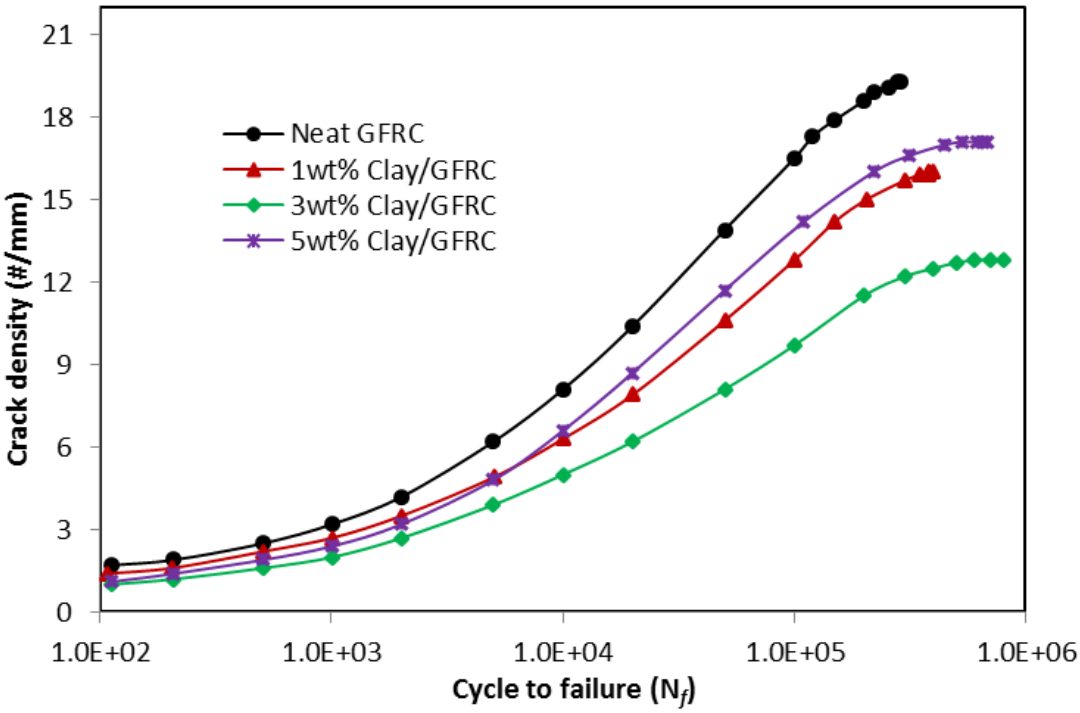

Figure 4.22: Matrix crack density evolution in neat GFRC and hybrid nanoclay/GFRC laminate specimens at 45% stress level

Before the saturation of the FCG was reached in the hybrid nanoclay/GFRC laminates, the crack growth rate was observed to be reducing to negligible values, which was considered as the fatigue threshold. At the fatigue threshold, some of the cracks in the transverse section began to couple along the gage length section with other transverse cracks. The coupling of the cracks led to the formation of delamination within the plies and along the interface region. It was observed that the application of clay in the composite material delayed the emergence of delamination. The delamination near the transverse crack emerged between the $0^0/90^0$ layers of the cross ply laminates around 400,000 cycles. The delamination spread rapidly along the

layer interface to form larger interfacial debonding. The separation of the $0^0/90^0$ layers were later found in most of the interface region when the cycles grew up to 1,000,000 cycles, thereafter leading to fatigue fracture. This basically occurred more at 3wt% clay loading because of the clay enhancement in the laminate. It can be stated that clay provided the fiber/matrix interface with sufficient interfacial strength for loads to transverse the interface, preventing early delamination, by which the fatigue period was made longer than other composite laminate samples. Figure 4.23 shows the crack behaviour of 3wt% nanoclay/GFRC sample at different intervals leading to interface debonding and delamination of the specimen.

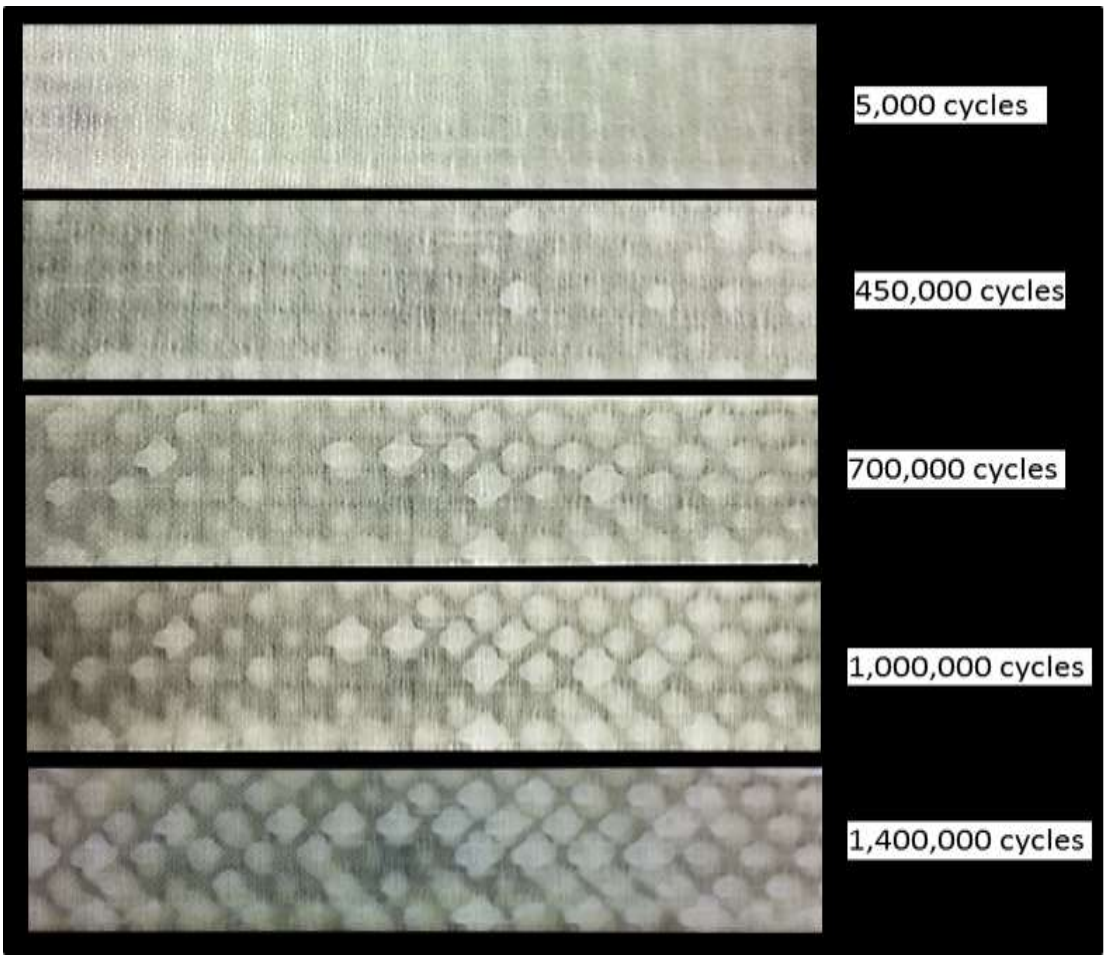

Figure 4.23: Matrix crack growth and interface delamination growth under tension-tension fatigue loading 3wt% nanoclay/GFRC laminate at 45% stress level

Delamination in the fiber layers grew up to the interface region as seen around 1,000,000 cycles and above. The causes of the delamination was as a result of localised interlaminar stresses generated within the transverse area as the cycle increases. At some certain stage of the fatigue test, it can be observed that the cracks coupling leading to interfacial debonding which causes delamination were arrested by the application of clays in the laminates. This is because the delamination growth did not connect with each other even as the fatigue test grew towards 1,000,000 cycles. This prevented interfacial separation of the layers leading to significant laminate stiffness and strength enhancement. However, with further increase of the cycles, delamination start to merge along the specimen edge, causing massive $0^0/90^0$ interface separation and leading to stiffness and strength reduction, and then final fatigue fraction.

4.6.3 Fatigue life damage

The Neat GFRC and hybrid nanoclay/GFRC were cycled to the final failure and the results were recorded in Table 4.12. The result of the cycle life at different stress levels were in agreement with Talreja's description. The failure of the specimens at 80% stress level loading were observed to be basically involved with the fiber fracture since cracks in the laminates did not propagate within and around the laminate edge before fracture occurred. This was as a result of high load testing that was closer to the initial static strength load. As observed from the fatigue result, neat GFRC laminate specimens went higher cycle before fracture. Nanoclay/GFRC up to 3 wt. % clay loading showed lower cyclic values than the neat GFRC. Contrary to the high static strength of the composite materials at all clay loading the effect of clay enhancement in the matrix of the material was not in play at fatigue loading. The fibers actually suffer much stress during high level fatigue loading. However, when the clay was increased to 5 wt. %, the cycle increased in the hybrid nanoclay/GFRC laminate. The improvement at 5 wt. % clay loading was a result of the clay cluster in the matrix the laminate. This is due to the intercalation of clay in the matrix. The fibers were assumed to be gathered

together by the clay-matrix, preventing easy breakage of the fiber at the fatigue failure.

The fatigue cycle increased when the stress level was reduced to the medium (60%) and material response to fatigue changed. The degradations that occurred in the composite laminate were accompanied by the combination of matrix cracking and interface failure. Few delaminations occurred within the fiber layers; but did not propagate along the specimen length before fracture occurred. Both the fiber and the matrix were greatly affected during the fatigue test at medium loading. Since the fibers have higher strength than the matrix, the stress application at 60% gave the neat GFRC tendency to compete with the hybrid nanoclay/GFRC. Neat GFRC undergo higher cycles that 1 wt. % and 5 wt. %, but lower in cycles when compared to 3 wt. % nanoclay/GFRC laminate.

Table 4.12: Fatigue life of neat GFRC and hybrid nanoclay/GFRC

Materials (GFRC)	Fatigue properties						
	Stress Level (%)	Maximum stress (MPa)	No of cycles (N_f)				
			Specimen 1	Specimen 2	Specimen 3	Specimen 4	Mean cycles
Neat	80	266	894	1038	1153	2885	1493
	60	199	17217	39349	4474	38442	24871
	45	149	292404	54110	154057	205282	176463
1 wt. % Clay	80	296	627	603	650	1671	888
	60	222	4605	12896	24985	14390	14219
	45	167	110751	327620	350430	419479	302070
3 wt. % Clay	80	288	779	1082	650	1355	967
	60	216	36596	11259	42013	68543	39602
	45	162	1298704	843380	1418554	1557752	1279598
5 wt. % Clay	80	286	1632	1453	1194	2007	1572
	60	214	6855	6320	8141	37613	14732
	45	161	67153	793272	275614	1204420	585115

The outstanding fatigue results of the hybrid nanoclay/GFRC laminate specimens, cycled to failure with respect to the application of clay in the matrix at low loading of 45% stress level over that of neat GFRC laminate specimens were amazing. At this stage, the matrix cracking was the area of concentration and the effect of the nanoclay enhancement was at play in the matrix of the composite. By reducing the stress amplitude, an increase in fatigue life for both the neat GFRC and hybrid nanoclay/GFRC laminates occurred. The presence of nanoclay significantly improves the fatigue life of the composite. It was observed after fracture of the laminates that the fatigue life of the hybrid nanoclay/GFRC at 3 wt. % clay loading showed the highest fatigue life value of 625% increase more that the neat GFRC laminate.

The graph of the fatigue test *S-N* curve is as shown in Figure 4.24; the linear graph shows the stress variation at the beginning of the test versus the number of cycles to failure. Considering the stress level applicable for GFRC materials under fatigue loading parameters, it was observed that hybrid nanoclay/GFRC samples at 1 wt. % and 3 wt. % clay loading; have almost similar behaviour at the low stress level of 45%.

From series of experiments conducted by Mandell [117] on different types of glass-fibre reinforced plastics (GFRP). He showed that when the number of cycles to failure lay between 10^2 and 10^6, the *S-N* curve can be approximated by a straight line. This can be calculated following the equation below:

$$\sigma_{max} = \Delta\sigma_{UTS} + blogN \tag{4.2}$$

Where; σ_{max} is the maximum applied stress, σ_{UTS} is the ultimate tensile strength, *N* is the number of cycles to failure and b is a constant. The ratio of b/σ_{UTS} was defined by Mandell [117] as the fractional loss in tensile strength per decade of cycles.

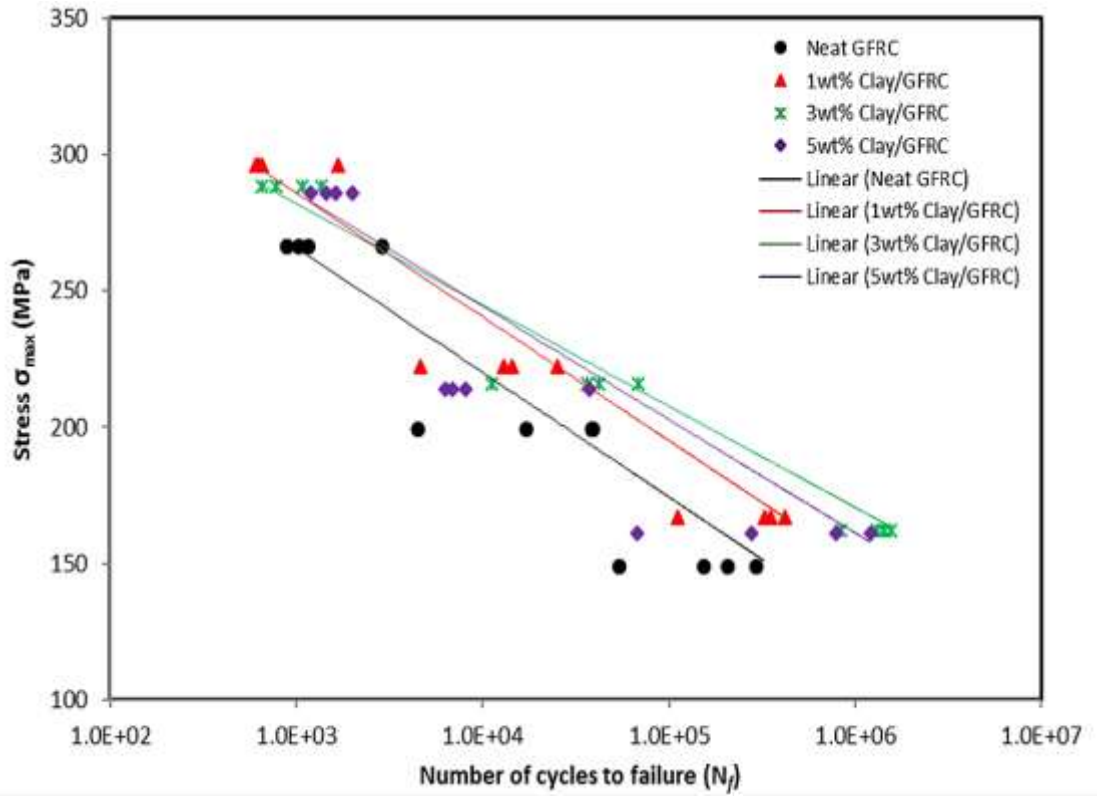

Figure 4.24: Maximum stress versus cycle to failure (*S-N* curve) of neat GFRC and hybrid nanoclay/GFRC

For this study, the values of the slope (b) from linear-regression data analysis and the strength degradation per decade of cycle (b/σ_{UTS}) are summarised in Table 4.13. It was observed that hybrid nanoclay/GFRC at 3 wt. % clay loading start to show less fractional loss, which is equivalent to the strength degradation per decade (b/σ_{UTS}) in the composite within 60% stress level. The fractional loss value reduced more within 45% stress level when compared to the neat GFRC and other hybrid nanoclay/GFRC materials. There was a reduction of 0.5% in the strength degradation per decade within 60% stress level and a reduction of 1.7% within 45% stress level in hybrid nanoclay/GFRC at 3 wt. %, when compared to neat GFRC material. The degradation per decade observed is as a result of nanoclay strength improvement properties at low stress level.

Table 4.13: Values of slope (b) and degradation of the fatigue strength per decade (b/σ_{UTS}) of the neat GFRC and hybrid nanoclay/GFRC material.

Materials GFRC	Degradation at Stress Levels					
	80%		60%		45%	
	Slope (b)	b/σ_{UTS} (%)	Slope (b)	b/σ_{UTS} (%)	Slope (b)	b/σ_{UTS} (%)
Neat	-21.22	6.39	-31.45	9.47	-35.47	10.68
1wt% Clay	-25.59	6.92	-36.41	9.84	-39.67	10.72
3wt% Clay	-24.31	6.75	-32.25	8.96	-32.49	9.02
5wt% Clay	-22.28	6.24	-35.68	9.99	-35.24	9.87

The fatigue failure modes of neat GFRC and hybrid nanoclay/GFRC at varying clay loading after fatigue, is as shown in Figure 4.25. From the figure, it was observed that the fracture behaviour of the neat GFRC and that of 5 wt. % clay loading looks similar. In neat GFRC, delamination of the fiber did not really occur so much at the interface; and the little delamination that occurred, transverse quickly along the length. This is associated with the debonding of some fibers, leading to rapid fracture of the sample. Similarly, the same fracture behaviour occurred in 5 wt. % clay loading. Although, the clay-matrix interaction extended the fatigue life of the composite material by about 232% when the clay was increased up to 5 wt. %; however, the morphological behaviour of the clay cluster in laminate limited the clay-matrix interaction by bridging the debonding at the interface. This caused delamination within the fibers, leading to the fracture of the laminate. This was attributed to the higher possibility of agglomeration of the clay in the epoxy of the composite material. It can therefore be concluded from the macrograph that 1 wt. % and 3 wt. % nanoclay/GFRC laminate went through a rigorous cyclic life during the fatigue testing as a result of clay enhancement of the composite materials.

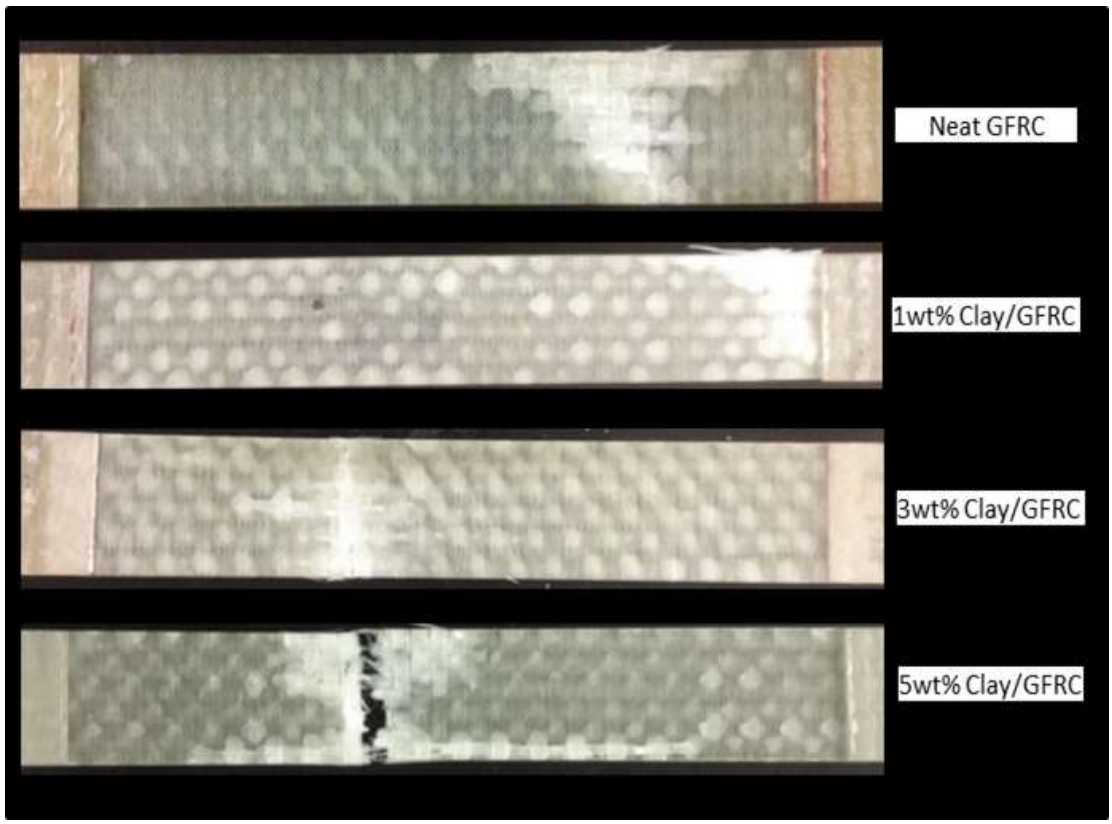

Figure 4.25: Failure modes of neat GFRC and hybrid nanoclay/GFRC specimens. Test were conducted at 45% stress level

4.6.4 Analysis of fatigue data

The degree of damage in a Neat GFRC laminate and that of hybrid nanoclay/GFRC laminate was followed by measuring the stress range variation and decrease in strength in the material as previously done by Farreira and Stinchcomb [210, 211]. Under constant amplitude loading condition of the fatigue testing, the composite specimens start to decrease in strength during the cyclic period. The rates of change in strength and stiffness and the lifetime of the composite material depends on the failure mode region where it is being loaded [212, 213]. These rates of change are defined as the damage growth rate. In order to generalize these considerations, these rates are normalised, and a non-linear relation between the normalized stress and the corresponding number of cycles is likely to be valid. Using this relation, the stiffness degradation at a given loading level for a prescribed number of cycles can be predicted. Variations of the stress during fatigue of the neat

and hybrid nanoclay/GFRC at the all stress levels (80%, 60% and 45%), were plotted in Figure 4.26 to 4.28. These illustrate the normalised stress ($\Delta\sigma/\Delta\sigma_{max}$) versus cycles to failure (N_f), where $\Delta\sigma$ is the fatigue stress range, $\Delta\sigma_{max}$ is the initial maximum stress range and N_f is the number of cycles to failure.

The strength degradation of the normalised stress is different at the various stress levels. In Figure 4.26, high drop of stress occurred in the linear regression graph of the fatigue at high stress level (80%). It was found that all normalised stress curve patterns show steep drop of stress variation. In the medium stress level (60%), a similar trend was found but does not actually correspond to that of the high stress level. However, the normalise stress reduced with the fatigue strength variation at medium stress level (60%) as seen in Figure 4.27. Following the progression of the normalise stress at the low stress level (45%) as shown in Figure 4.28, it is obvious that significant drops of the stress (13±10%) occurred at the early stage of the fatigue life of the neat GFRC and hybrid nanoclay/GFRC.

From these observations, the significant drops of the normalised stress did not reduce drastically in the composite material. It was found that normalise stress decreases slowly in the neat GFRC and the hybrid nanoclay/GFRC laminates. However, least strength progression drop was observed in 3 wt. % nanoclay/GFRC sample. This showed consistency in the stress distribution during the low stress level of the fatigue loading.

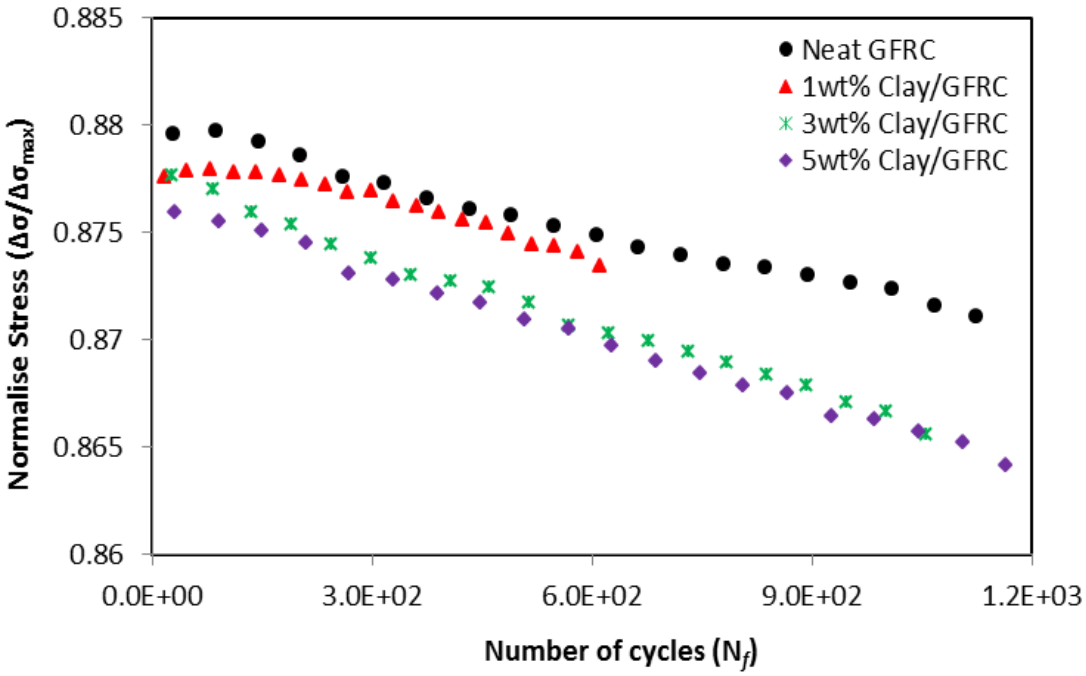

Figure 4.26: Stress range variation during the fatigue test of neat GFRC and hybrid nanoclay/GFRC at 80% stress level

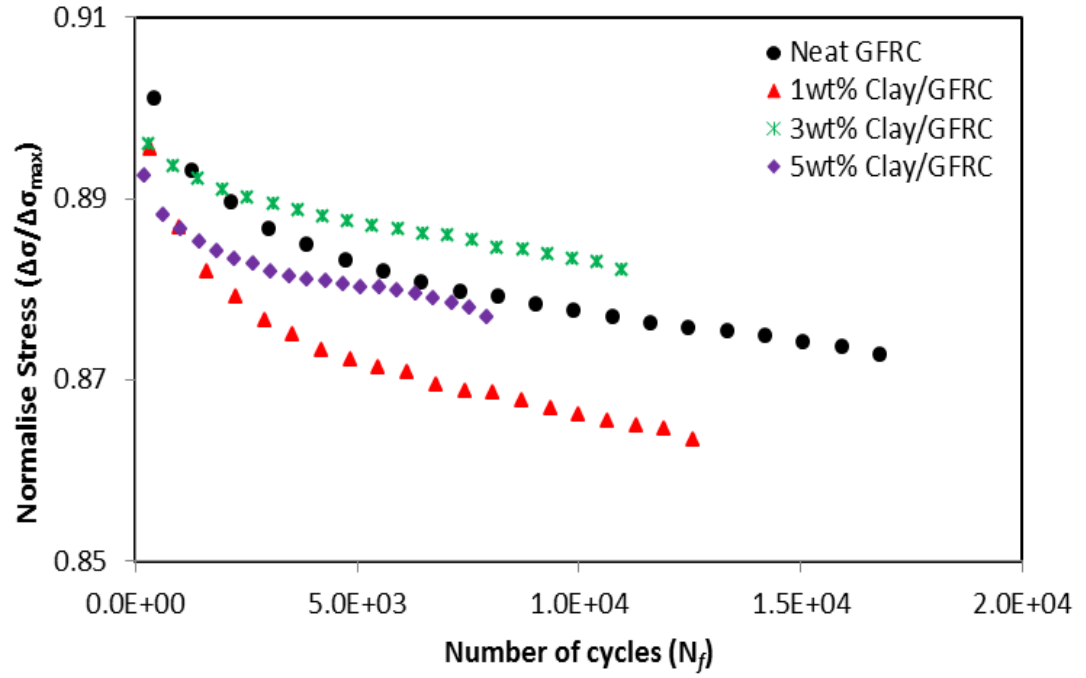

Figure 4.27: Stress range variation during the fatigue test of neat GFRC and hybrid nanoclay/GFRC at 60% stress level

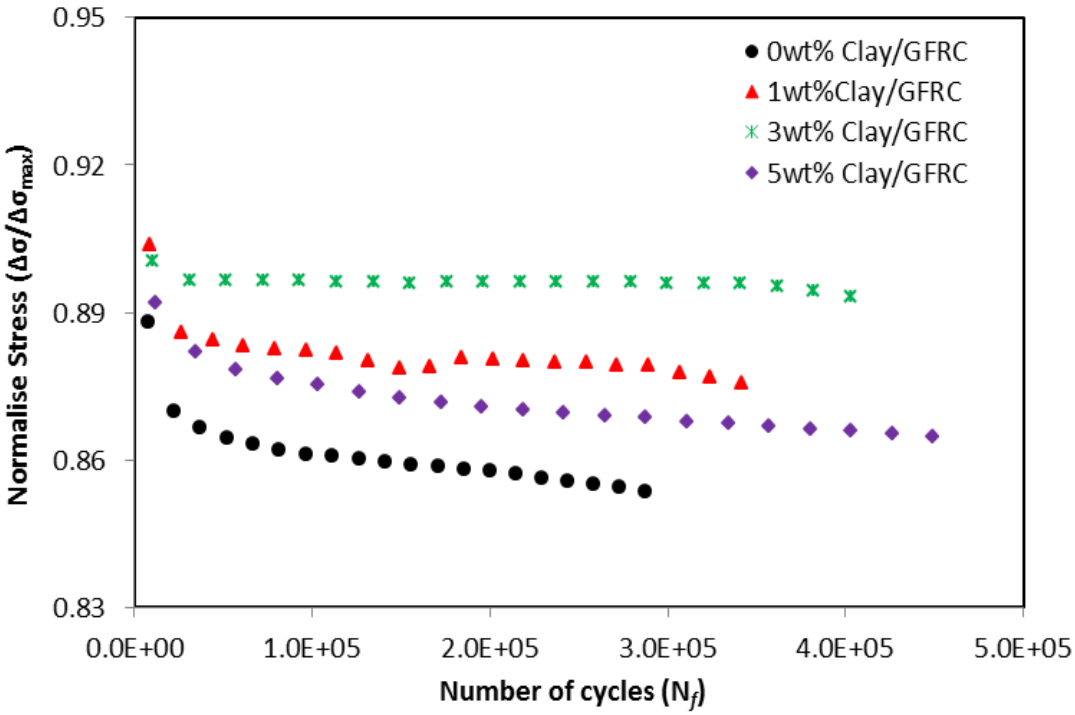

Figure 4.28: Stress range variation during the fatigue test of neat GFRC and hybrid nanoclay/GFRC at 45% maximum stress level

Normalize stress was generalized for all stress levels (80%, 60% and 45%) in order to show the strength degradation variations within the entire cycle life of the neat and hybrid nanoclay/GFRC. In Figure 4.29, it was observed that hybrid nanoclay/GFRC at 3 wt. % clay loading gave the best linear regression behaviour. Less strength degradation in terms of normalised stress level was found within the composite materials. This was more predominant in laminate sample with 3 wt. % clay loading. GFRC with 1 wt. % clay also showed a more closed behaviour to that of GFRC with 3 wt. % clay. This implies that nanoclay proved better strength enhancement in the composite material up to 3 wt. % clay loading.

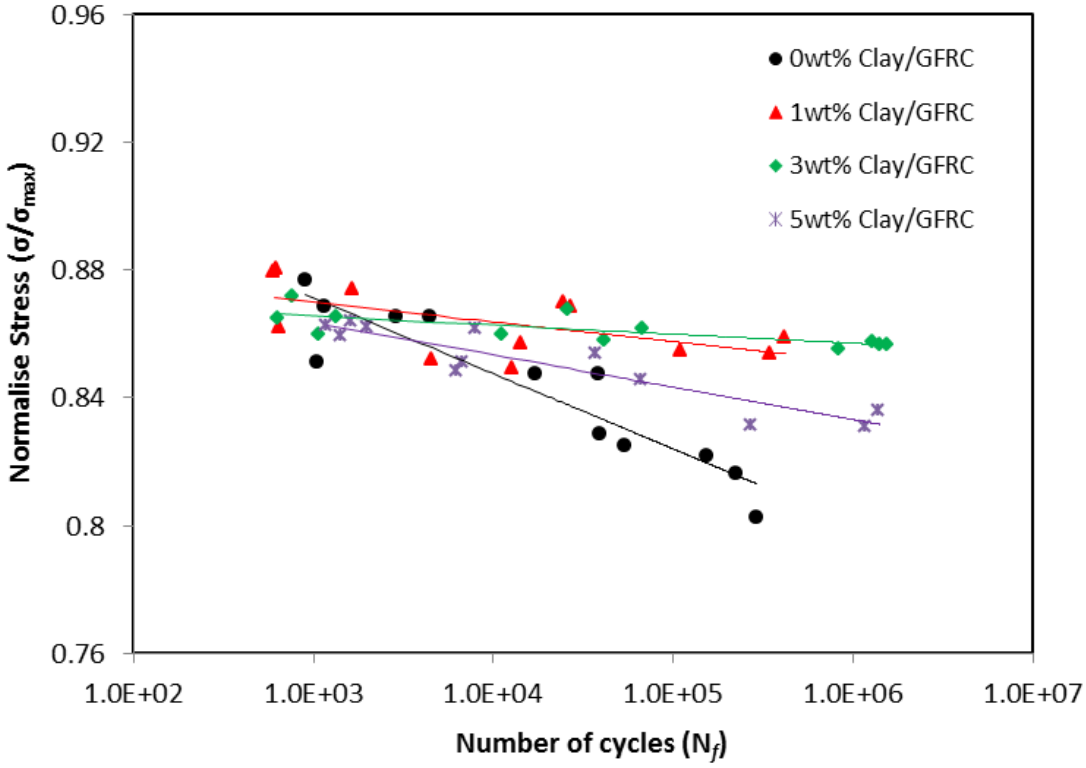

Figure 4.29: Peak stress at fatigue failure of the neat GFRC and hybrid nanoclay/GFRC at all maximum stress

It was assumed that the fatigue test run conducted on the neat GFRC and the hybrid nanoclay/GFRC specimen was true and the result was valid for the prediction of the fatigue life. In order to justify the fatigue result, for the benefit of doubt, one-way analysis of variance (ANOVA) was used to verify the significant differences between and within the four independent groups of the neat GFRC and the hybrid nanoclay/GFRC specimens. A significance level was chosen during data collection, this was set to 0.05 (5%). In the variance analysis, if the *p*-value is less than the significance level (e.g., $p < 0.05$), that means no significant difference is found between and within the groups. The variability descriptive values are tabulated in Tables 4.14, 4.15 and 4.16 respectively for all different stress level (80%, 60% and 45%). The tables present the variability of the statistical values, 95% confidence interval for mean and the *p*-value.

Table 4.14: Statistical result of the neat GFRC and hybrid nanoclay/GFRC materials at 80% stress level

Materials GFRC	Statistical Values			95% Confidence Interval for Mean		ANOVA test (*p*-value)
	Mean	Standard Deviation	Standard Error	Lower Bound	Upper Bound	
Neat	1492.5	934.36	467.18	5.73	2979.28	0.276
1 wt% Clay	887.75	522.52	261.26	56.31	1719.2	
3 wt% Clay	966.5	316.02	158.01	463.65	1469.35	
5 wt% Clay	1571.5	341.5	170.75	904.68	2114.91	

Table 4.15: Statistical result of the neat GFRC and hybrid nanoclay/GFRC materials at 60% stress level

Materials GFRC	Statistical Values			95% Confidence Interval for Mean		ANOVA test (*p*-value)
	Mean	Standard Deviation	Standard Error	Lower Bound	Upper Bound	
Neat	24870.5	17013.78	8506.89	-2202.22	51943.22	0.171
1 wt% Clay	14219	8368.9	4184.45	902.22	27535.78	
3 wt% Clay	39602.75	23492.95	11746.48	2220.22	76985.28	
5 wt% Clay	14732.25	15272.96	7636.48	-9570.44	39034.94	

Table 4.16: Statistical result of the neat GFRC and hybrid nanoclay/GFRC materials at 45% stress level

Materials GFRC	Statistical Values			95% Confidence Interval for Mean		ANOVA test (*p*-value)
	Mean	Standard Deviation	Standard Error	Lower Bound	Upper Bound	
Neat	176463.25	99574.32	49787.16	18018.29	334908.21	0.001
1 wt% Clay	302070	133391	66695.41	89815.45	514324.55	
3 wt% Clay	1279598	309478	154739	787149.2	1772000	
5 wt% Clay	58114.75	513466	256733	-231925.02	1402200	

Multiple comparisons for all fatigue stress level of the neat GFRC and hybrid nanoclay/GFRC materials was analysed based on the each specimen dependent variables. Using the *p*-value approach, the values of the multi-variance comparison calculated is tabulated in Table 4.17 to show significance difference of the fatigue specimens.

Table 4.17: Multi-variance comparison of neat GFRC and hybrid nanoclay/GFRC materials

Specimen group	Tukey HSD					
Nanoclay GFRC	*p*-value		*p*-value		*p*-value	
	80% Stress level	Sig.	60% Stress level	Sig.	45% Stress level	Sig.
Neat – 1 wt%	0.486	*S	0.81	S	0.939	S
Neat – 3 wt%	0.595	S	0.62	S	0.001	*NS
Neat – 5 wt%	0.997	S	0.831	S	0.295	S
1 wt% - 3 wt%	0.997	S	0.201	S	0.004	NS
1 wt% - 5 wt%	0.386	S	1	S	0.588	S
3 wt% - 5 wt%	0.486	S	0.214	S	0.036	NS

(*NS = No significant; *S = Significant)

From Table 4.16, it can be observed that there was no significant difference between the neat GFRC and 3 wt. % nanoclay/GFRC; 1 wt. % and 3 wt. % nanoclay/GFRC; and 3 wt. % and 5 wt. % nanoclay/GFRC materials at 45% stress level. On the other hand there is a significant difference between neat GFRC and 1 wt. % nanoclay/GFRC; neat and 5 wt. % nanoclay/GFRC; and 1 wt % and 5 wt. % nanoclay/GFRC materials at 45% stress level. It can therefore be concluded that the addition of clay up to 3 wt. % enhanced the fatigue strength and life of the composite material. The insignificance between the 3 wt. % nanoclay/GFRC and other composite materials is therefore justified by the fatigue result. It is therefore concluded that nanoclay/GFRC laminate at 3 wt. % clay loading show the best variability within and among the specimen samples.

4.6.5 Fatigue microscopy analysis

The surface of the neat GFRC and the hybrid nanoclay/GFRC fatigued specimens were observed using scanning electron microscope (SEM). Figure 4.30a shows matrix cracking propagation in the neat GFRC. The propagation of the matrix cracking was seen to cut across the width section of the specimen surface. The crack propagated on the surface was uninterrupted because of the brittleness of the matrix. This causes the laminate to undergo extensive deformation. However, there is a distinct deviation of matrix crack propagation on the hybrid nanoclay/GFRC surface. This was classified as crack arrest. As shown in Figure 4.30b, matrix cracking on the laminate surface was arrested by the nanoclay at certain points during the propagation along width of the laminate. The crack propagation reveals a step-like formation as the nanoclay diverts the crack. It can be concluded that the nanoclay contributed to the crack energy delay in the Hybrid nanoclay/GFRC laminate.

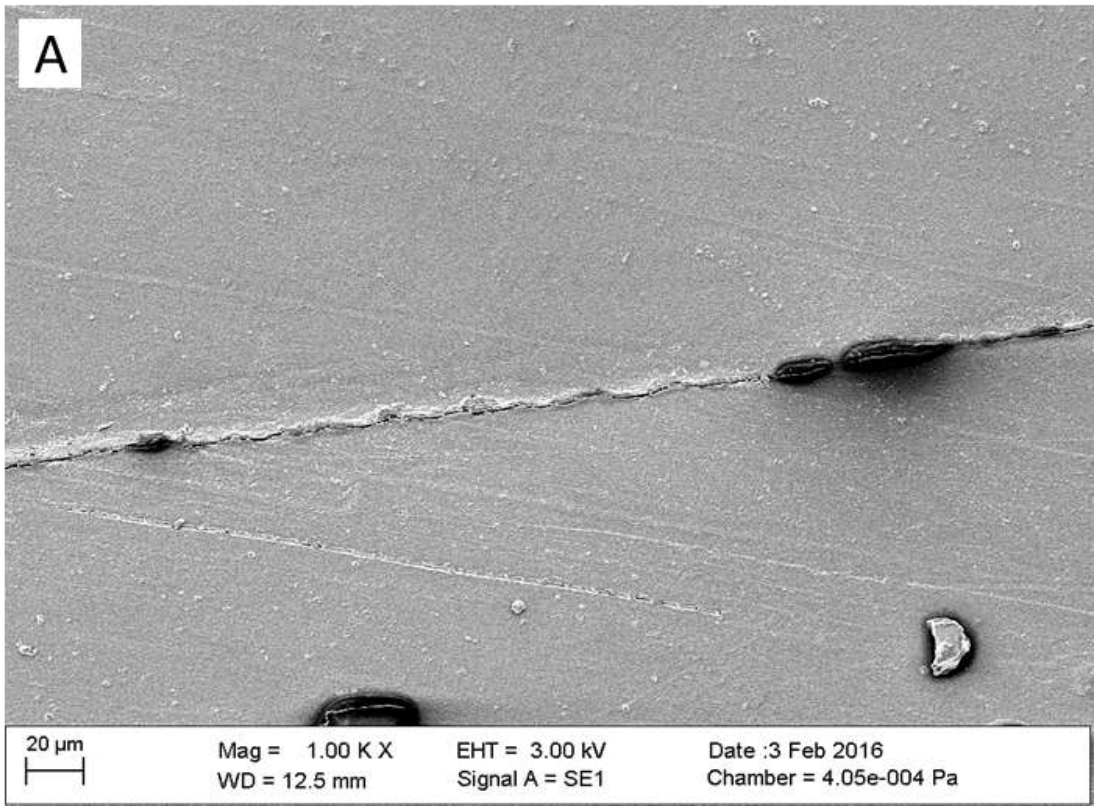

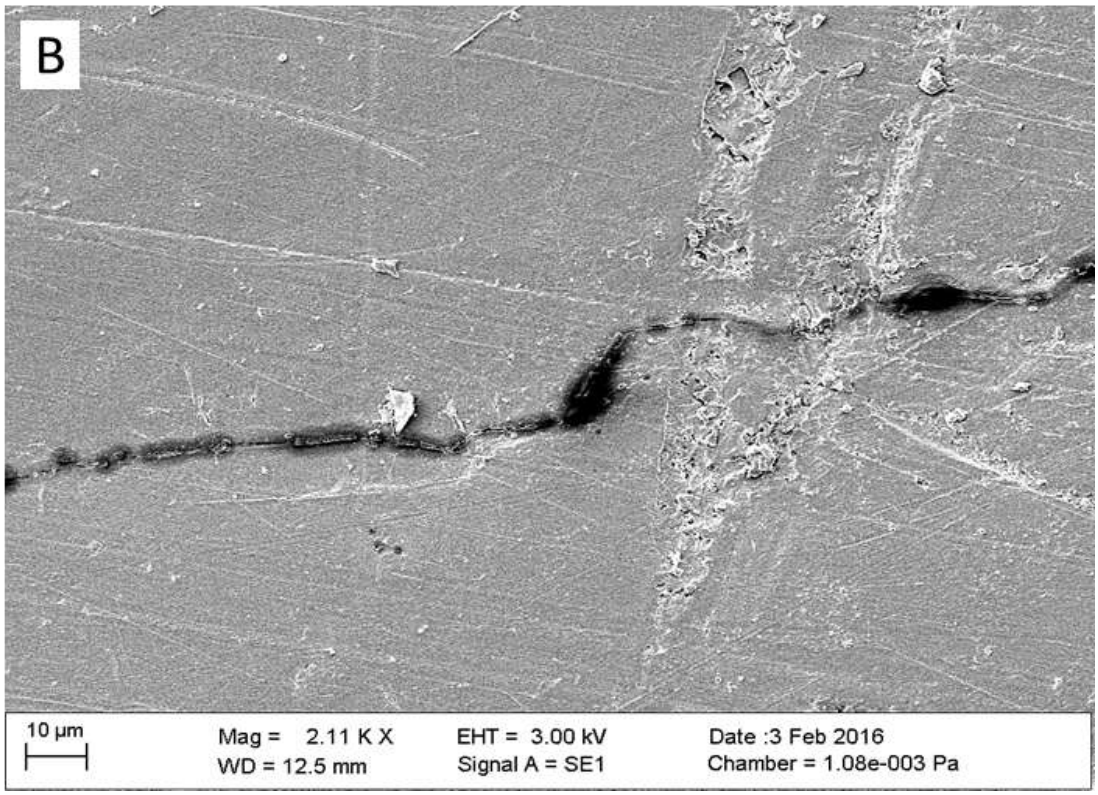

Figure 4.30: Fatigue specimen showing SEM image of matrix crack propagation: (a) across neat GFRC laminate surface and (b) along hybrid nanoclay/GFRC surface.

A substantial amount of matrix deformation occurred during fatigue test of the neat GFRC specimen. Counterscarp formation at the transverse (width) section of the specimen was revealed, by uneven brittleness in the epoxy-matrix as shown in Figure 4.31a. This is classified as weakness in the fiber matrix interfacial adhesion of the neat GFRC. The matrix cracking led to fiber-matrix debonding, causing delamination (fiber-matrix separation) within the mid-part of the laminated specimen. A clean fiber track during the delamination was observed along the laminates specimen depth. The gap between the fiber and the matrix is clearly visible as shown in Figure 4.31b. This indicated a poor fiber-matrix adhesion. The reason was because the separation revealed a clean fiber surface on one side and matrix fragment attached to the fiber on the other side.

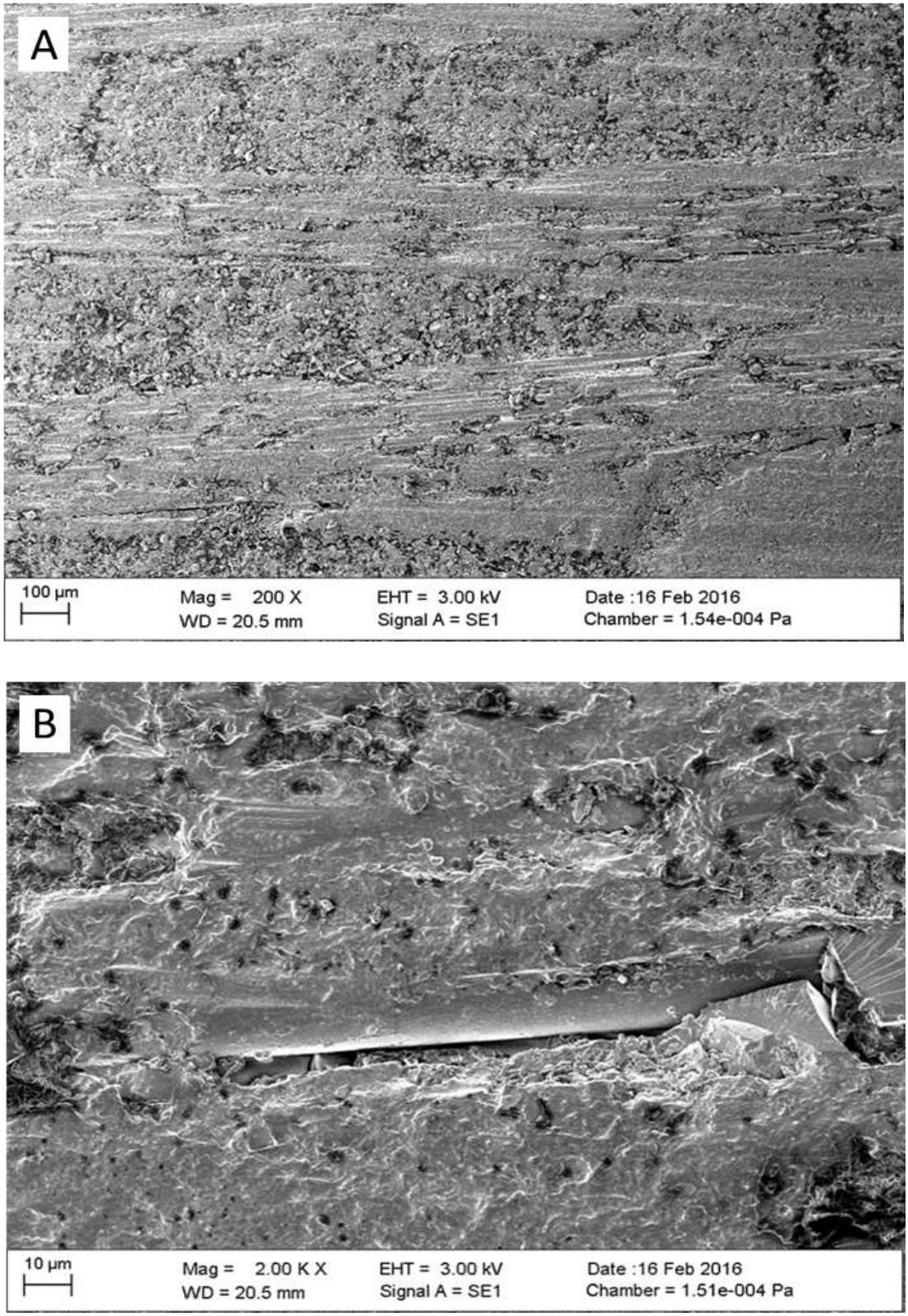

Figure 4.31: Fatigue specimen showing SEM image of: (a) matrix crack deformation across neat GFRC laminate thickness and (b) fiber-matrix separation of the neat GFRC along laminate thickness.

In the hybrid nanoclay/GFRC, the fracture energy in the crack propagation region along the laminate edge is a combination of the matrix and fiber toughening mechanisms. Addition of nanoclay enhanced the fiber-matrix interfacial bonding, and contributed towards increase matrix stiffness and matrix adherent to the fiber. The toughening improvement observed in Figure 4.32a, can be admitted as homogeneous dispersion of the nanoclay throughout the matrix, which significantly enhance the bonding within the fiber region. Although cracks occurred and propagated across the depth of the laminate, but the cracks were evenly deformed as they cut across the laminate thickness. The fiber-matrix interaction observed during the crack propagation depicted a good bonding of the matrix to the fiber as shown in Figure 4.32b. This was considered as strength enhancement in the hybrid nanoclay/GFRC laminate.

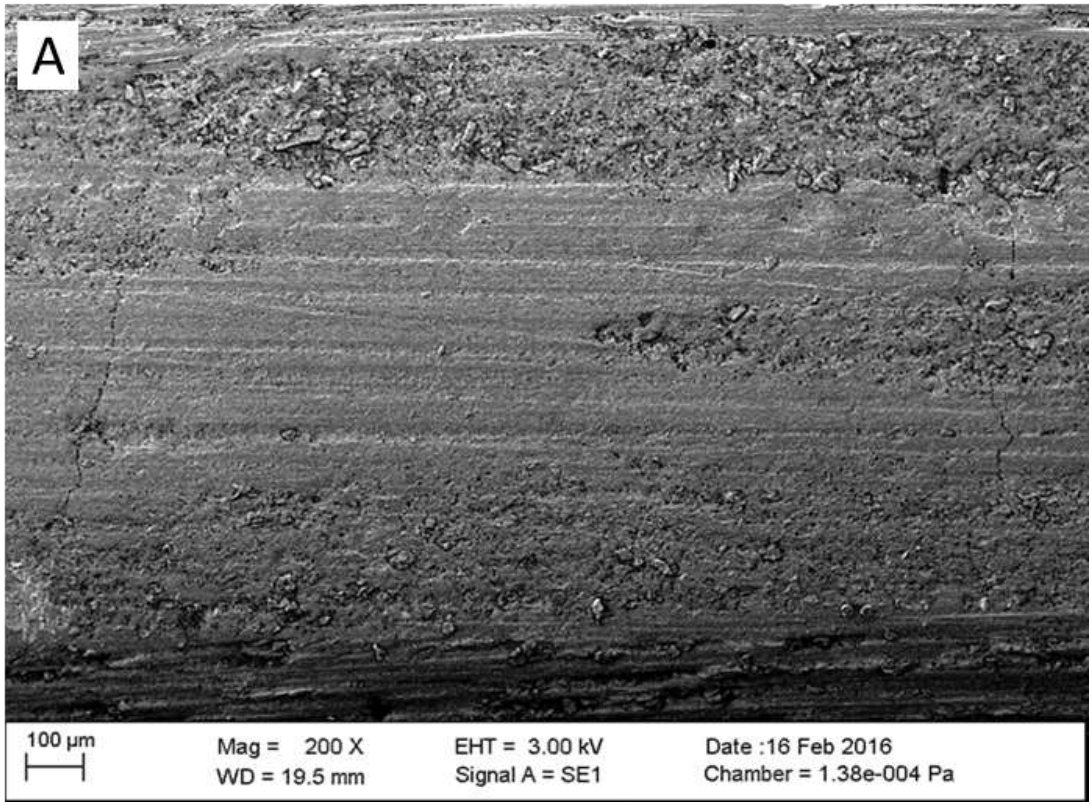

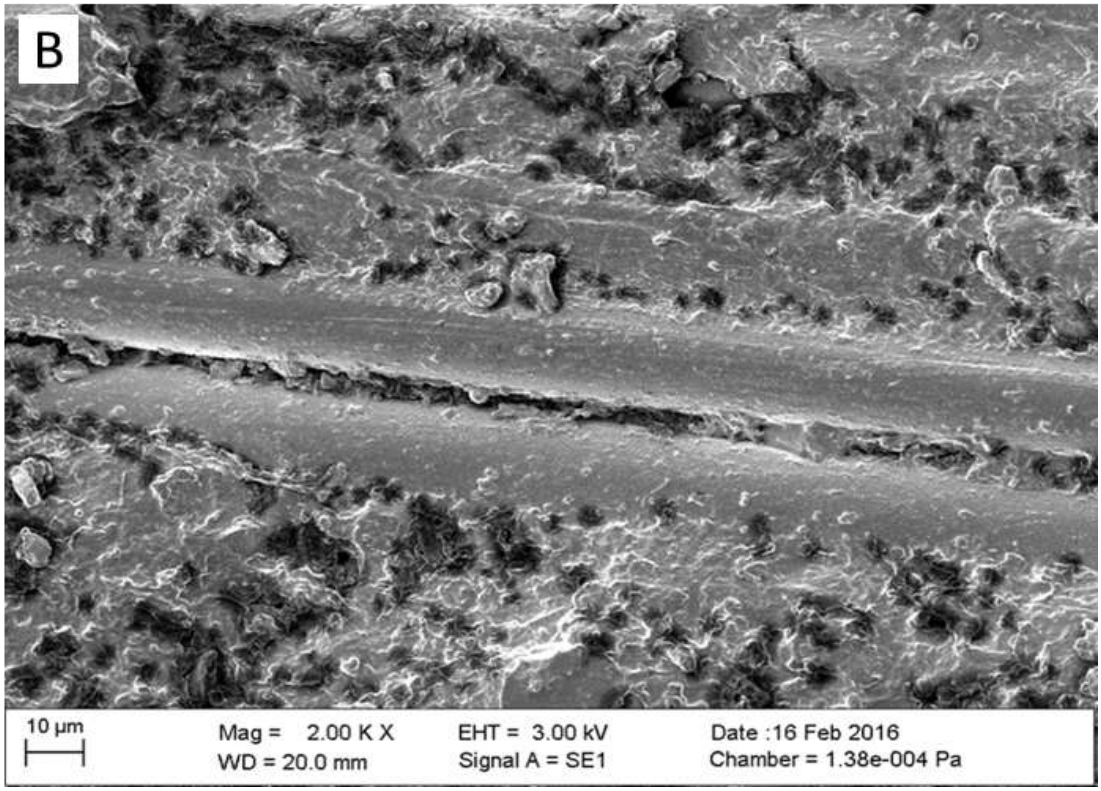

Figure 4.32: Fatigue specimen showing SEM image of: (a) matrix crack across hybrid nanoclay/GFRC laminate thickness (b) fiber-matrix interaction along the hybrid nanoclay/GFRC laminate thickness.

4.7 RESIDUAL STRENGTH OF FATIGUED HYBRID NANOCLAY/GFRC MATERIALS

In most structural designs where fatigue damage is a concern, materials experience fatigue loading of various amplitudes throughout their lifetime. The amplitude and mean values of the loading may have some repeating order during application or they may be completely random ordered. However, fatigue durability characterization of materials is usually performed for constant amplitude loading due to the relative ease of running tests and reporting data, and uncertainty in the real world load history that the material will encounter [214]. If a specific variable amplitude loading is performed, the test might be useful for one application. However, another set of tests would have to be performed for each additional situation. Therefore, if the

engineering design world requires methods for predicting fatigue life of materials based on constant amplitude fatigue loading; hence, the residual strength for such constant amplitude fatigue loading of the composite material needed to be explored.

One of the ways to study the residual strength of the composite laminate is the use of dynamic mechanical analysis (DMA). This process has previously been done studied by Towo and Ansell [215], where DMTA was conducted on failed untreated and treated sisal fiber epoxy resin fatigued specimen, to examine the influence of fatigue history on storage modulus and tan δ T_g of the composites. Figure 4.33 presents the (DMA) storage modulus data for the fatigued neat GFRC and hybrid nanoclay/GFRC laminates samples.

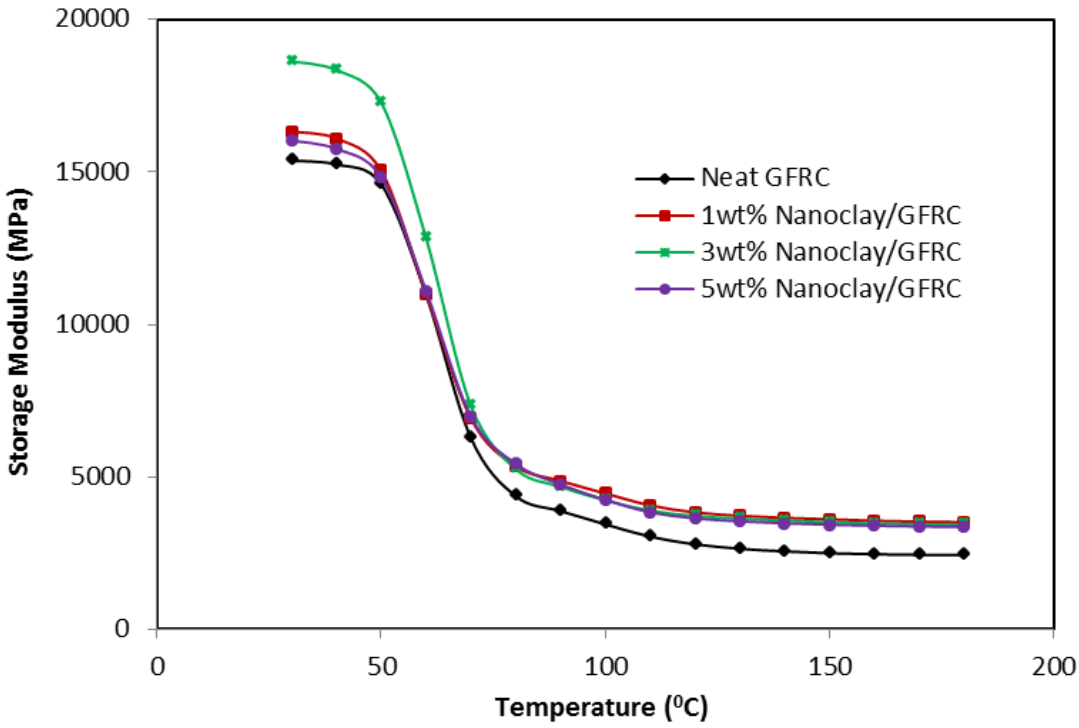

Figure 4.33: Temperature dependency of storage modulus for neat GFRC and hybrid nanoclay/GFRC fatigued to failure at 45% of the mean stress

From the initial DMA of the unfatigued specimen in section 4.3.2; the storage modulus peak values of the unfatigued composite specimens were observed to be higher when compared with the fatigued composite specimens. This

indicated decrease in stiffness of the materials after fatigue test. Also, the hybrid nanoclay/GFRC storage modulus peaks are higher than the neat GFRC modulus values of both unfatigued and fatigued composite materials. GFRC with 3 wt. % clay addition gave the highest storage modulus values of 18856 MPa and 18626 MPa for unfatigued and fatigued samples respectively. When the unfatigued composite material and fatigued composite material were compared, it was found that 3 wt. % nanoclay/GFRC fatigued specimen gave the lowest stiffness reduction of 1.21^0C, while neat GFRC fatigued specimen gave highest reduction of 3.74^0C. The storage modulus plots in Figure 4.33 for the fatigued specimens, showing a shift to the left of the unfatigued specimens suggests that there is a decrease in the glass transition temperature (T_g) of the fatigued composite samples. Lowest T_g reduction of 2.920C was found in 3 wt. % nanoclay/GFRC fatigued sample when compared to 4.11^0C found in the neat GFRC samples. However, 1 wt. % and 5 wt. % nanoclay/GFRC samples have T_g reduction of 6.14^0C and 4.33^0C respectively, which are quite higher than that of the neat GFRC T_g reduction value. The storage modulus properties for both un-fatigued and fatigue composite results are recorded in Table 4.18.

Table 4.18: Storage modulus data of neat GFRC and hybrid nanoclay/GFRC (unfatigued and fatigued) materials

Material (GFRC)	Storage modulus (unfatigued)		Storage modulus (fatigued at 45% stress level)		Change in storage modulus	
	Peak value (MPa)	T_g (^{0}C)	Peak value (MPa)	T_g (^{0}C)	Stiffness reduction (%)	T_g reduction (^{0}C)
Neat	15964±416	66.10	15367±521	61.99	3.74	4.11
1 wt. % Clay	16635±303	68.17	16322±454	62.03	1.88	6.14
3 wt. % Clay	18856±284	68.32	18626±327	65.40	1.21	2.92
5 wt. % Clay	16496±422	66.26	16030±471	61.93	2.83	4.33

The nanoclay dispersion in the resin-matrix showed a good modification to the GFRC material interfacial properties as revealed by the residual strength of the material after fatigue. In a structural application irrespective of the structural change, the hybrid nanoclay/GFRC can serve as reliable materials. Moreover, the minor reduction in the 3 wt. % nanoclay/GFRC T_g value is a confirmation of an excellent thermal property.

Figure 4.34 presents tan δ versus temperature data for the neat and hybrid nanoclay/GFRC laminate samples that were obtained from the un-fatigued and fatigue composite samples. The tan δ peak value for the neat GFRC and the hybrid nanoclay/GFRC fatigued samples are greater than the unfatigued samples up to 3 wt. % clay loading. At 5 wt. % clay loading, the peak value reduced in the fatigued sample.

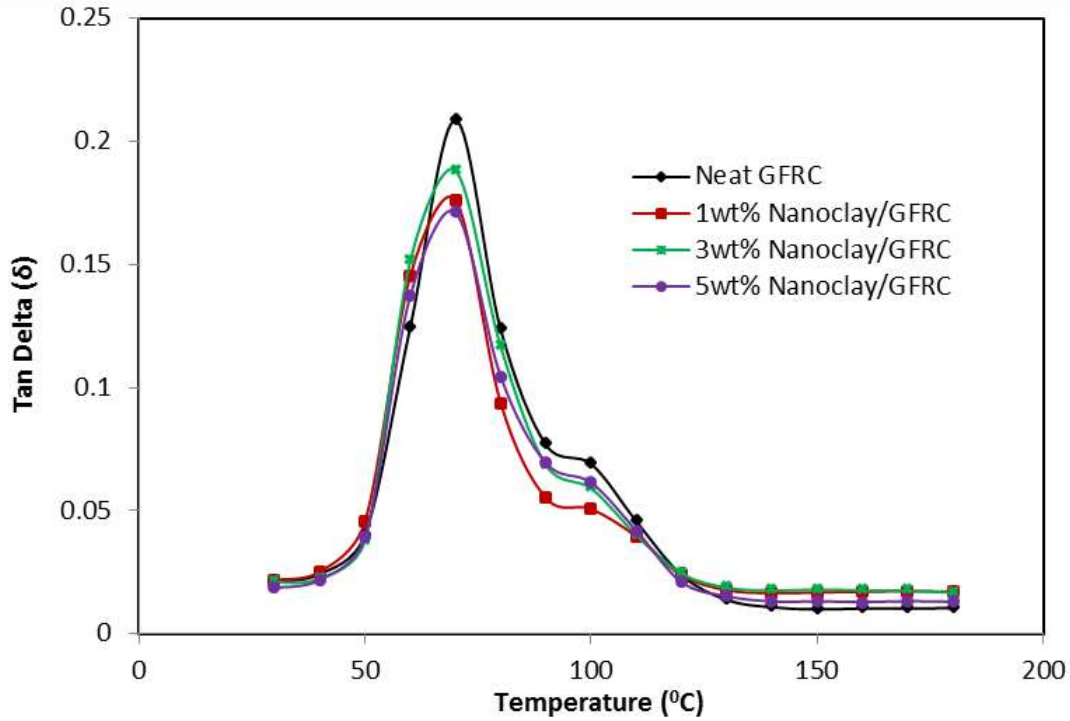

Figure 4.34: Temperature dependency of tan δ for neat GFRC and hybrid nanoclay/GFRC fatigue to failure at 45% of the mean stress

As recorded in Table 4.19, it was observed that 5wt% nanoclay/GFRC has the highest tan δ peak value of 0.1816 in the unfatigued sample, while neat GFRC has the highest tan δ peak value of 0.2086 in the fatigued samples.

The low tan δ peak values in the hybrid nanoclay/GFRC fatigued sample are likely due to the rigorous cycle life the materials undergo before fracture. It was apparent that the neat GFRC did not undergo much matrix cracking before failure occurred, by which the cycle life was smaller when compared to the hybrid nanoclay/GFRC material. However, the hybrid nanoclay GFRC materials went through rigorous amount of cracks during cycle period, which must have resulted in fiber matrix debonding during fatigue. From the tan δ data T_g it was observed that only 3wt% nanoclay/GFRC fatigued sample has tan δ peak temperature 69.09^0C, which is about a positive shift of 1.81^0C when compared to the unfatigued composite T_g sample. On the other hand, the neat GFRC fatigued sample and (1 wt. % and 5 wt. %) nanoclay/GFRC fatigued samples had negative T_gs shift when compare to unfatigued composite samples.

Table 4.19: Tan δ peak data for the neat GFRC and hybrid nanoclay/GFRC (unfatigued and fatigued) materials

Material (GFRC)	Tan δ (un-fatigued)		Tan δ (fatigued at 45% stress level)		Change in Tan δ	
	Peak value	T_g (^{0}C)	Peak value	T_g (^{0}C)	Change in Peak (%)	Shift in T_g (^{0}C)
Neat	0.1662	74.84	0.2086	69.17	25.51	- 4.33
1 wt. % Clay	0.1701	72.91	0.1763	65.88	3.65	- 7.03
3 wt. % Clay	0.1615	67.28	0.1882	69.09	16.53	1.81
5 wt. % Clay	0.1816	75.08	0.1713	66.69	- 5.67	- 8.39

It can therefore be concluded that a reflection of better bonding and good clay enhancement was found between the fiber and matrix during fatigue as proved by DMA analysis. The residual strength of the hybrid nanoclay/GFRC composite material can be reliable during application and the materials can continue to carry load irrespective of structural change, both mechanically and thermally, pending the time that the structure is replaced.

CHAPTER 5

CONCLUSIONS AND RECOMMENDATIONS

5.1 GENERAL CONCLUSIONS

In this chapter, the evaluation of the fatigue study of hybrid nanoclay/glass fiber reinforced composite (GFRC) laminates was highlighted. The percentage weight ratio of nanoclay suitable for the strength enhance of GFRC for maximum fatigue life was clearly identified. The structural behaviour and microscopy analysis of nanoclay dispersion in polymer-matrix as well as the thermal analysis of the hybrid nanoclay/GFRC were outlined. The quasi-static and fatigue properties of the hybrid nanoclay/GFRC results and the residual strength of the hybrid nanoclay/GFRC investigated were summarised. Results obtained have shown that the main objective of the research, which was to study the structure-properties relationship and the improved performance of nanocomposite materials for maximum fatigue life was achieved. The residual strength of the hybrid nanoclay/GFRC equally proved that good fabrication of the nanocomposite laminate was truly met.

From the characterisation of the nanocomposite materials, the range of the peak patterns in the XRD corresponds to the varying weight percentages of nanoclay. It was observed that epoxies with up to 3 wt. % nanoclay show no distinct XRD peak corresponding to the diffraction peak of nanoclay. The absence of diffraction peak suggested that nanoclay is randomly dispersed in the matrix. Generally, such type of structure can be referred to as an exfoliated nanocomposite structure. However, epoxy with nanoclay up to 5 wt. % shows a sharp diffraction pattern corresponding to incomplete dispersion of nanoclay in the polymer matrix. The increased interlayer spacing suggests that the epoxy has intercalated into the gallery spacing of the clays. Thus, such types of nanocomposite materials are been referred to as intercalated structure. The micrograph of polymer-nanocomposite showed homogeneous dispersion of nanoclay in the epoxy-resin up to 3 wt. % clay loading. This resulted in proper homogeneous structures, since uniformed dispersion clay were found in the ECN. At the addition of more nanoclay,

Agglomeration of clay were found as there are formation of clusters in the polymer-matrix.

DSC result showed that samples with nanoclay undergo less absorption of energy during the heating process. The nanoclay in the polymer nanocomposite sample prevented the relaxation of polymer chain during the heating of the sample along the temperature range. Sample with 3 wt. % nanoclay was observed to have shown lowest heat absorption to reach the enthalpy of the rubbery state. This was attributed to a good crosslink density of nanoclay and epoxy with respect to the exfoliation of clay particles in the samples. Furthermore, the glass transition temperature (T_g), increased with the addition of nanoclay. 3^0C increase was found at 3 wt. % clay loading, which was the highest T_g value increase when compared with the neat epoxy.

The viscoelastic properties of the hybrid nanoclay/GFRC improved with the presence of nanoclay in the composite material. The stored energy in the elastic portion of the composite as measured by the storage modulus measures showed that increase in the storage modulus of the hybrid nanoclay/GFRC was observed in all clay loading. GFRC with 3 wt. % clay loading however increased by 18% at the peak level more that the neat GFRC. Incorporation of nanoclay in the glass fibre laminates caused broadening of the loss modulus peak; and this was more visible at 3 wt. % clay loading. Highest peak value of 41% was observed, which was more than the neat GFRC peak value. Hence, a shift of 2^0C increase in the loss modulus T_g towards the right was found at 3 wt. % clay addition. This is due to the increase in the number of chain segments upon clay addition. The shift in the temperature was quite significant; and this depicted an improvement in the T_g with addition of nanoclay. However, tan delta which is also known as the mechanical loss factor gave peaks increase in intensity with increase in the amount of nanoclay content. Sample with 5 wt. % clay loading, which has the highest peak value was 9.3% higher than neat GFRC. At a point between 90^0 and 110^0, the polymer surrounding the clay undergoes high T_g because the clay acts as a thermal barrier in the medium of the soft segment. This

caused another peak within the variation of tan δ at 1 wt. % and 3 wt. % nanoclay/GFRC. An indication of improved clay-epoxy interaction in the glass fibre reinforced laminate was confirmed.

DMA-RM studies revealed the cure properties of hybrid nanoclay/GFRC laminate through changes in loss modulus T_g of the bulk specimen sample. The changes in the first heating process and the second reheating process reveal the level of cure of the composite laminates. Neat GFRC specimen showed higher increase of 11^0C in the T_g when compared to the hybrid nanoclay/GFRC samples. However, hybrid nanoclay/GFRC at 1 wt. % and 3 wt. % clay loading showed the lowest T_g of 7^0C increase after reheating of the materials. The increase in T_g value was as a result of the uncured properties in the laminates at the first heating process. The low increase in T_g at the second reheat process depict a better cure properties in the hybrid nanoclay/GFRC laminate. The degree of cure calculated from the percentage difference of the cured to uncured values of the neat GFRC was 74%, while hybrid nanoclay/GFRC up to 3 wt. % clay loading was 78%. This shows that hybrid nanoclay/GFRC laminate was more fully cured.

Quasi-static properties of neat GFRC and that of the hybrid nanoclay/GFRC laminates were compared, it was found that the properties of the hybrid nanoclay/GFRC improved with the dispersion of nanoclay in the composite material. Tensile strength of the neat GFRC laminate was 332 MPa, while that of the hybrid nanoclay/GFRC laminates were 370 MPa, 360 MPa and 357 MPa, for composite enhanced with 1 wt. %, 3 wt. % and 5 wt. % nanoclay respectively. An increase of 12% was found in the tensile strength at 1 wt. % clay loading. Also highest tensile strain of 0.0299 mm/mm was found in 1 wt. % nanoclay/GFRC material. This was 8.3% higher that the neat GFRC. However, in the tensile modulus; highest stiffness of 20.6 GPa was found at 3 wt. % clay loading, which was 17% higher than the neat GFRC. The improved tensile strength and strain were attributed to the homogeneous dispersion of clay and crosslink effect of the clay with epoxy. Hence, the

improved tensile modulus was related to the enhancement effect of clay fillers.

The improvement found in the both flexural strength and flexural modulus of the hybrid nanoclay/GFRC laminate was astonishing. The highest flexural strength and flexural modulus values of 396 MPa and 24 GPa respectively, were found in 3 wt. % nanoclay/GFRC materials. These make a difference of 18% and 24% higher than the neat GFRC values. The improvement in flexural properties was be attributed to matrix enhancement due to nanoclay addition. Likewise, flexural strain at maximum strength was increased up to 3 wt. % clay loading but decrease at more addition of clay. The detrimental effect of clay content at higher wt. % was as a result of the formation of agglomerates in the epoxy.

In impact strength of the composite material, impact resistance improved at all varying clay addition in the GFRC laminates. It was apparent that the impact resistance of the neat GFRC laminate was 210 KJ/m^2. The impact resistance however increased to 314 KJ/m^2 at the addition nanoclay up to 3 wt. %. This depict 56% impact resistance increase. It is worth mentioning that the high impact resistance at 3 wt. % clay loading depict great improvement of the composite material.

Hardness test results of neat GFRC and hybrid nanoclay/GFRC proved beyond benefit of doubt that nanoclay improve the laminates interphase. Small amount of nanoclay in the composite laminate gave better hardness properties. The addition of 1 wt. % nanoclay gave the best hardness value of 61.8 Hv with a variance-of-average of 0.8 and a value of 1.3 as the coefficient of variation. Closer to this result is 3 wt. % hybrid nanoclay/GFRC, with hardness value of 61.4 Hv. Having a variance-of-average of 1.1 and a coefficient of variation 1.6. Lowest hardness value of 56.6 Hv was found in neat GFRC laminate, while 5 wt. % nanoclay/GFRC have 58.2 Hv as hardness value. This shows that the hardness value of the composite laminate up to 3 wt. % clay addition is commendable as materials with better surface toughness.

The fatigue investigation of the neat composite laminate reveals the materials resistance to cracks initiation and propagation in the hybrid nanoclay/GFRC. The fatigue crack growth (FCG) in neat GFRC laminate rapidly led to higher crack density (CD), without an evidence of crack saturation in the FCG before fracture. However, saturation of FCG was reached around 400,000 to 500,000 cycles in hybrid nanoclay/GFRC laminates before fracture occurred. The application of nanoclay as filler for strength enhancement in the epoxy promoted reduction in the fatigue crack propagation of the hybrid nanoclay/GFRC laminates. In terms of mechanical performance and fatigue life of the composite laminates; hybrid nanoclay/GFRC laminates performed better than neat GFRC laminate at low stress level (45%). Significant improvement in the fatigue was achieved in the hybrid nanoclay/GFRC and more predominant at 3 wt. % clay loading. The presence of nanoclay significantly improves the fatigue life of the composite by 625%. The degree of damage observed from stress range variation showed that strength degradation variation was reduced in all composite samples. However, strength progression drop of the normalise stress at the low stress level (45%) was not as much in hybrid nanoclay/GFRC when compared to the neat GFRC material. List strength progression drop was observed more at 3 wt. % clay loading.

The SEM images of the materials after fatigue revealed that dispersion of nanoclay in the resin-epoxy of the GFRC laminate at 3 wt. % gave better strength enhancement and fatigue life of the composite material. In the neat GFRC sample, uneven brittleness of matrix deformation was substantially found in the image tested sample. The hybrid nanoclay/GFRC however display an increase matrix stiffness as the matrix adherent to the fiber. The matrix and fiber interaction was regarded as the fracture energy by which the fiber-matrix interfacial debonding was reduced as a result of clay addition. This also reduced the rate of matrix cracking propagation in the hybrid nanoclay/GFRC laminates.

The residual strength of the fatigued composite laminates showed that Neat GFRC lost more strength than hybrid nanoclay/GFRC material. Relative to the residual strength of the composite from the unfatigued-to-fatigue composite, sample with 3 wt. % clay addition showed the lowest storage reduction of 1.21% and T_g reduction of 2.92^{0}C. While neat GFRC fatigued sample has 3.74% and 4.11^{0}C reductions at both storage modulus and T_g respectively after fatigue. Likewise, a positive shift of 1.81^{0}C toward the right was found in the tan delta glass transition temperature (T_g) at 3 wt% nanoclay/GFRC laminate after fatigue. A reflection of better bonding between the fiber and matrix after fatigue was proved by the residual strength. It can be concluded that the application of nanoclay in GFRC improved the performance of the material. Therefore, the hybrid nanoclay/GFRC can be recommended for structural application, be it mechanically or thermally, pending the time that the structure is replaced.

5.2 RECOMMENDATIONS FOR FUTURE RESEARCH

This study is focus on the application of nanoclay in resin-epoxy for strength enhancement of woven GFRC laminate that can basically be used in aerodynamic applications. It was observed experimentally that Cloisite 30B montmorillonite clay improved the properties of the GFRC laminate. With this findings, application of nanoclay in GFRC material to form hybrid nanoclay GFRC material can be recommended for the manufacturing of aerospace/aerodynamic components and structures. However, fiber orientations and different processing conditions should be considered and utilised to understand the hybrid nanocomposite system. This is because Shiravand *et al* [216]; have reported that the performance of nanocomposite was difficult to compare. With prove that nanoparticles have produced different effects in different matrices; and even in the same matrix under different processing.

In order to fully understand the behaviour of the nanoclay in the GFRC material, quasi-static and fatigue testing should be conducted under elevated temperature conditions that are suitable for aerodynamic applications. Finally,

the manufacturing and testing of a composite structural component rather that lab scale small specimens is highly recommended for future research.

REFERENCES

[1] Campbell F. C. *Structural Composite Materials. ASM International, Ohio.* . Available: http://www.asminternational.org/documents/10192/3449376/05287G_Frontmatter.pdf/99be6880-dfa9-41d3-89b6-bfd96d63b878. Accessed (February 2012)

[2] Masuelli M. A. *Introduction of Fibre-Reinforced Polymers – Polymers and Composites: Concepts, Properties and Processes*. Available: http://cdn.intechopen.com/pdfs-wm/41941.pdf. Accessed (February 2013)

[3] Khan S. U, Munir A, Hussain R, and Kim J. K., "Fatigue damage behaviors of carbon fiber-reinforced epoxy composites containing nanoclay," *Composite Science and Technology,* vol. 70, pp. 2077-85, 2010.

[4] Manjunatha C. M, Bojja R, Jagannathan N, Kinloch A. J, and Taylor A. C., "Enhanced fatigue behavior of a glass fiber reinforced hybrid particles modified epoxy nanocomposite under WISPERX spectrum load sequence," *International Journal of Fatigue,* vol. 54, pp. 25-31, 2013.

[5] Kristofer Gamstedt E and Svend Ib Andersen. (2001). *Fatigue degradation and failure of rotating composite structures – materials characterisation and underlying mechanisms*. Available: http://orbit.dtu.dk/fedora/objects/orbit:91229/datastreams/file_7727033/content. Accessed (August 2015)

[6] Leon Mishnaevsky Jr. *"Composite materials in wind energy technology", Riso Nantional Laboratory for Sustainable Energy, Technical University of Denmark, Roskilde, Denmark.* Available: http://www.eolss.net/Eolss-sampleAllChapter.aspx. Accessed (February 2014)

[7] Richardson R., "New design tool improves manufacture of composite wind turbine blades," *Power,* vol. 154, pp. 62-65, 2010.

[8] Awang Ngah S, "Static and fatigue behaviour of fiber composite infused with rubber and silica nanoparticle-modified epoxy," Mechanical Engineering, Imperial College London, 2013.

[9] Scott J. G. (2014). *New 3D Printing Material Mimics Light Weight Balsa Wood for use in Wind Turbine Construction*. Available: http://3dprintingindustry.com/2014/07/04/3d-printing-material-light-weight-balsa-wood/ Accessed (September 2014)

[10] Compston P, Jar P. Y. B, Burchil P. J, and Takahashi K., "The effect of matrix toughness and loading rate on the mode-II interlaminar fracture toughness of glass fibre/vinyl-ester composites," *Composites Science and Technology,* vol. 61, pp. 321-33., 2001.

[11] Kawai M, Yakima S, Hachinohe A, and Takano Y., "Off-axis fatigue behaviour of unidirectional carbon fiber-reinforced composites at room and high temperatures," *Journal of Composite Materials,* vol. 35, pp. 545-576, 2001.

[12] Degrieck J and Paepegem W. V., "Fatigue damage modeling of fiber-reinforced composite materials," *Appl Mech Rev* vol. 54, pp. 279–300, 2001.

[13] Raif Sakin and Irfan Ay., "Statistical analysis of bending fatigue life data using Weibull distribution in glass-fibre reinforced polyester composites," *Materials and Design,* vol. 29, pp. 1170-1181, 2008.

[14] Mar-Bal. *History of Composite*. Available: http://www.mar-bal.com/applications/history-of-composites. Accessed (March 2015)

[15] Cooperative Research Centre for Advanced Composite Structures Ltd. *Putting it together – the science and technology of composite materials.* Available: http://www.science.org.au/nova/059/059key.htm. Accessed (November 2014)

[16] Wikipedia. *Composite Material, Wikipedia, the free encyclopaedia*. Available: http://en.wikipedia.org/wiki/Composite_material. Accessed (November 2015)

[17] RSC. *Composite materials*. Available: http://www.rsc.org/Education/Teachers/Resources/Inspirational/resources/4.3.1.pdf. Accessed (January 2014)

[18] Johnson T. *History of Composite*. Available: http://composite.about.com/od/aboutcompositesplastics/a/HistoryofComposites.htm. Accessed (March 2014)

[19] HSC Engineering studies. *Polymer composite*. Available: http://hsc.csu.edu.au/engineering_studies/focus/aero/2579/polymer_answers.html#act3. Accessed (March 2014)

[20] Goodrich. *Why Composites*. Available: http://www.epp.goodrich.com/why.shtml. Accessed (March 2014)

[21] AZO. *Composite matrix materials*. Available: http://www.azom.com/article.aspx?ArticleID=9814. Accessed (August 2013)

[22] Warren R., "Ceramic and Metal Matrix Composites, Course Notes," Luleå, University of Technology 1999.

[23] Smith P. A and Yeomans J. A., "Benefit of Fibre and Particulate Reinforcement," *Material Science and Engineering,* vol. 2, 2002.

[24] Composite Learning Center. *Types of Fiber Reinforcement.* Available: http://www.automateddynamics.com/article/thermoplastic-composite-basics/types-of-fiber-reinforcement. Accessed (March 2015)

[25] Johnson T. *Benefit of Composite*. Available: http://composite.about.com/od/aboutcompositesplastics/tp/Benefits-Of-Composites.htm. Accessed (March 2014)

[26] American Composite Manufacturers Association. *Why Composite.* Available: http://acmanet.org/composites/why-composites/ . Accessed (February 2015)

[27] David Cripps. Guide to Composite. *NetComposite*. Available: http://www.netcomposites.com/guide/fibre-properties/27. Accessed (May 2015)

[28] Lopez J. P, Mutje P, Pelach M. A, Mansouri N. E, Boufi S, and Vilaseca F., "Analysis of the tensile modulus of polypropylene composites reinforced with stone groundwood fiber from soft wood," *BioResources,* vol. 7, pp. 1310-1323, 2012.

[29] Abdel Ghafaar M and Mazen A. A., "Application of the rule of mixtures and halpin-tsai equations to woven fabric reinforced epoxy composites," *Journal of Engineering Sciences, Assiut University,* vol. 34, pp. 227-236, 2006.

[30] Khan S. U, Iqbal K, Munir A, and Kim J., "Quasi-static and impact fracture behaviors of CFRPs with nanoclay-filled epoxy matrix," *Composite Part A,* vol. 42, pp. 253–264, 2011.

[31] Chehroudi B. *Composite Materials and Their Uses in Cars*. Available: http://advtechconsultants.com/CompositeMaterial.htm. Accessed (August 2014)

[32] Bryan Harris. (1999). *Engineering composite material*. Available: http://www.cantab.net/users/bryanharris/Engineering%20Composites.pdf. Accessed(February 2014)

[33] Kulkari S. G. *Svnit composite materials: Introduction to composite materials*. Available: http://www.slideshare.net/neerajparmar68/svnit-composite-materials. Accessed (February 2015)

[34] Taylor R. P., "Fibre composite aircraft – capability and safety," *ATSB - AR,* pp. 2007-012, 2008.

[35] Brimhall T., "Composite Automotive Crash Structures," *Composites Technology,* 2007.

[36] Rakow J and Pettinger A., "Failure Analysis of Composite Structures in Aircraft Accidents," *International Society of Air Safety Investigators* 2006.

[37] Cantwell W. J and Morton J., "The impact resistance of composite materials -- a review," *Composites,* vol. 22, pp. 347–62, 1991.

[38] Jamison R. D, Schulte K, Reifsnider K. L, and Stinchcomb W. W., "Characterization and analysis of damage mechanisms in tension–tension fatigue of graphite/epoxy laminates," *ASTM-STP* vol. 836, pp. 21–55, 1984.

[39] Baron C, Schulte K, and Harig H., "Influence of fibre and matrix failure strain on static and fatigue properties of carbon fibre-reinforced plastics," *Composite Science Technology,* vol. 29, pp. 257-72, 1987.

[40] Njuguna J, Pielichowski K, and Alcock J. R., "Epoxy-based fibre reinforced nanocomposites," *Advanced Engineering Material,* vol. 9, pp. 835–47, 2007.

[41] Hull D and Clyne T. W, *An introduction to composite materials*, 2nd ed. UK: Cambridge University Press, 1996.

[42] Wikipedia. *Hybrid Material, Wikipedia, the free encyclopedia*. Available: http://en.wikipedia.org/wiki/Hybrid_material. Accessed (October 2014)

[43] Suyama Y., "Research and Development of Organic-Inorganic Nanohybrids Materials," *Ceramics Japan,* vol. 39, pp. 92-93, 2004.

[44] John M. J, Anandjiwala R. D., and Thomas S., "Hybrid composites," in *Natural fibre reinforced polymer composites*, Thomas S. and Laly A. Pothen., Eds., ed: Old City Publishing, 2009, pp. 315-328.

[45] Isaac M. Daniel and Joel S. Fennernd. *Hybrid Nano/Micro Composite Materials for Greatly Enhanced Fatigue Life*. Available: https://isen.northwestern.edu/doc/pdf/Booster_IDaniel.Mar10_Final.NarrativeReport.pdf. Accessed (February 2015)

[46] Fu Shao-Yun, Guanshui Xu, and Yiu-Wing Mai., "On the elastic modulus of hybrid particle/short-fiber/polymer composites," *Composites Part B: Engineering* vol. 33, pp. 291-299, 2002.

[47] Mirbagheri J, Tajvidi M, Ghasemi I, and Hermanson J. C., "Prediction of the Elastic Modulus of Wood Flour/ Kenaf Fiber/ Polypropylene Hybrid Composites," *Iranian Polymer Journal,* vol. 16, pp. 271-278, 2007.

[48] Swolfs Y, Gorbatikh L, and Verpoest I., "Fibre hybridisation in polymer composites: A review,," *Composites Part A: Applied Science and Manufacturing,* vol. 67, pp. 181–200, 2014.

[49] De Greef N, Gorbatikh L, Godara A, Mezzo L, Lomov S. V, and Verpoest I., "The effect of carbon nanotubes on the damage development in carbon fiber/epoxy composites," *Carbon,* vol. 49, pp. 4650-4664, 2011.

[50] De Greef N, Gorbatikh L, Lomov. S. V, and Verpoest I., "Damage development in woven carbon fiber/epoxy composites modified with carbon nanotubes under tension in the bias direction," *Composite: Part A,* vol. 42, pp. 1635-1644, 2011.

[51] Kornmann X, Rees M, Thomann Y, Necola A, Barbezat M., and Thomann R., "Epoxy layered silicate nanocomposites as matrix in glass fibre-reinforced composites," *Composite Science Technology,* vol. 65, pp. 2259-68, 2005.

[52] Subramaniyan A. K and Sun C. T., "Enhancing compressive strength of unidirectional polymeric composites using nanoclay," *Composites: Part A,* vol. 37, pp. 2257-68, 2006.

[53] Siddiqui N. A, Woo R. S. C, Kim J. K, Leung C. C. K, and Munir A., "Mode I interlaminar fracture behavior and mechanical properties of CFRPs with nanoclay-filled epoxy matrix," *Composites: Part A,* vol. 38, pp. 449-60, 2007.

[54] Tsai J. L and Wu M. D., "Organoclay effect on mechanical responses of glass/epoxy nanocomposites," *Journal of Composite Materials,* vol. 41, pp. 2513-28, 2007.

[55] Tsai J. L and Wu M. D., "Organoclay effect on transverse tensile strength and in-plane shear strength of unidirectional glass/epoxy nanocomposites," *Key Engineering Material* pp. 334-335:773–6, 2007.

[56] Hofer K. E. Jr, Stander M, and Bennett L. C, "Degradation and enhancement of fatigue behaviour of glass/grahhite/epoxy hybrid composite after accelerated aging," in *32nd Annual Technical Conference*, 1977.

[57] Manders P.W and Bader M. G, "The strength of hybrid glass/carbon fiber composite, Part 2," *Journal of Material Science,* vol. 16, pp. 2246-2256, 1981.

[58] Liao K, Schultheisz C.R, Hunston D L, and Brinson L. C, "Long-term durability of fiber-reinforced polymer-matrix composite materials for infractructure applications: a review," *Journal of Advanced Materials,* vol. 30, pp. 2-40, 1998.

[59] Gururaja M. N. A. N. and Hari Rao., "A Review on Recent Applications and Future Prospectus of Hybrid Composites," *International Journal of Soft Computing and Engineering (IJSCE) ISSN,* vol. 1, pp. 2231-2307, 2012.

[60] Manjunatha C. M, Taylor A. C, Kinloch A. J, and Sprenger S., "The tensile fatigue behaviour of a silica nanoparticle-modified glass fibre reinforced epoxy composite," *Composite Science and Technology,* vol. 70, pp. 193-199, 2010.

[61] Kinloch A. J, Masania K, Taylor A. C, Sprenger S, and Egan D., "The fracture of glassfibre- reinforced epoxy composites using nanoparticle-modified matrices," *Journal Material Science,* vol. 43, pp. 1151-4, 2008.

[62] Gojny F. H, Wichmann M. H. G, Fiedler B, Bauhofer W., and Schulte K., "Influence of nano-modification on the mechanical and electrical properties of conventional fibre-reinforced composites," *Composites A,* vol. 36, pp. 1525-35, 2005.

[63] Zhou Y, Pervin F, Jeelani S., and Mallick P. K., "Improvement in mechanical properties of carbon fabric-epoxy composite using carbon nanofibers," *Journal of Material Process Technology,* vol. 198, pp. 445-53, 2008.

[64] Haque A, Shamsuzzoha M, Hussain F., and Dean D., "S2-glass/epoxy polymer nanocomposites: manufacturing, structures, thermal and mechanical properties," *Journal of Composite Materials,* vol. 37, pp. 1821-37, 2003.

[65] Johnsen B. B, Kinloch A. J, Mohammed R. D, Taylor A. C., and Sprenger S., "Toughening mechanisms of nanoparticle-modified epoxy polymers," *Polymer,* vol. 48, pp. 530-41, 2007.

[66] Ma J, Mo M. S, Du X. S, Rosso P, Friedrich K, and Kuan H. C., "Effect of inorganic nanoparticles on mechanical property, fracture toughness and toughening mechanism of two epoxy systems," *Polymer,* vol. 49, pp. 3510-3523, 2008.

[67] Kinloch A. J, Mohammed R. D, Taylor A. C, Sprenger S, and Egan D. J., "The interlaminar toughness of carbon-fibre reinforced plastic composites using 'hybrid toughened' matrices," *Journal of Material Science,* vol. 41, pp. 5043-6, 2006.

[68] Grimmer C and Dharan C., "High-cycle fatigue of hybrid carbon nanotube/glass fiber/polymer composites," *Journal of Material Science,* vol. 43, pp. 4487-92, 2008.

[69] Kostopoulos V, Vavouliotis A, Karapappas P, Loutas T, Voyatzi T, and Paipetis A., "Multi-stage fatigue life monitoring on carbon fibre reinforced polymers enhanced with multi-wall carbon nanotubes," *ECCM-13 Conference Proceedings* vol. 1, pp. 1-9, 2008.

[70] Borrego L. P, Costa J. D. M, Ferreira J. A. M, and Silva H., "Fatigue behaviour of glass fibre reinforced epoxy composites enhanced with nanoparticles," *Composites: Part B,* vol. 62, pp. 65-72, 2014.

[71] Gojny F. H, Wichmann M. H. G, Köpke U, Fiedler B, and Schulte K, "Carbon nanotubereinforced epoxy-composites: enhanced stiffness and fracture toughness at low nanotube content," *Composite Science and Technology,* vol. 64, pp. 2363–2371, 2004.

[72] Lars Böger, Jan Sumfleth, Hannes Hedemann., and Karl Schulte., "Improvement of fatigue life by incorporation of nanoparticles in glass fibre reinforced epoxy," *Composite: Part A,* vol. 41, pp. 1419-1424, 2010.

[73] Manjunatha C. M, Sprenger S, Taylor A. C, and Kinloch A. J., "The tensile fatigue behavior of a glass-fiber reinforced plastic composite using a hybrid-toughened epoxy matrix," *Journal of Composite Material,* vol. 44, pp. 2095-2109, 2010.

[74] Dahlen C and Springer G. S, "Delamination growth in composites under cyclic loads," *journal of polymer Materials,* vol. 28, pp. 732–781, 1994.

[75] Blackman B. R. K, Kinloch A. J, Sohn Lee J., and Taylor A. C., "The fatigue and fracture behaviour of nano-modified epoxy polymers," *Journal of Material Science* vol. 42, pp. 7049-7051, 2007.

[76] Reifsnider K. L., "Modelling of the interphase in polymer-matrix composite material systems," *Composites,* vol. 25, pp. 461-469, 1994.

[77] Drzal L. T and Madhukar M, "Fiber-matrix adhension and its relationship to compsite materialproperties," *Journal of Materail Science,* vol. 28, pp. 569-610, 1993.

[78] Cech V, Prikryl R, Balkova R, Vanek J, and Grycova A., "The influence of surface modifications of glass on glass fiber/ polyester interphase properties," *J. Adhension Sci. Technol,* vol. 17, pp. 1299–1320, 2003.

[79] Yong X. Gan., "Effect of Interface Structure on Mechanical Properties of Advanced Composite Materials," *International Journal of Molecular Science,* vol. 10, pp. 5115-5134., 2009.

[80] GAO Z and REIFSNIDE K. L., *Journal Composite Technology and Res.,* vol. 14, p. 201, 1992.

[81] Lin W. P and Hu H. T., "Parametric study on the failure of fiber reinforced composite laminates under biaxial tensile load," *Journal Composite Material,* vol. 36, pp. 1481–503, 2002.

[82] Harizia W, Chakia S, Boursea G, and Ourak M., "Mechanical damage assessment of Glass Fiber-Reinforced Polymer composites using passive infrared thermography," *Composites Part B: Engineering,* vol. 59, pp. 74–79, 2014.

[83] Okoli O. I and Smith G. F., "Failure modes of fibre reinforced composites: The effects of strain rate and fibre content," *Journal of Materials Science* vol. 33, pp. 5415 – 5422, 1998.

[84] Barsom J. M and T Rolfe S. T., *Fracture and Fatigue control in structures: Application of Fracture Mechanics*, 2nd ed. Prentice Hall. Inc. USA, 1987.

[85] Silva R. V, Spinelli D, Bose Filho W. W, Claro Neto S, Chierice G. O, and Tarpani J. R., "Fracture toughness of natural fibers/castor oil polyurethane composites," *Composite Science and Technology,* vol. 66, pp. 1328-1335, 2006.

[86] Barikani M, Saidpour H, and Sezen M., "Mode-I Interlaminar Fracture Toughness in Unidirectional Carbon-fiber/Epoxy Composites," *Iranian Polymer Journal,* vol. 11, pp. 413-423, 2002.

[87] Lee J. W and Daniel I. M., "Progressive transverse cracking of cross-ply composite laminates," *Journal of Composite Materials,* vol. 24, pp. 1225-1243, 1990.

[88] Highsmith A.L and Reifsnider K.L., "Stiffness-reduction mechanisms in composite laminates," *Damage in Composite Materials,* vol. 775, pp. 103-117, 1982.

[89] Garrett K.W and Bailey J.E., "Multiple transverse fracture in 90° cross-ply laminates of a glass fibre-reinforced polyester," *Journal of Materials Science,* vol. 12, pp. 157-168, 1977.

[90] Hahn H.T and Tsai S.W., "On the behaviour of composite laminates after initial failures," *Journal of Composite Materials,* vol. 8, pp. 288-305, 1974.

[91] Salkind M. J., "Fatigue of composites," in *Composite materials: testing and design*, ed: 2nd conf, ASTM STP 497. American Society for Testing and Materials, 1972, pp. 143–169.

[92] Browning C. E and Schwartz H. S., "Testing and Design " in *Composite Materials*, J.M.Whitney, Ed., ed ASTM STP 893: Philadelphia, 1986, pp. 256–265.

[93] Cantwell W. J and Morton J, "The significant of damage and defect and their detection in composite materials: A review," *The Journal of Strain Analysis for Engineering Design,* vol. 27, pp. 29 – 42, 1992.

[94] Bolotin V. V., "Delamination in composite structures; Its origin, buckling, growth and stability," *Composites Part B: Engineering,* vol. 27, pp. 129-145, 1996.

[95] Davies P, Sims G. D, Blackman B. R. K, Brunner A. J, Kageyama K, Hojo M*, et al.*, "Comparison of test configurations for determination of mode II interlaminar fracture toughness results from international collaborative test programme," *Plastic Rubber Composite,* vol. 28, pp. 432–437, 1999.

[96] Hochard C., "Optimum design of laminated composite structures," *Composite Structures* vol. 63, pp. 159–165, 2004.

[97] Zhuang H and Wightman J. P., "The Influence of Surface Properties on Carbon/Epoxy Matrix Interfacial Adhesion," *The Journal of Adhesion* vol. 62, pp. 213-245, 1997.

[98] Silberschmidt V.V., "Matrix cracking in cross-ply laminates: effect of randomness," *Composite A,* vol. 36, pp. 129–135, 2005.

[99] Center for Nondestructive Evaluation. (March 2015). Available: https://www.cnde.iastate.edu/ultrasonics-and-composites/modeling-cracks-and-delaminations-carbon-fiber-composites-frank-margetan

[100] Wisnom M. R., "The role of delamination in failure of fibre-reinforced composites," *Philos Trans A Math Phys Eng Sci,* vol. 370, pp. 1850-70, 2012.

[101] Johnson A. F and Toso-Pentecote., "Determination of Delamination Damage in Composite Under Impact Loads: Delamination Damage in Low Velocity Impact," in *Delamination Behaviour of Composites*, S. Sridharan, Ed., ed Washington: Woodhead, 2008, pp. 570 – 583.

[102] Choi S. R and Kowalik R. W., "Interlaminar crack growth resistances of various ceramic matrix composites in Mode I and Mode II loading," *Journal of Engineering for Gas Turbine Power,* vol. 130, p. 031301, 2008.

[103] Benzeggagh M. L and Kenane M, "Measurement of Mixed-Mode delamination fracture toughness of unidirectional glass/epoxy composites with Mixed- Mode Bending apparatus," *Composite Science Technology,* vol. 56, pp. 439–49, 1996.

[104] Hashemi S and Kinloch A. J, "Williams JG. The effects of geometry, rate and temperature on the Mode I, Mode II and Mixed-Mode I/II interlaminar fracture of carbon-fiber/poly(ether-ether ketone) composites," *Journal Composite Material,* vol. 24, pp. 918–56, 1990.

[105] Madhukar M. S and Drzal L. T, "Fiber-Matrix Adhesion and its Effect on Composite Mechanical Properties: IV. Mode I and Mode II Fracture Toughness of Graphite/Epoxy Composte," *journal Composite Materials,* pp. 936 – 968, 1992.

[106] Dorey G, Bishop S. M, and Curtis P. T, "On the Impact Performance of Carbon Fiber Laminates with Epoxy and PEEK Matrices," *Composite Science and Technology,* vol. 23, pp. 221 – 237, 1985.

[107] Garg A. C, "Delamination – A damage mode in composite structures," *Engineering Fracture Mechanics,* vol. 29, pp. 557 – 584, 1988.

[108] David Hogg. *Aircraft Composites - Damage Through Rain Erosion*. Available: http://www.azom.com/article.aspx?ArticleID=1740. Accessed (June 2013)

[109] Jenq S. T, Jing H. S, and Chung C., "Predicting the ballistic limit for plain woven glass/epoxy composite laminate," *International Journal of Impact Engineering* vol. 15, pp. 451–64, 1994.

[110] Zhu G, Goldsmith W, and Dharan C. K., "Penetration of laminated Kevlar by projectiles—II. analytical model," *International Journal of Solids and Structure* pp. 421–436, 1992.

[111] Morye S. S, Hine P. J, Duckett R. A, Carr D. J, and Ward I. M., "Modelling of the energy absorption by polymer composites upon ballistic impact," *Composite Science and Technology,* vol. 60, pp. 2631–2642, 2000.

[112] Billon H. H and Robinson D. J., "Models for the ballistic impact of fabric armour," *International Journal of Impact Engineering,* vol. 25, pp. 411–422, 2001.

[113] Cheeseman B. A and Bogetti T. A, "Ballistic impact into fabric and compliant composite laminate," *Composite Structures,* vol. 61, pp. 161–73, 2003.

[114] Kate Galbraith. *When Lightning Strikes Wind Turbines II*. Available: http://betterplan.squarespace.com/todays-special/2009/7/3/7209-if-a-wind-turbine-blade-explodes-in-a-german-forest-and.html. Accessed (May 2014)

[115] Broutman L. J and Sahu S., "Progressive damage of a glass reinforced plastic during fatigue," in *Proceedings of the Reinforced Plastics and Composites Institute Annual Conference*, New York, 1969, pp. 1-12.

[116] Kinloch A. J and Young R. J., "Fracture Behavior of Polymers," *Elsevier Applied Science, New York,* pp. 182-225, 1983.

[117] Mandell J. F, Huang D. D, and McGarry F. J., "Tensile Fatigue Performance of Glass Fiber Dominated Composites," *Composites Technology,* vol. 3, pp. 96-102, 1981.

[118] Hahn H. T and Kim R. Y., "Fatigue Behavior of Composite Laminate," *Journal of Composite Materials,* vol. 10, p. 156, 1976.

[119] Okamoto H and Ohde Y., "Failure of Plastics," W. Brostow and R. Corneliussen, Eds., ed: Hanser Publications, Munich, 1986, pp. 330-332

[120] Mandell J. F, McGarry F. J, Huang D. D, and C. G. Li, "Some Effects of Matrix and Interface Properties on the Fatigue of Short Fiber Reinforced Thermoplastics," in *Proc 36th Annual Conference of Reinforced Plastics/Composites*, SPI, 1982, pp. 330-332

[121] Mandell J. F., "Fatigue Behavior of Short Fiber Composite Materials," in *The Fatigue Behavior of Composite Materials*, K. L. Reifsnider, Ed., ed: Elsevier, 1991.

[122] Nairn J. A and Hu S., "Micromechanics of Damage: A Case Study of Matrix Microcracking," in *Damage Mechanics of Composite Materials*, R. Talreja, Ed., ed: Elsevier, Amsterdam, 1994, p. 187(243).

[123] J. A. Nairn., "Polymer Matrix Composite: Matrix Microcracking in Composites," in *Comprehensive Composite Materials*, A. Kelly and C. Zweben, Eds., ed: Salt Lake City: Elsevier Science, 2000, pp. 1-7.

[124] Iddin M. F and Sun C. T., "Strength of unidirectional glass/epoxy composite with silica nanoparticle-enhanced matrix," *Composite Science and Technology,* pp. 1637–43, 2008.

[125] Kim B. C, Park S. W, and Lee D. G., "Fracture toughness of the nano-particle reinforced epoxy composite," *Composite Structures,* vol. 86, pp. 69–77, 2008.

[126] Hussain F, Hojjati M, Okamoto M, and Gorga R. E., "Review article: polymer–matrix nanocomposites, processing, manufacturing, and application," *Journal of Composite Materials,* vol. 40, pp. 1511–1575, 2006.

[127] Hussain F, Hojjati M, Okamoto M, and Gorga R. E., "Polymer–matrix nanocomposites, processing, manufacturing, and application," *Journal of Composite Materials,* vol. 40, pp. 1511–75, 2006.

[128] Manias and Evangelos., "Nanocomposites: Stiffer by design," *Nature Materials* vol. 6, pp. 9–11, 2007.

[129] Amazigo J. C and B. Budiansky, "Interaction of particulate and transformation toughening," *Journal of the Mechanics and Physics of Solids* pp. 581-595, 1988.

[130] Ray S. S and Okamoto M., "Polymer/layered silicate nanocomposites: a review from preparation to processing.," *Progress in polymer science,* vol. 28, pp. 1539-1641, 2003.

[131] Pavlidou S and Papaspyrides C. D., "A review on polymer-layered silicate nanocomposites," *Prog Polym Sci,* vol. 33, pp. 1119–98, 2008.

[132] Dennis H. R, Hunter D. L, Chang D, Kim S, White J. L, Cho J. W*, et al.*, "Effect of Melt Processing Conditions on the Extent of Exfoliation in Organoclay-Based Nanocomposites," *Polymer,* vol. 42, pp. 9513-9522 2001.

[133] Ali Olad., "Polymer/Clay Nanocomposites," in *Advances in Diverse Industrial Applications of Nanocomposites*, B. Reddy, Ed., ed: ISBN: 978-953-307-202-9, InTech, 2011.

[134] Alexandre M and Dubois P., "Polymer-layered silicate nanocomposites: preparation, properties and uses of a new class of materials," *Material Science and Engineering,* vol. 28, pp. 1–63, 2000.

[135] Vaia R. A and Giannelis E. P., "Polymer melt intercalation in organically modified layered silicates: model predictions and experiment," *Macromolecules,* vol. 30, pp. 8000–9, 1997.

[136] Zilg C, Mulhaupt R, and Finter J., "Morphology and toughness/stiffness balance of nanocomposites based upon anhydride-cured epoxy resins and layered silicates," *Macromol Chem Phys* vol. 70, pp. 661–70, 1999.

[137] Boo W. J, Liu J, and Sue H. J., "Fracture behaviour of nanoplatelet reinforced polymer nanocomposites," *Material Science Technology,* vol. 22, pp. 829–34, 2006.

[138] Eckel D. F, Balogh M. P, Fasulo P. D, and Rodgers W. R., "Assessing organo-clay dispersion in polymer nanocomposites," *Journal of Applied Polymer Science,* vol. 93, pp. 1110–1117, 2004.

[139] Usuki A, Kojima Y, Kawasumi M, Okada A, Fukushima Y, and Kurauchi T., "Synthesis of nylon 6-clay hybrid," *J Mater Res,* vol. 8, p. 1179, 1993.

[140] Silvestre C, Cimmino S, Duraccio D, and Kotsilkova R., "Structure and Morphology of Epoxy Nanocomposite with Clay, Carbon and Diamon," in *Thermoset Nanocomposites for Engineering Applications*, R. Kotsilkova, Ed., ed UK: Smithers Rapra Technology Limited, 2007, pp. 117 – 118.

[141] Wang Z, Massam J, and Pinnavaia T. J., "Epoxy–clay nanocomposites," in *Polymer–clay nanocomposites*, Pinnavaia T. J and Beall G. W, Eds., ed New Jersey:: Hoboken 2000, pp. 127–49.

[142] Rana H. T, Gupta R. K, Gangarao H. V. S, and Sridhar L. N., "Measurement of moisture diffusivity through layered-silicate nanocomposites," *AICHE Journal,* vol. 51, pp. 3249–56, 2005.

[143] Rana H. T., "Moisture diffusion through neat and glass-fiber reinforced vinyl ester resin containing nanoclay," Masters Thesis, Department of Chemical Engineering, West Virginia University, 2003.

[144] Sarathi R, Sahu R. K, and Rajeshkumar P., "Understanding the thermal, mechanical and electrical properties of epoxy nanocomposites," *Materials Science and Engineering A 445–446* pp. 567–578, 2007.

[145] Quaresimin M, Salviato M, and Zappalorto M., "Fracture and interlaminar properties of clay-modified epoxies and their glass reinforced laminates," *Engineering Fracture Mechanics,* vol. 81, pp. 80–93, 2012.

[146] Yasmin A, Luo J. J, Abot J. L, and Daniel I. M., "Mechanical and thermal behavior of clay/epoxy nanocomposites," *Composites Science and Technology* vol. 66, pp. 2415–2422, 2006.

[147] Jumahat A, Soutis C, Mahmud J, and Ahmad N., "Compressive properties of nanoclay/epoxy nanocomposites," *Procedia Engineering,* vol. 41, pp. 1607-1613, 2012.

[148] Jones F. R., *Handbook of Polymer Composites*: Longman Scientific and Technical, 1994.

[149] Evans A. G, Zok F. W, and Mackin T. J., *High temperature mechanical behavior of ceramic composites*: Butterworth-Heinemann Boston, 1995.

[150] Thouless M. D, Szaibero O, Sigl L. S, and Evans A. G., "Effect of interface mechanical properties on pullout in a SiC-fiber-reinforced lithium aluminum silicate glass ceramic," *Journal of the American Ceramic Society,* vol. 72, pp. 525-532, 1989.

[151] Heredia F. E, Spearing S. M, He M-Y, Mackin T. J, Evans A. G, Mosher P*, et al.*, "Notch effects in carbon matrix composites," *Journal of the American Ceramic Society,* vol. 77, pp. 2817–2827, 1994.

[152] Mackin T. J, Purcell T. E, He M. Y, and Evans A. G., "Notch sensitivity and stress redistribution in three ceramic-matrix composites," *Journal of the American Ceramic Society,* vol. 78, pp. 1719–1728, 1995.

[153] Cao H. C, Bischoff E, Sbaizero O, Ruhle M, Evans A. G, Marshall D. B*, et al.*, "Effect of interfaces on the properties of fiber-reinforced ceramics," *Journal of the American Ceramic Society,* vol. 73, pp. 1691-1699, 1990.

[154] Lin G, Geubelle P. H, and Sottos N. R., "Simulation of fiber debonding with friction in a model composite push-out test," *International Journal of Solids and Structures,* vol. 38, pp. 8547-8562, 2001.

[155] Timmerman J. F, Hayes B, and Seferis J. C., "Nanoclay reinforcement effects on the cryogenic micro cracking of carbon fiber/epoxy composites," *Composite Science and Technology,* vol. 62, pp. 1249–58, 2002.

[156] Muhi R. J, Najim F, and de Moura M. F. S. F., "The effect of hybridization on the GFRP behavior under high velocity impact," *Composites Part B: Engineering* vol. 40, pp. 798-803, 2009.

[157] Mc Coll I. R and Morley J. G., "Crack growth in hybrid fibrous composites," *Journal of Material Science,* vol. 12, pp. 1165–75, 1977.

[158] Bunsell A. R and Harris B., "Hybrid carbon and glass fibre composites," *Composites,* vol. 5, pp. 157–164, 1974.

[159] Harris B and Bunsell A. R., "Impact properties of glass fibre/carbon fibre hybrid composites," *Composites,* vol. 6, pp. 197–201, 1975.

[160] Mingkang A, Daofang S, and Guojun W., "Study on the structure and properties of a hybrid resins," *International Journal of Chemistry,* vol. 1, p. 1646, 2009.

[161] Jang B. Z, Chen L. C, Wang C. Z, Lin H. T, and Zee R. H., "Impact resistance and energy absorption mechanisms in hybrid composites," *Composite Science and Technology,* vol. 34, pp. 305–335, 1989.

[162] Karippal J. J, Murthy H. N. N, Rai K. S, Sreejith M, and Krishna M., "Study of mechanical properties of epoxy/glass/nanoclay hybrid composites," *Journal of Composite Materials,* vol. 45, 2011.

[163] Reifsnider K. L., "Introduction," in *Fatigue of Composite Materials*, K. L. reifsnider, Ed., ed Elsevier Science Publishers B.V., 1990, pp. 1-9.

[164] Boger L, Sumfleth J, Hedemann H, and Schulte K., "Improvement of fatigue life by incorporation of nanoparticles in glass fibre reinforced epoxy," *Composites: Part A* vol. 41, pp. 1419–1424, 2010.

[165] Manjunatha C. M, Jagannathan N, Padmalatha K, Kinloch A. J, and Taylor A., "Improved variable-amplitude fatigue behavior of a glass-fiber-reinforced hybrid-

toughened epoxy composite," *Journal of Reinforced Plastic Composite,* vol. 30, pp. 1783–1793, 2011.

[166] Manjunatha C. M, Taylor A. C, Kinloch A. J, and Sprenger S., "The tensile fatigue behaviour of a GFRP composite with rubber particle modified epoxy matrix," *Journal of Reinforced Plastic Composite,* vol. 21, pp. 2170–2183, 2010.

[167] Manjunatha C. M, Taylor A. C, Kinloch A. J, and Sprenger S., "The Effect of Rubber Micro-Particles and Silica Nano-Particles on the Tensile Fatigue Behaviour of a Glass Fiber Epoxy Composite," *Journal of Material Science,* vol. 44, pp. 342-345, 2009.

[168] Joel S. Fenner and Isaac M. Daniel, "Hybrid nanoreinforced carbon/epoxy composites for enhanced damage tolerance and fatigue life," *Composites: Part A,* vol. 65, pp. 7–56, 2014.

[169] Withers G. J, Yu Y, Khabashesku V. N, Cercone L, Hadjiev V. G, Souza J. M*, et al.*, "Improved mechanical properties of an epoxy glass–fiber composite reinforced with surface organomodified nanoclays," *Composites: Part B,* vol. 72, pp. 175-182, 2015.

[170] Patil P. N, Rath S. K, Sharma S. K, Sudarshan K, Maheshwari P, Patri M*, et al.*, "Free volumes and structural relaxations in diglycidyl ether of bisphenol-A based epoxy–polyether amine networks," *Soft Matter,* vol. 9, pp. 3589-3599, 2013.

[171] European coatings. *Dispersion is the key to performance*. Available: http://www.european-coatings.com/Editorial-archive/Dispersion-is-the-key-to-performance. Accessed (March 2013)

[172] Lam C.K, La K.T, Cheung H.Y, and Ling H.Y., "Effect of ultrasound sonication in nanoclay clusters of nanoclay/epoxy," *Composites Material Lett,* vol. 59, pp. 1369–1372, 2005.

[173] Bilotti E, Fischer H.R, and Peijs T, "Polymer nanocomposites based on needle-like sepiolite clays: Effect of functionalized polymers on the dispersion of nanofiller, crystallinity, and mechanical properties," *Journal of Applied Polymer Science,* vol. 107, pp. 1116–1123, 2008.

[174] Agubra V. A, Owuor P. S, and Hosur M. V., "Influence of Nanoclay Dispersion Methods on the Mechanical Behavior of E-Glass/Epoxy Nanocomposites," *Nanomaterials* vol. 3, pp. 550-563, 2013.

[175] Wu C.L, Zhang Q.M, Rong Z.M, and Klaus F, "Tensile performance improvement of low nanoparticles filled polypropylene composites," *Composite Science Technology,* vol. 62, pp. 1327–1340, 2002.

[176] Yasmin A, Abot J.L, and Daniel I.M, "Processing of clay/epoxy nanocomposites by shear mixing," *Scriptal Materialia,* vol. 49, pp. 81-86 2003.

[177] Ngo T. D, Ton-That M. T, Hoa S. V, and Cole K. C., "Effect of temperature, duration and speed of pre-mixing on the dispersion of clay/epoxy nanocomposites," *Composite Science Technology,* vol. 69, pp. 1831–1840, 2009.

[178] America Society for testing Testing Materials, "Standard Test Method for Content of Composite Materials," vol. ASTM D 3171 - 99, ed. West Conshohocken, PA 19428 - 2959, United state: ASTM International, 1999.

[179] Abraham D, Matthews S, and Mclhagger R., "A comparison of physical properties of glass fiber epoxy composites produced by wet lay-up with autoclave consolidation and resin transfer moulding," *Composite Part A: Applied Science and Manufacturing,* vol. 29, pp. 795-801, 1998.

[180] Annual Book of ASTM Standards, "Standard Practice for Plastics: Dynamic Mechanical Properties: Determination and Report of Procedures," vol. D 4065-01, ed: ASTM International, West Conshohocken, PA, 2001.

[181] America Society for testing Testing Materials, "Standard Test Method for Tensile Properties of Polymer Matrix Composite Materials," vol. ASTM D 3039 – 14, ed: United state: ASTM International, 2014.

[182] America Society for testing Testing Materials, "Standard Test Methods for Flexural Properties of Unreinforced and Reinforced Plastics and Electrical Insulating Materials," vol. D 790-02, ed: United state: ASTM International, 2002.

[183] America Society for testing Testing Materials, "Standard Test Method for Determining the Charpy Impact Resistance of Notched Specimens of Plastics," vol. ASTM D6110 – 10, ed: United state: ASTM International, 2010.

[184] America Society for testing Testing Materials, "Standard Test Method for Indentation Hardness of Rigid Plastics by Means of a Barcol Impressor," vol. ASTM D 2583 - 07 ed: United state: ASTM International, 2007.

[185] America Society for testing Testing Materials, "Standard Test Method for Tension–Tension Fatigue of Polymer Matrix Composite Materials," vol. ASTM D3479 – 96, ed: United state: ASTM International, 1996.

[186] Comsol. *Material Fatigue*. Available: https://www.comsol.com/multiphysics/material-fatigue. Accessed (February 2014)

[187] Sanglimsuma, Apiradee, Narumon Seeponkai, and J. Wootthikanokkhan., "Effect of concentration of organically modified nanoclay on properties of sulfonated poly (vinyl alcohol) nanocomposite membranes.," *International Journal of Electrochemistry* 2011.

[188] Xu H. H. K, Ostertag C. P, Braun L. M, and Lloyd I. K, "Effects of Fibre Volume Fraction on Mechanical Properties of SiCfibre/ Si[3]N[4]-Matrix Composites," *Journal of the American Ceramic Society,* vol. 77, pp. 1897-1900, 1994.

[189] David Cripps. *Guide to Composite: Fiber properties*. Available: http://www.netcomposites.com/guide/fibre-properties/27. Accessed (May 2015)

[190] Kanny K and Mohan T. P., "Resin infusion analysis of nanoclay filled glass fiber laminates," *Composite part B,* vol. 58, pp. 328-334, 2014.

[191] Chen Wen-Yi, Wang Yez-Zen, and Chang Feng-Chih., "Study of curing kinetics and 517 curing mechanism of epoxy resin based on diglycidyl ether of bisphenol A and 518 melamine phosphate," *Journal of Applied Polymer Science,* vol. 92, pp. 892-900, 2004.

[192] Bilyeu B, Brostow W, and Menard K. P., "Epoxy thermosets and their applications. II. Thermal analysis," *Journal of Materials Education,* vol. 22, pp. 107-129, 2000.

[193] Wilso T. W, Fornes R. E, Gilbert R. D, and Memory J. D., "Cross-Linked Polymers," ed R. A. Dickie, S. S. Labana, R. S. Bauer,: American Chemical Society, Washington D.C., 1988.

[194] American Standard Test Method, "Standard Test Method for Glass Transition Temperature (DMA Tg) of Polymer Matrix Composites by Dynamic Mechanical Analysis (DMA)," in *ASTM D7028 - 07e1, DOI: 10.1520/D7028-07E0*, ed, 2007.

[195] Messersmith P. B and Giannelis E. P., "Synthetic and characterization of layered silicate epoxy nanaocomposites," *Chem. Materials,* vol. 6, pp. 1719-1725, 1994.

[196] Chen J. S., "Study of interlayer expansion mechanism and thermal mechanical properties of surface initiated epoxy nanocomposites," *Polymer,* vol. 43, pp. 4895-4904, 2002.

[197] Feng W, Ait-Kadi A, and Riedl B., "Polymerization compounding: epoxy-montmorillonite nanocomposites," *Polymer Engineer Science,* vol. 42, pp. 1827–1836, 2002.

[198] Pham J. Q, Mitchell C. A, Bahr J. L, Tour J. M, Krishanamoorti R, and Green P. F., "Glass transition of polymer/single-walled carbon nanotube composite films," *Journal Polymer Science Part B: Polymer Physics,* vol. 41, pp. 3339-3345, 2003.

[199] Ash B. J, Schadler L. S, and Siegel R.W., "Glass transition behaviour of alumina/polymethacrylate nanocomposites," *Mater. Lett.,* vol. 55, pp. 83-87, 2002.

[200] Becker O, Varley R, and Simon G., "Morphology, thermal relaxations and mechanical properties of layered silicate nanocomposites based upon high-functionality epoxy resin," *Polymer,* vol. 43, pp. 4365-4373, 2002.

[201] Kornmann X, Lindberg H, and Berglund L. A., "Synthesis of epoxy-clay nanocomposite: Influence of the nature of the curing agent on the structure," *Polymer,* vol. 42, pp. 4493–4499, 2001.

[202] Nigam V., "Epoxy-montmorillonite clay nanocomposites: synthesis and characterization," *Journal of Applied Polymer Science,* vol. 93, pp. 2201-2210, 2004.

[203] Liu T., "Morphology and fracture behaviour of intercalated epoxy clay nanocomposites," *Journal of Applied Polymer Science,* vol. 94, pp. 1236–1244.

[204] Bozkurt E, Kaya E, and Tanoglu M, "Mechanical and thermal behavior of non-crimp glass fiber reinforced layered clay/epoxy nanocomposites," *Composite Science and Technology,* vol. 67, pp. 3394–3403, 2007.

[205] Aktas L and Altan M. C., "Effect of nanoclay content on properties of glass–waterborne epoxy laminates at low clay loading," *Material Science and Technology,* vol. 26, pp. 626–629, 2010.

[206] Yang J.P, Yang G, Xu G, and Fu ShY, "Cryogenic mechanical behaviours of MMT/epoxy nanocomposite," *Journal of Composite Science,* vol. 67, pp. 2934–40, 2007.

[207] Isik I, Yilmazer U, and Bayram G., "Impact modified epoxy/montmorillonite nanocomposites: synthesis and characterization," *Polymer* vol. 44, pp. 6371–6377, 2003.

[208] Wetzel B, Haupert F, and Zhang M. Q, "Epoxy nanocomposites with high mechanical and tribological performance," *Composite Science Technology,* vol. 63, pp. 2055–67, 2003.

[209] Talreja R, "Fatigue of polymer matrix composites," in *Compressive composite materials* vol. 2, Talreja R and Manson Zweben C, Eds., ed polymer matrix Elsevier, Oxford, 2000, pp. 529–52.

[210] Ferreira J. A. M, Costa J. D. M, and Reis P. N. B., "Static and fatigue behaviour of glass-fibre-reinforced polypropylene composites," *Theoretical and Applied Fracture Mechanics,* vol. 31, pp. 67-74, 1999.

[211] Stinchcomb W. W and Bakis C. E, "Fatigue behavior of composite laminates," in *Fatigue of Composite Materials*, K. L. Riefsnider, Ed., ed Amsterdam: Elsevier, 1990, pp. 105–180.

[212] Brøndsted P, Lilholt H, and Andersen S. I., "Fatigue damage prediction by measurements of the stiffness degradation in polymer matrix composites," in *Int. Conf. Fatigue Compos*, 1st, Paris, 8. International spring meeting of ICFC. Paris, 1997, pp. 370–77.

[213] Brøndsted P and J. B. S., "Measurement of damage progress in FRP materials," *Plastic Rubber Composite,* vol. 28, pp. 458– 62, 1999.

[214] Post N. L, Cain J, McDonald K. J, Case S. W, and Lesko J. J., "Residual strength prediction of composite materials: Random spectrum loading," *Engineering Fracture Mechanics* vol. 75, pp. 2707–2724, 2008.

[215] Towo A. N and Ansell M. P., "Fatigue evaluation and dynamic mechanical thermal analysis of sisal fibre–thermosetting resin composites," *Composites Science and Technology,* vol. 68, pp. 925-932, 2008.

[216] Shiravand F, Huchinson J. M, Calventus Y, and Ferrando F., "Comparison of the nanostructure and mechanical performance of highly exfoliated epoxy-clay nanocomposite prepared by three different protocols," *Materials,* vol. 7, pp. 4196-4223, 2014.

LIST OF PAPERS SUBMITTED ON THE BASIS OF THIS DESSERTATION

Refereed Journal

1. Olusanya John, Krishnan Kanny and Shalini Singh, (2015). Bulk cure study of nanoclay filled epoxy glass fiber reinforced composite material. *Journal of Polymer Engineering; POLYENG. 2015.0086.* Accepted May 21, 2016.

Conference Proceedings

1. Olusanya John, Krishnan Kanny and Mohan TP (2013). Study of fiber matrix interface properties and thermal stability of clay filled epoxy-resin nanocomposites. Paper presented at the *1st International Conference for Composite, Bio-composite and Nanocomposite, (ICCBN), ISBN: 978-1-919858-25-8*; 2 – 4 December, 2013, Durban, South Africa.
2. Olusanya John and Krishnan Kanny (2015). Dynamics mechanical thermal analysis of hybrid nanoclay glass fiber reinforced composite structure. Paper presented at the *2nd International Conference for Composite, Bio-composite and Nanocomposite (ICCBN) Proceedings, ISBN: 978-0-620684-56-9*; 28 – 30 October, 2015, Durban, South Africa.

Abstract Accepted

1. Olusanya John, Krishnan Kanny and Mohan TP (2015). Fatigue evaluation of hybrid nanoclay glass fiber reinforced composite structure. Presented at the *Durban University of Technology Research Day,* 26 November, 2015, Durban, South Africa.